

# *Tracing the Dark Matter Web*

Sergei Shandarin

Univ. of Kansas, Lawrence, KS, USA

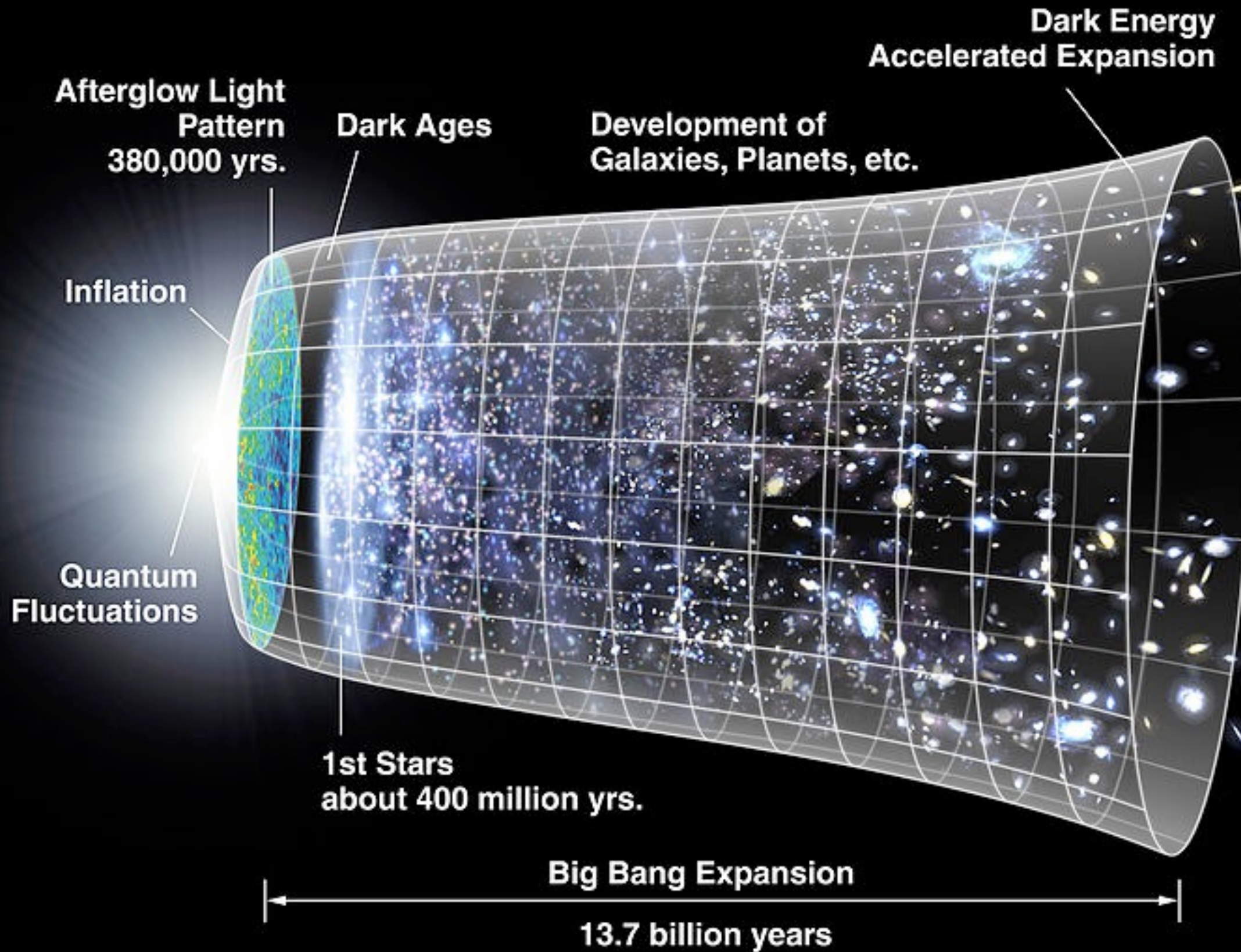
Collaborators: N. Ramachandra, M. Medvedev

# Outline of the talk

- Brief cosmological introduction
- Beginning of the dark matter web story
  - The Zeldovich approximation
  - Geometrical and topological challenges
  - Web of galaxies
- Dark matter web
  - Flip-flop field as a record of halo merging
  - Multi stream field
  - A comparison project “Tracing the Cosmic Web”
  - Caustics
- Summary

# Outline of the talk

- Brief cosmological introduction
- Beginning of the dark matter web story
  - The Zeldovich approximation
  - Geometrical and topological challenges
  - Web of galaxies
- Dark matter web
  - Flip-flop field as a record of halo merging
  - Multi stream field
  - A comparison project “Tracing the Cosmic Web”
  - Caustics
- Summary

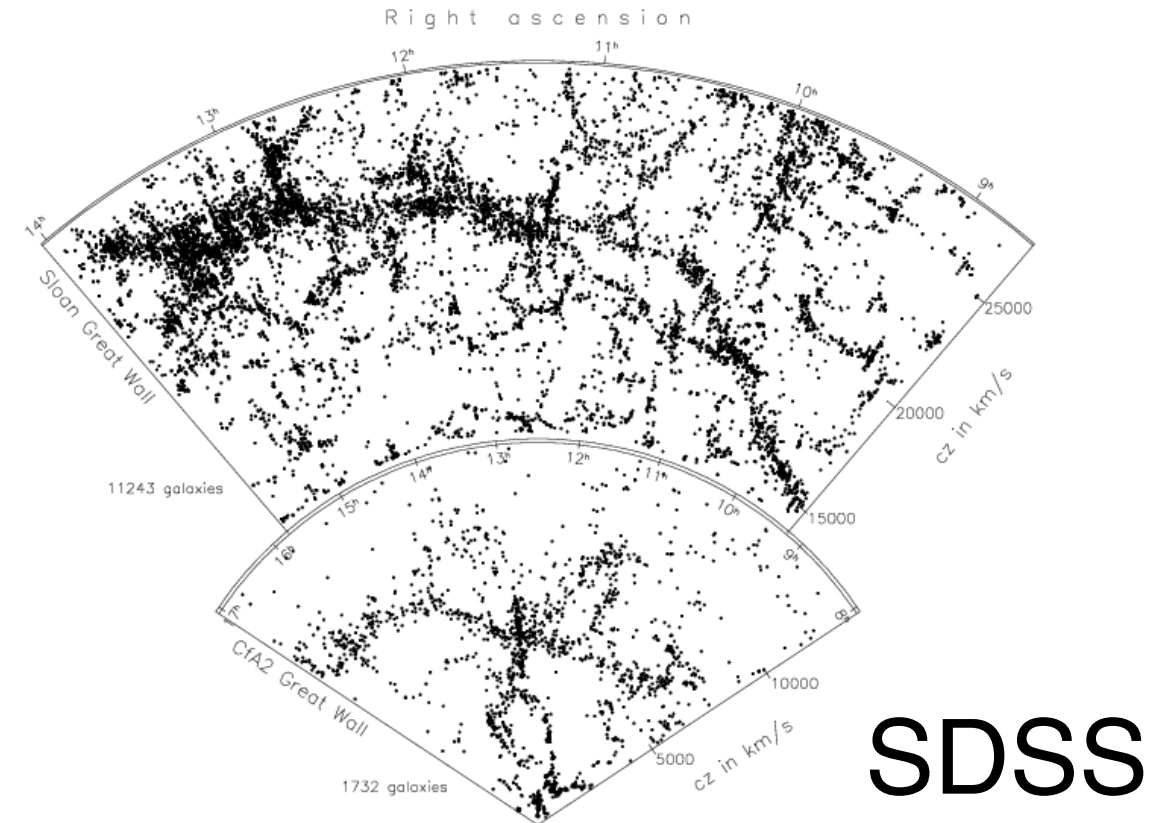
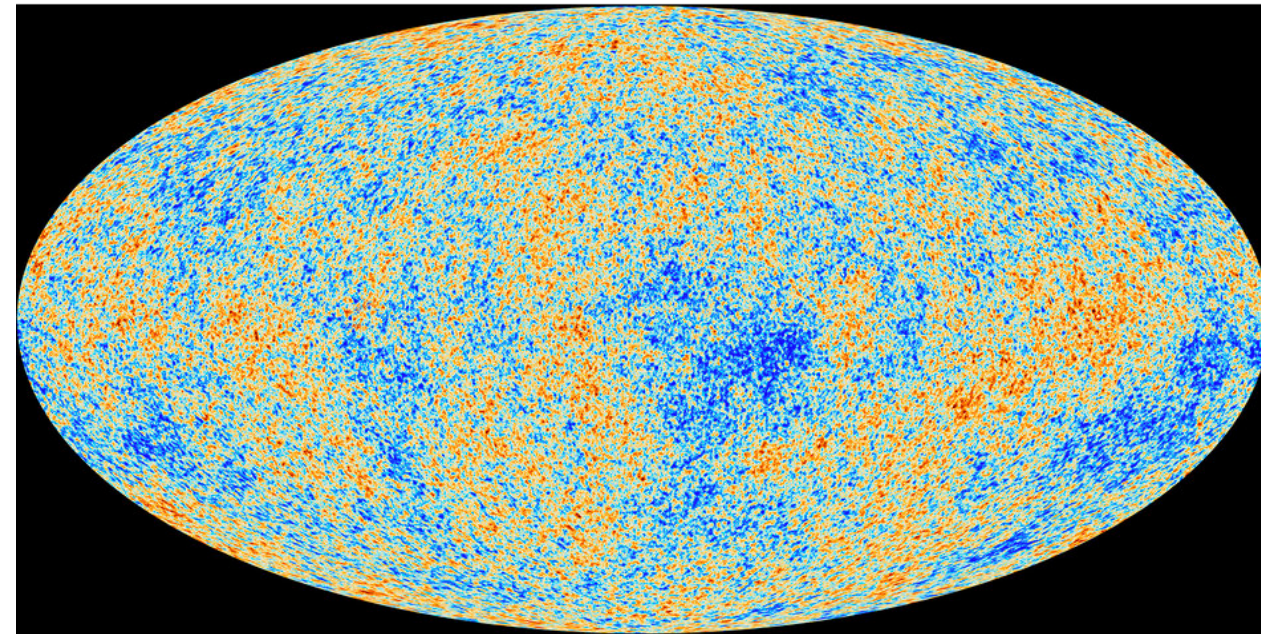


# Structure in the Universe

*Universe, 380,000 year old  
Gaussian random Field*

**At present (13.7 billion year old)  
Highly non-Gaussian**

Below is the image in its original context on the page: [www.astro.princeton.edu/~mjuric/universe/](http://www.astro.princeton.edu/~mjuric/universe/)



Plank map

Temperature fluctuations of Cosmic Microwave Background

$T=2.73$  K

(fluctuations:

of the order of  $1/100,000$ )

Galaxy distribution in a thin slice

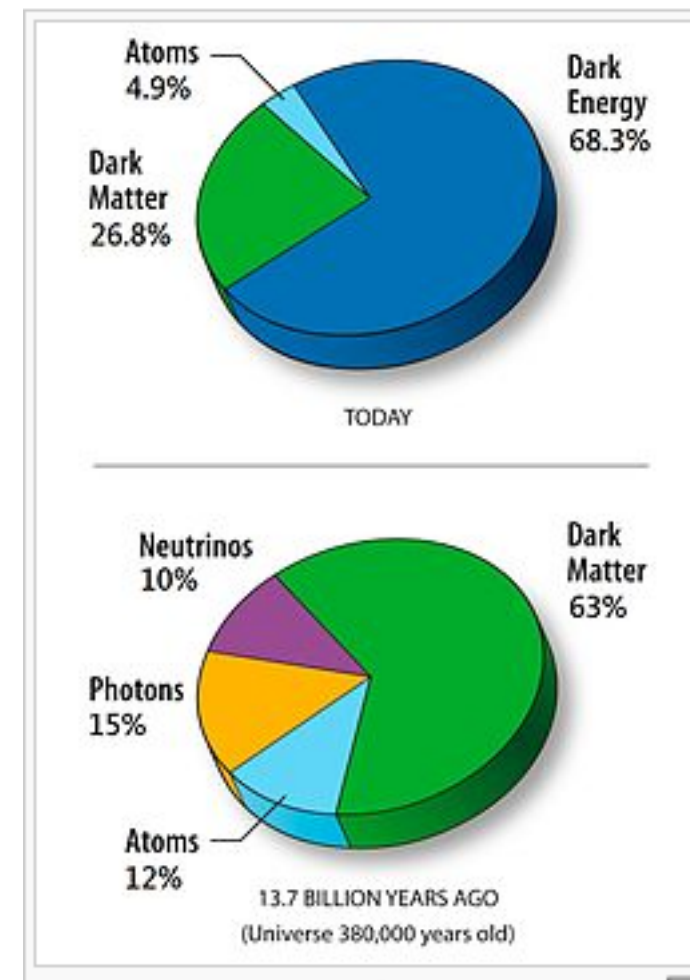
# Why did inhomogeneities grow?

- Thanks to gravitational instability of Dark Matter

Why only Dark matter?

more mass - stronger gravity

NOW



*13.7 billion years ago*

Atoms **alone** could NOT develop structures because they were unable to overcome the expansion of the universe!

That's why we focus on the growth of structure in Dark Matter.

# Cosmological parameters (Planck 2015)

Calculated values	Hubble constant	0.7%	$H_0$	$67.74 \pm 0.46 \text{ km s}^{-1} \text{ Mpc}^{-1}$
	Baryon density parameter <sup>[b]</sup>	2%	$\Omega_b$	$0.0486 \pm 0.0010^{[e]}$
	Dark matter density parameter <sup>[b]</sup>	2.2%	$\Omega_c$	$0.2589 \pm 0.0057^{[f]}$
	Matter density parameter <sup>[b]</sup>	2%	$\Omega_m$	$0.3089 \pm 0.0062$
	Dark energy density parameter <sup>[b]</sup>	0.9%	$\Omega_\Lambda$	$0.6911 \pm 0.0062$
	Critical density	1.4%	$\rho_{\text{crit}}$	$(8.62 \pm 0.12) \times 10^{-27} \text{ kg/m}^3^{[g]}$
	Fluctuation amplitude at $8h^{-1} \text{ Mpc}$	1%	$\sigma_8$	$0.8159 \pm 0.0086$
	Redshift at decoupling		$z_*$	$1\,089.90 \pm 0.23$
	Age at decoupling		$t_*$	$377\,700 \pm 3200 \text{ years}^{[16]}$
	Redshift of reionization (with uniform prior)		$z_{\text{re}}$	$8.5^{+1.0}_{-1.1}^{[17]}$

## Linear growth of density inhomogeneities:

- *linearized equations  $\Rightarrow$  analytic solution*
- *amplitude grows but shapes do not change (Gaussian)*
- *density contrast:  $(den - \langle den \rangle) / \langle den \rangle \ll 1$*

## Nonlinear evolution

- *non-linear equations  $\Rightarrow$  approximations and numerical*
- *both geometry and topology evolve dramatically (non G)*
- *density contrast:  $(den - \langle den \rangle) / \langle den \rangle \gg 1$*

# Outline of the talk

- Brief cosmological introduction
- Beginning of the dark matter web story
  - **The Zeldovich approximation**
  - Geometrical and topological challenges
  - Web of galaxies
- Dark matter web
  - Flip-flop field as a record of halo merging
  - Multi stream field
  - A comparison project “Tracing the Cosmic Web”
  - Caustics
- Summary

# Gravitational Instability

Usually the growth of density perturbations is described in the comoving coordinates

$$\mathbf{x} \equiv \frac{1}{a(t)} \mathbf{r}$$

and in terms of peculiar velocity

$$\mathbf{v}_p \equiv \mathbf{v} - H(t)\mathbf{r},$$

where  $a(t)$  is the scale factor describing the uniform expansion of the universe and  $H(t) \equiv \dot{a}/a$  is the Hubble parameter.

$$\Omega = 1; \quad a(t) \propto t^{2/3}$$

# Rescaling Variables

$$\eta \equiv a^3 \rho$$

$$\mathbf{v} \equiv (a\dot{D})^{-1} \mathbf{v}_p = \dot{D}^{-1} \frac{d\mathbf{x}}{dt} = \frac{d\mathbf{x}}{dD}$$

$$\varphi \equiv \left( \frac{3}{2} \Omega_0 \dot{a}^2 D \right)^{-1} \phi$$

Significantly simplifies the equations

(1) continuity or conservation of mass  $\frac{\partial \eta}{\partial D} + \nabla_x \cdot (\eta \mathbf{v}) = 0,$

(2) Euler equation,  $\frac{\partial \mathbf{v}}{\partial D} + (\mathbf{v} \cdot \nabla_x) \mathbf{v} = -\frac{3}{2} \frac{\Omega_0}{D f^2} (\nabla_x \varphi + \mathbf{v}),$   
*=0 in linear regime*

(3) Poisson  $\nabla_x^2 \varphi = \frac{\delta}{D}$

where  $D = D(t)$  is a monotonically growing function of time,  
 $\Omega_0 \approx 0.27$  is the dimensionless mean density of matter in the universe at present,  
 $f(t) = d \ln D / d \ln a$ , and  $\delta = (\eta - \bar{\eta}) / \bar{\eta} = (\rho - \bar{\rho}) / \bar{\rho}$ .

$$\Omega = 1; \quad D(t) = a(t); \quad f = 1$$

**Gravitational Instability:  
An Approximate Theory for Large Density Perturbations**

YA. B. ZELDOVICH

Institute of Applied Mathematics, Moscow

Received September 19, 1969

# Zel'dovich approximation (1970)

Comoving coordinates:  $\mathbf{x}_i$ ,

Zel'dovich approximation is a map:  $\mathbf{x}_i(\mathbf{q}, t) = q_i + D(t)s_i(\mathbf{q})$

If  $\Phi(\mathbf{q})$  is the linear perturbation of grav. potential then  $s_i(\mathbf{q}) = -\partial\Phi/\partial q_i$

Density can be found from the conservation of mass

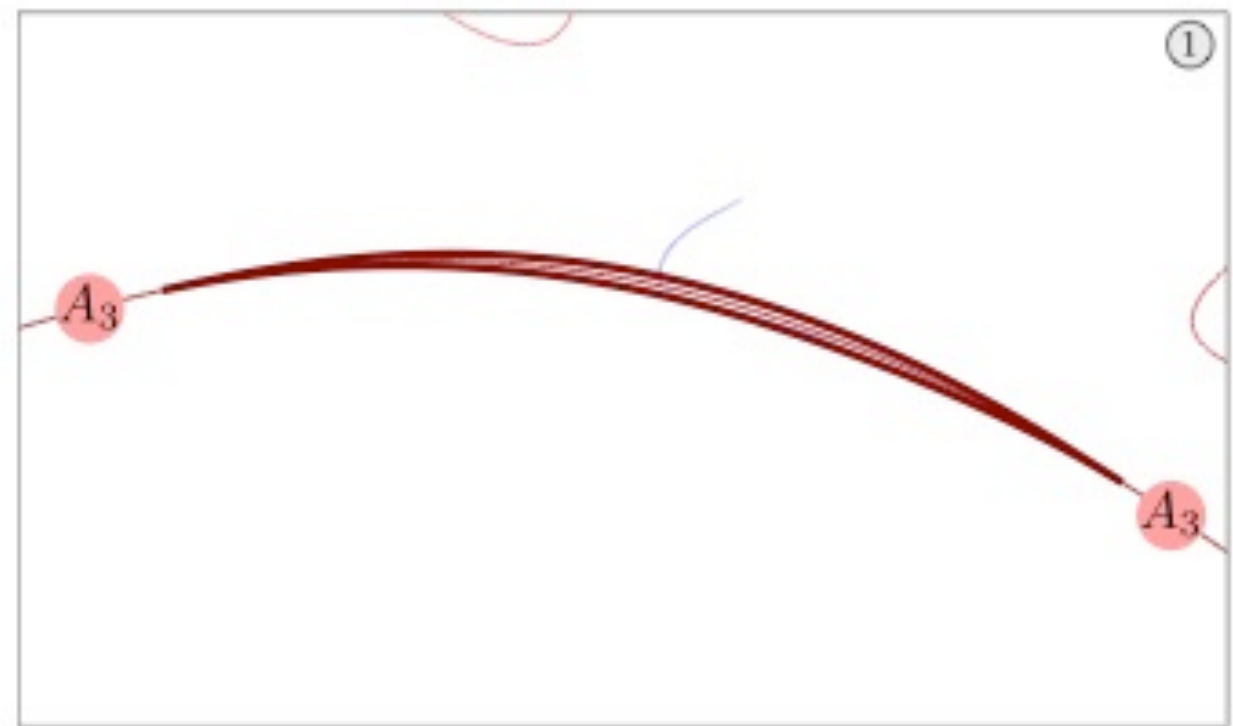
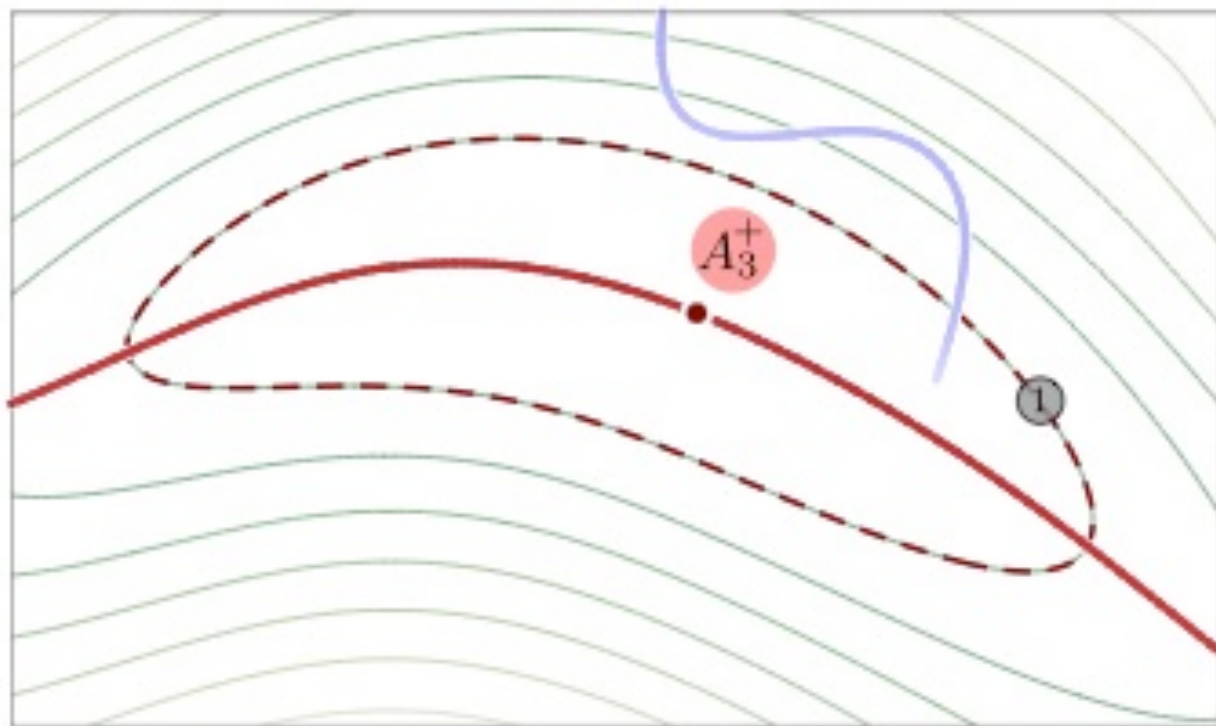
$$\rho(\mathbf{q}, t) = \bar{\rho}(t) \left| \frac{\partial r_i}{\partial q_k} \right|^{-1} = \bar{\rho} \left[ (1 - D(t)\alpha(\mathbf{q}))^{-1} [(1 - D(t)\beta(\mathbf{q}))^{-1} [(1 - D(t)\gamma(\mathbf{q}))^{-1} \right]$$

$\alpha(\mathbf{q}) \geq \beta(\mathbf{q})$  and  $\beta(\mathbf{q}) \geq \gamma(\mathbf{q})$  are the eigen values of the deformation tensor

$$d_{ik}(\mathbf{q}) = \frac{\partial s_i}{\partial q_k} = -\frac{\partial^2 \Phi}{\partial q_i \partial q_k}$$

Linear density fluctuations:  $\delta\rho/\rho = D(t)(\alpha + \beta + \gamma)$ .

The Zel'dovich approximation describes anisotropic collapse and motion.



Hidding, Shandarin, van de Weygaert 2014

Assumptions are not realistic, approximation is kinematic,  
pancakes are unstable therefore no observable traces

# Lagrangian Submanifold (LS) is N-dim surface in 2N-dim space

Zel'dovich 1970

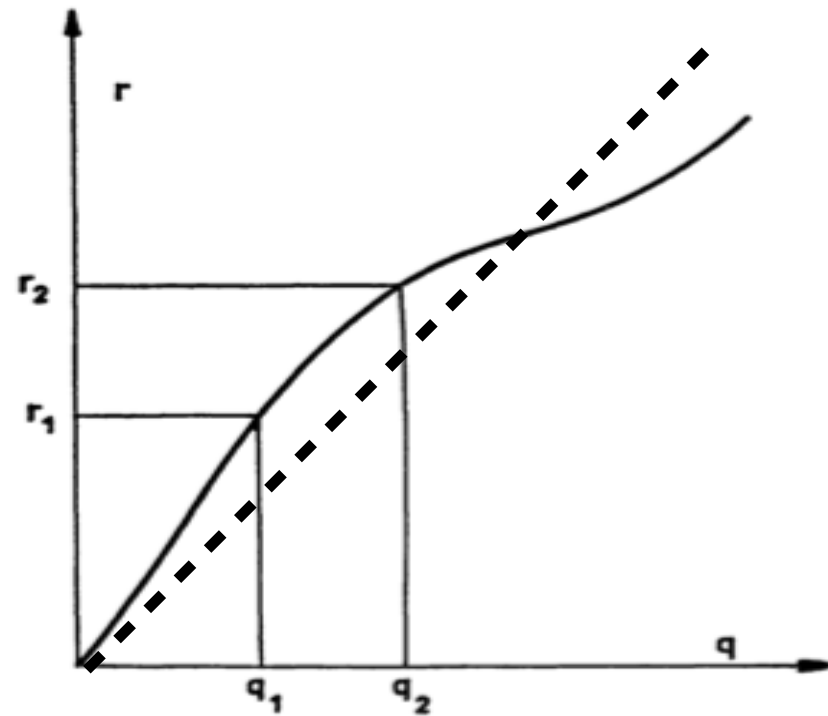
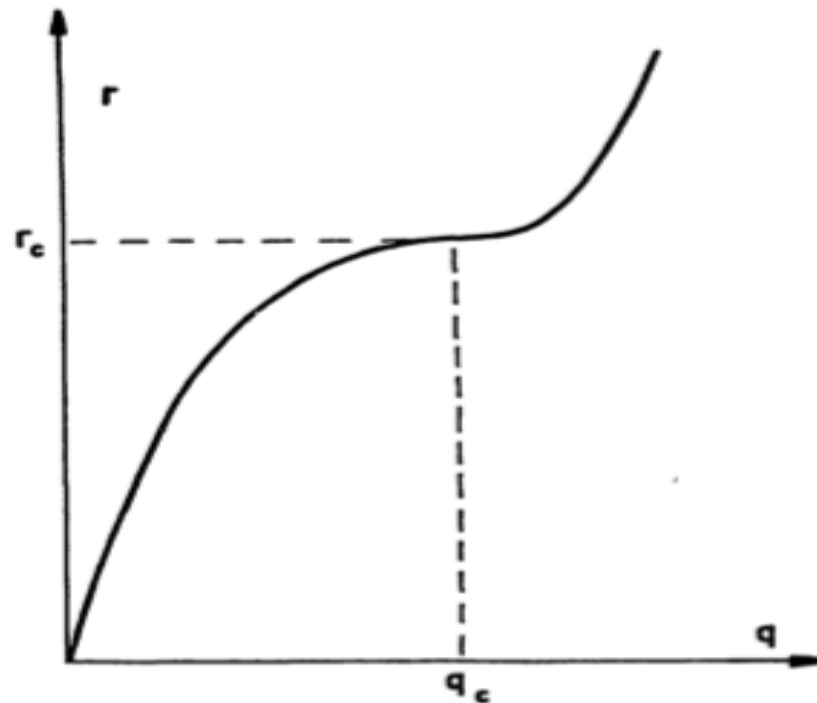
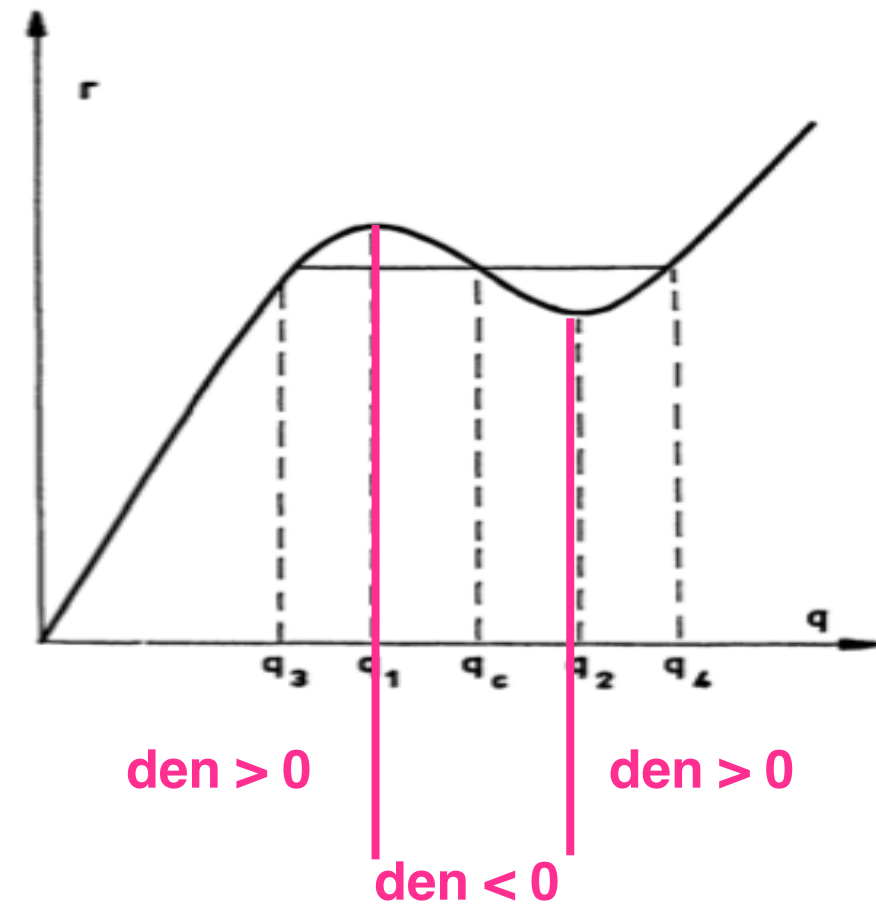


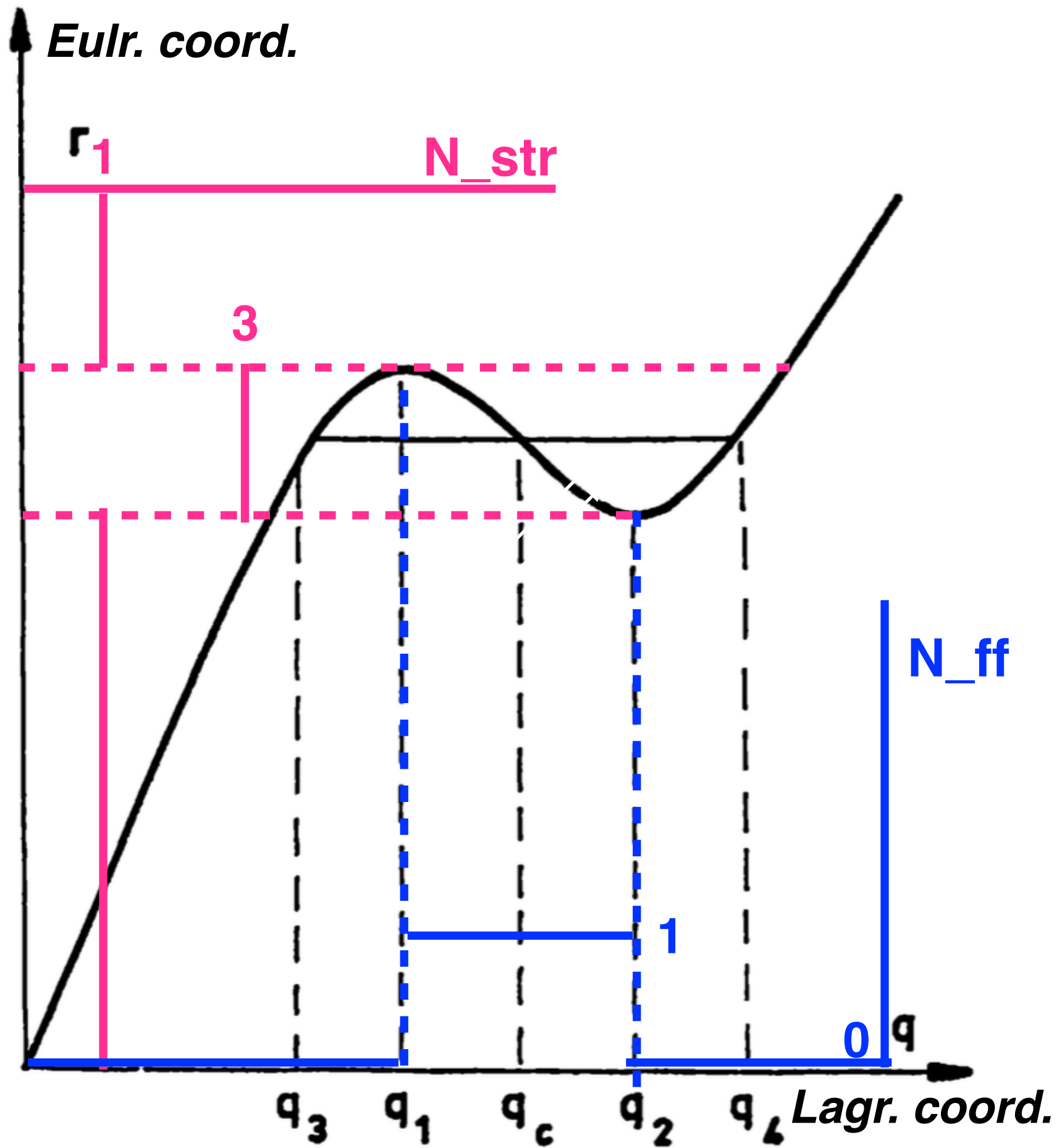
Fig. 1



The Evaluation of Density:  
density =  $(q[i+1]-q[i]) / (r[i+1] - r[i])$

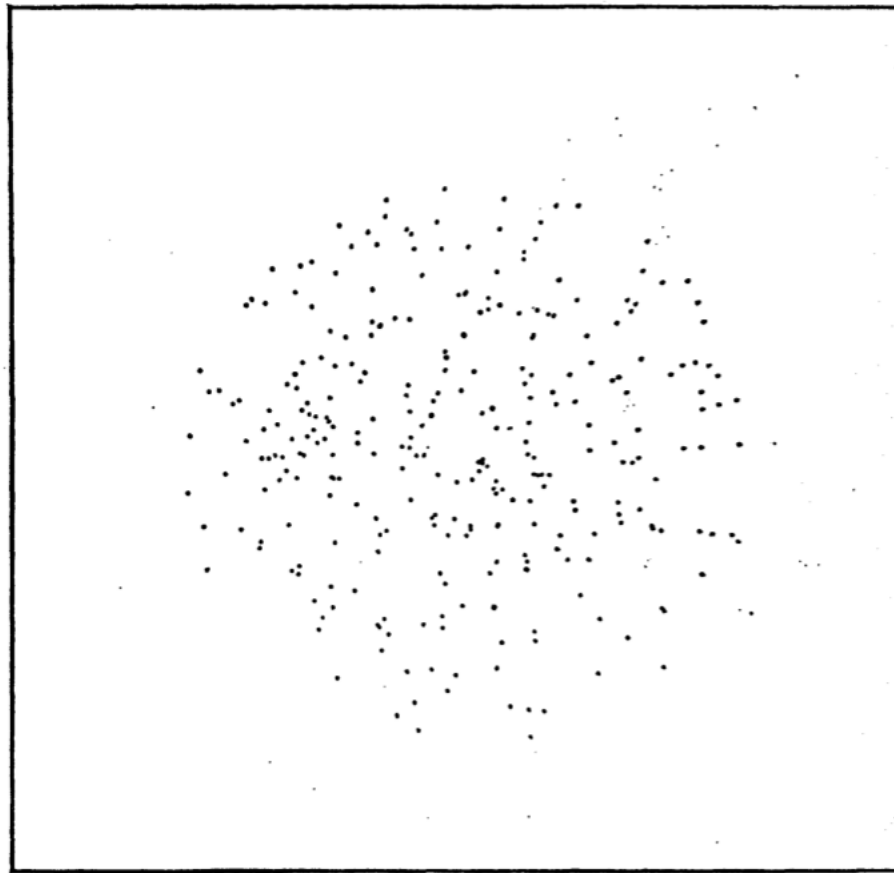


# Number of streams and number of flip-flops

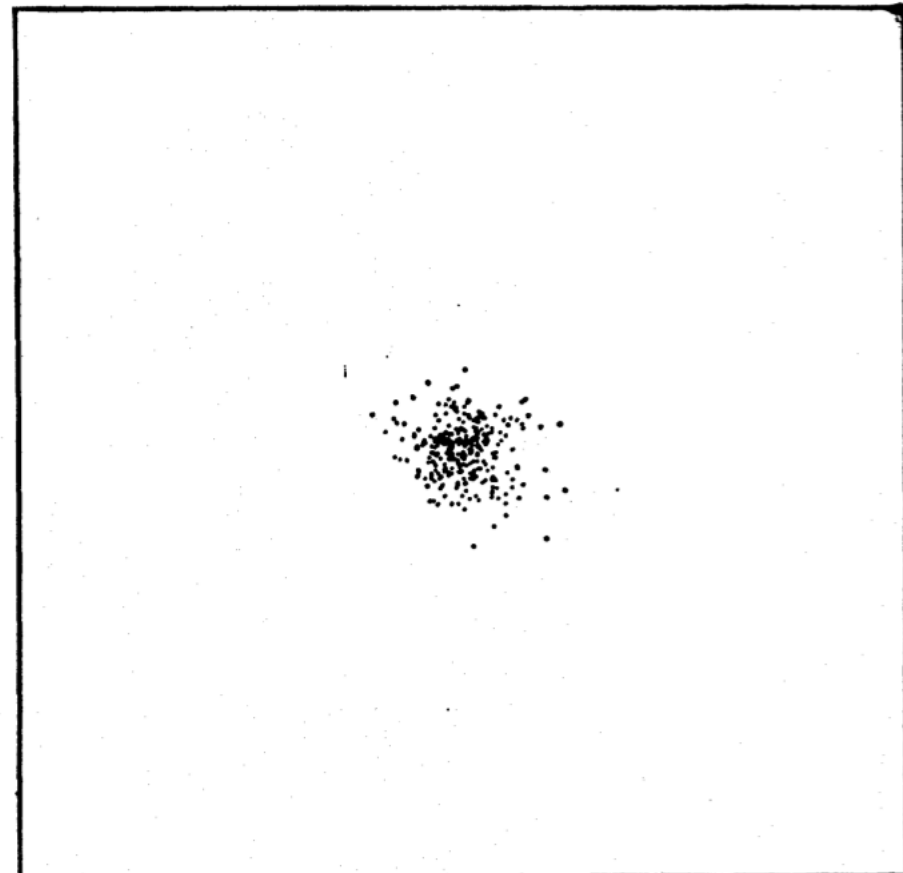


# Outline of the talk

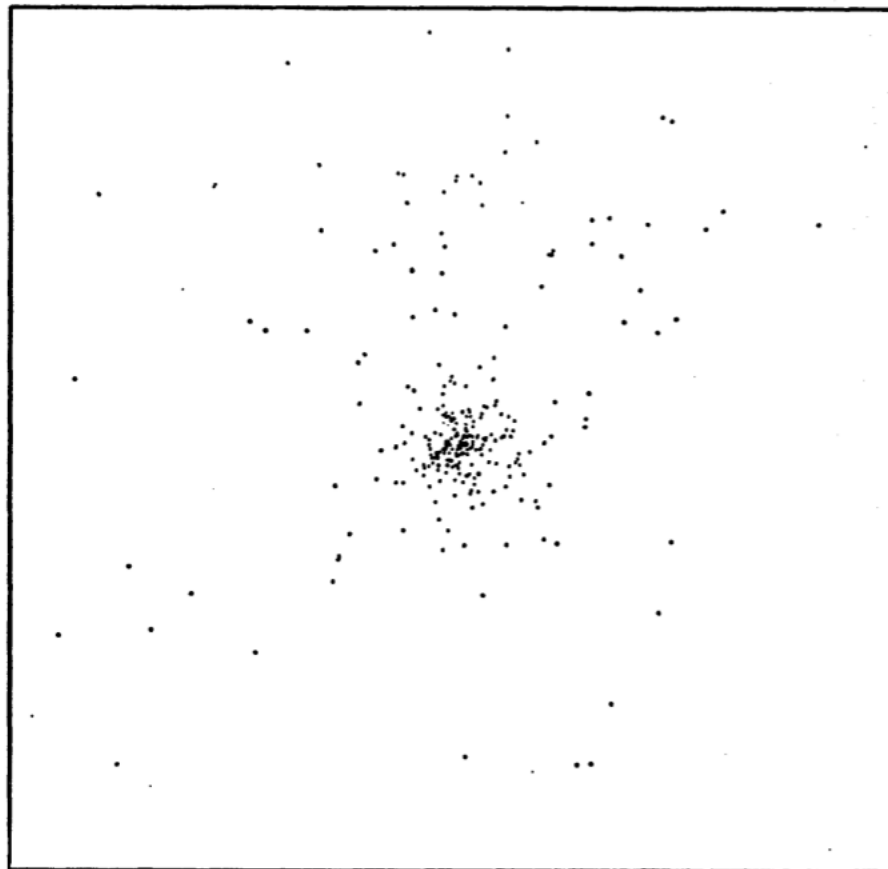
- Brief cosmological introduction
- Beginning of the dark matter web story
  - The Zeldovich approximation
  - Geometrical and topological challenges
  - Web of galaxies
- Dark matter web
  - Flip-flop field as a record of halo merging
  - Multi stream field
  - A comparison project “Tracing the Cosmic Web”
  - Caustics
- Summary



(a)



(b)



(c)

FIG. 1. Model 1 positions: (a) initial positions,  $t=2.8$  b.y.;  
(b)  $t=5.6$  b.y.; and (c)  $t=8.4$  b.y.

# State of art *N*-body simulations

*Clustering of particles in an expanding Universe*

511

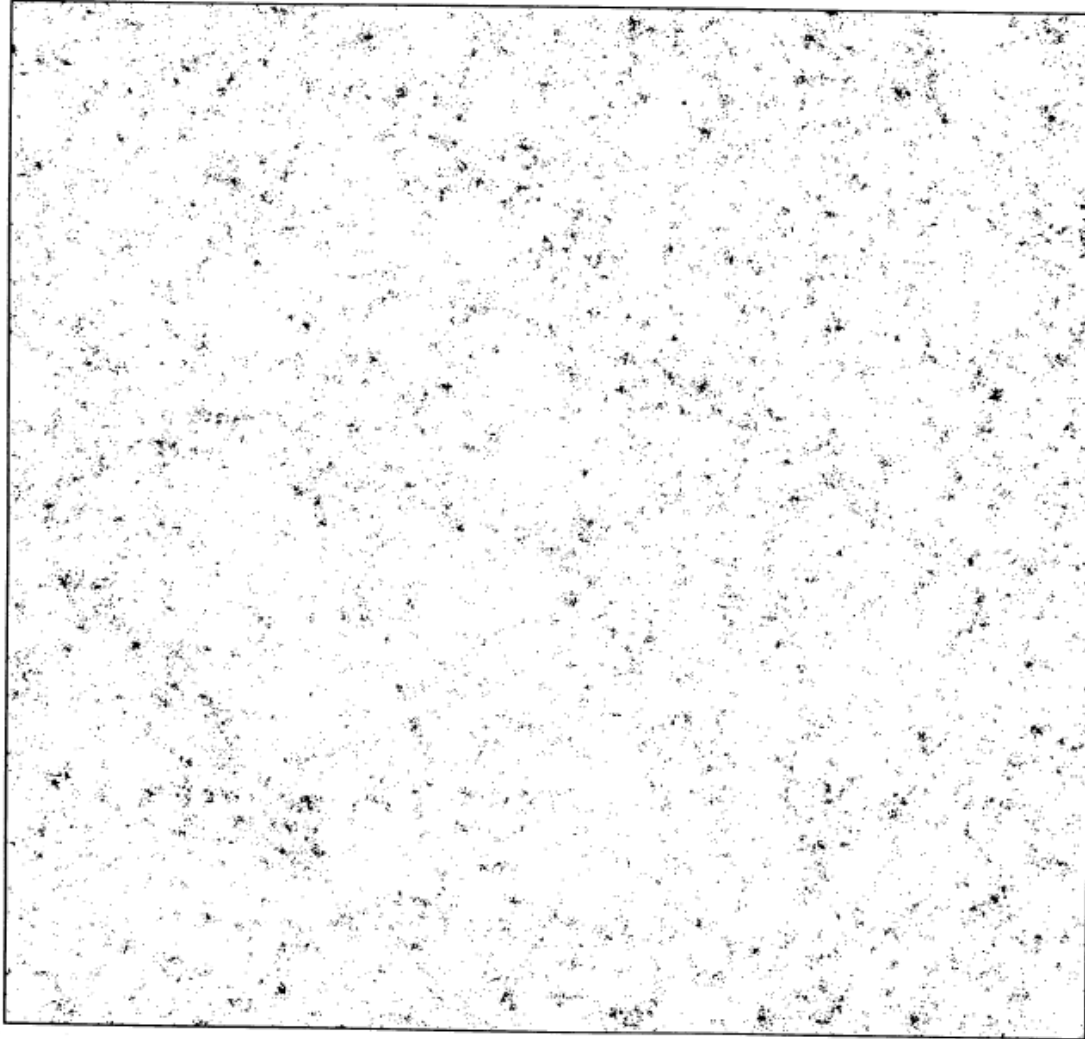


Figure 1. *X*–*Y* projection of the particle positions for a 20 000-body numerical experiment after the system has expanded by a factor of 9.9. In this case the expansion follows that of an Einstein–de Sitter model,  $\Omega_0 = 1.0$ .

**1981** Efstathiou, Eastwood,  
MNRAS, 194, 503

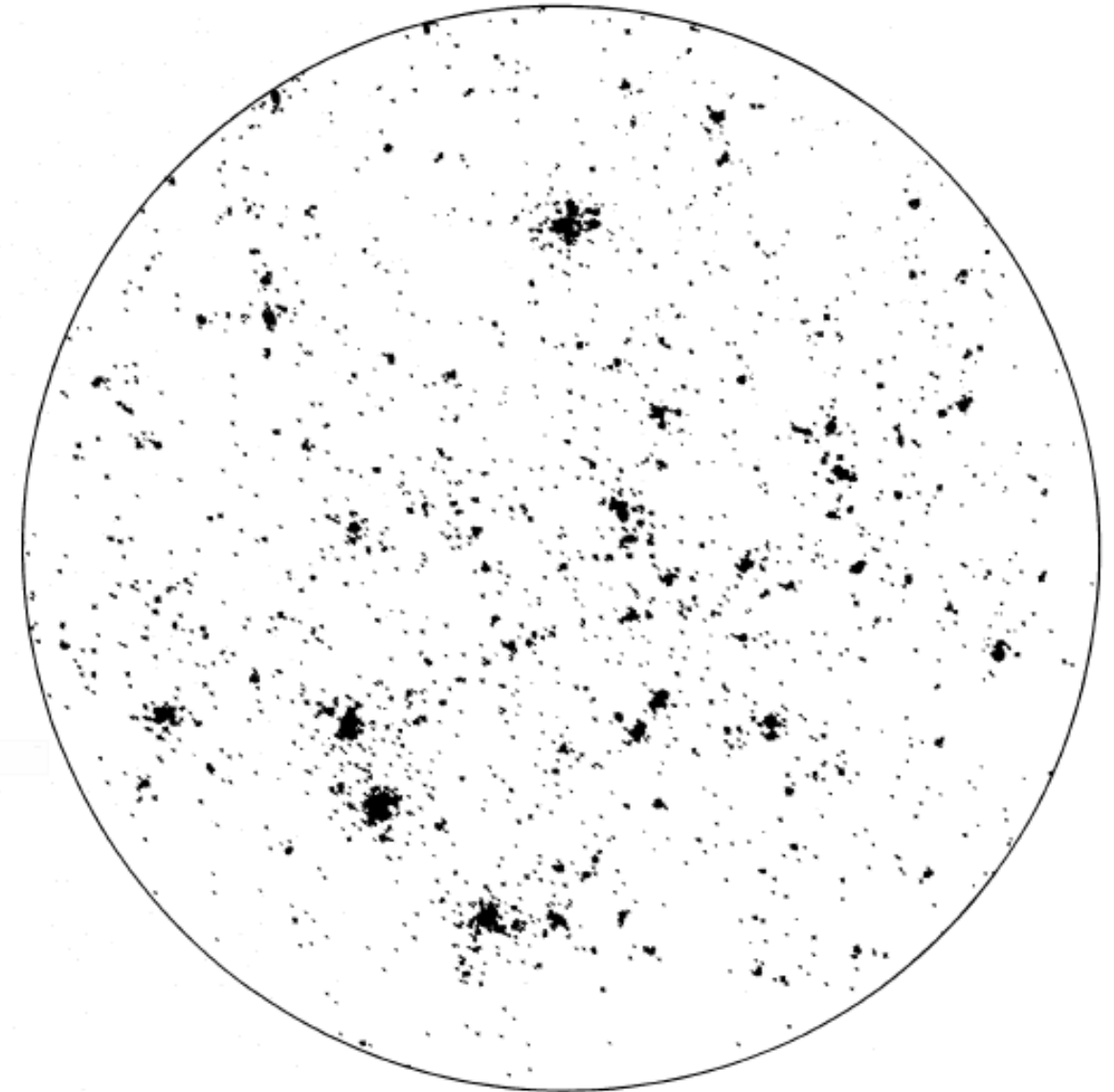
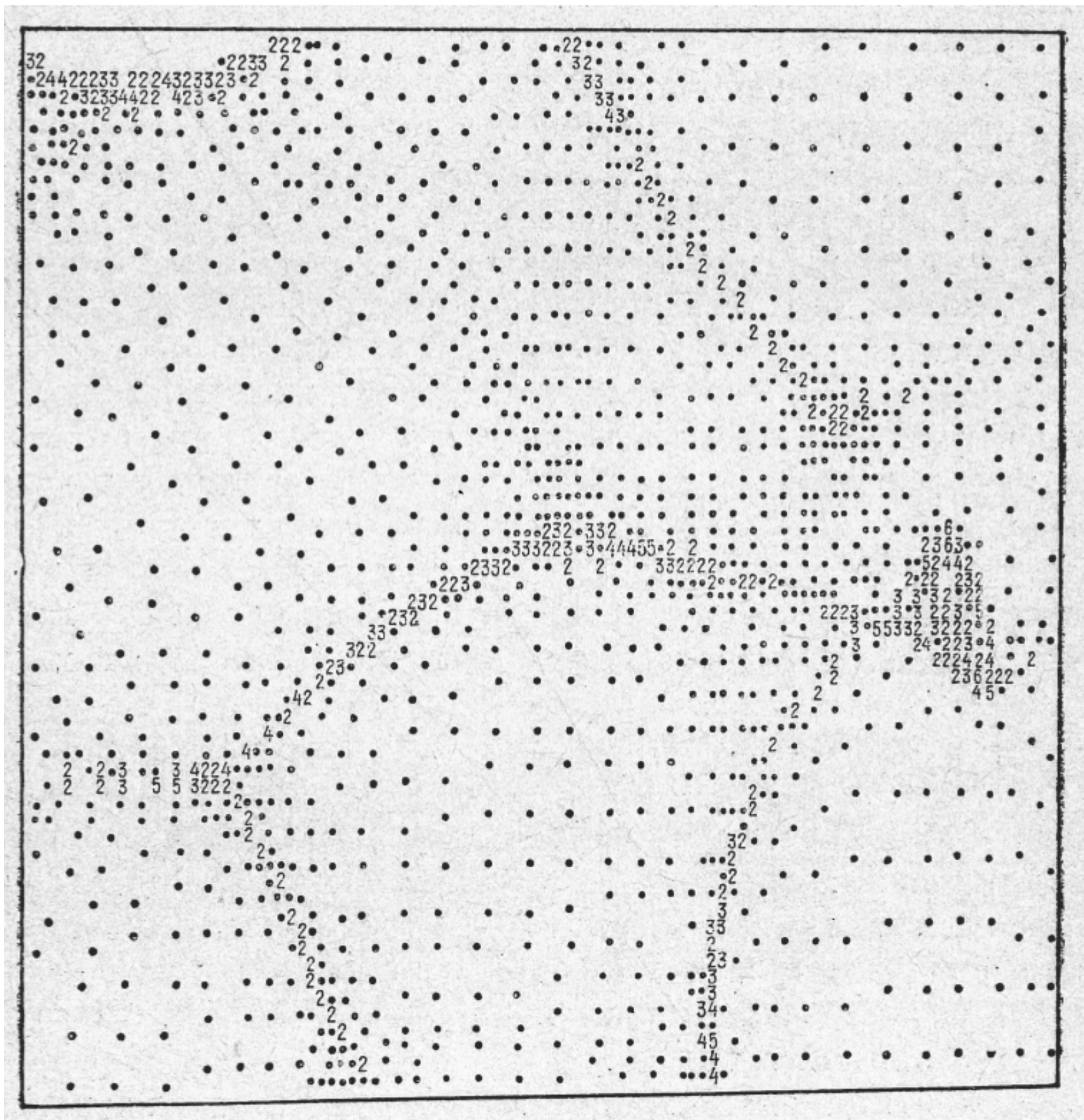


Fig. 1f

**1979** Aarseth, Gott, Turnet,  
Astrophys. J. 228, 644



**Structure predicted  
by “Zeldovich  
Approximation” aka  
“Pancake model”**

**Published in  
a review paper by  
Doroshkevich,  
Zeldovich,  
Sunyaev 1976  
(only in Russian)**

**Caption says:  
“the figure is made  
by S. Shandarin”**

**and also by  
Doroshkevich and  
Shandarin, 1978  
Sov.Astron. 22(6), 653**

# Shandarin in

The Origin and Evolution of Galaxies:  
Proceedings of the  
NATO Advanced Study Institute  
held at Erice, Italy, May 11–23, 1981.  
VII-th Course of the ... and Gravitation

(Nato Science Series C:) Hardcover – December 31, 1982  
page 171

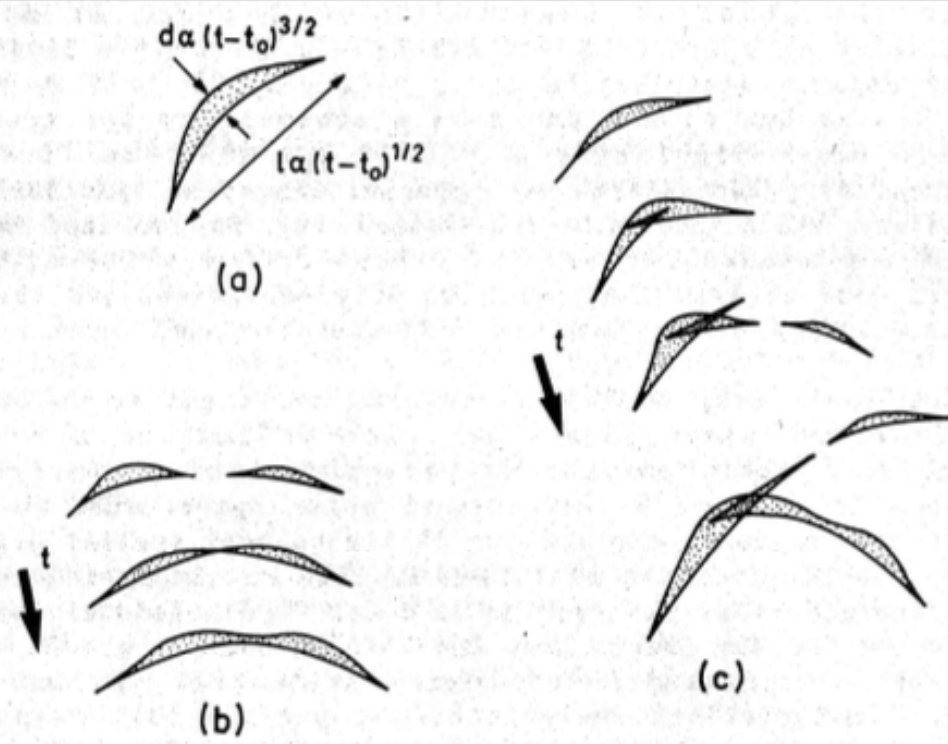


Figure 1. Examples of the general patterns arising in two-dimensional models. The dark regions are regions of three streams flows. a) 'pancake', b) and c) two types of merging of pancakes. Solid lines are caustics - lines of infinite density.

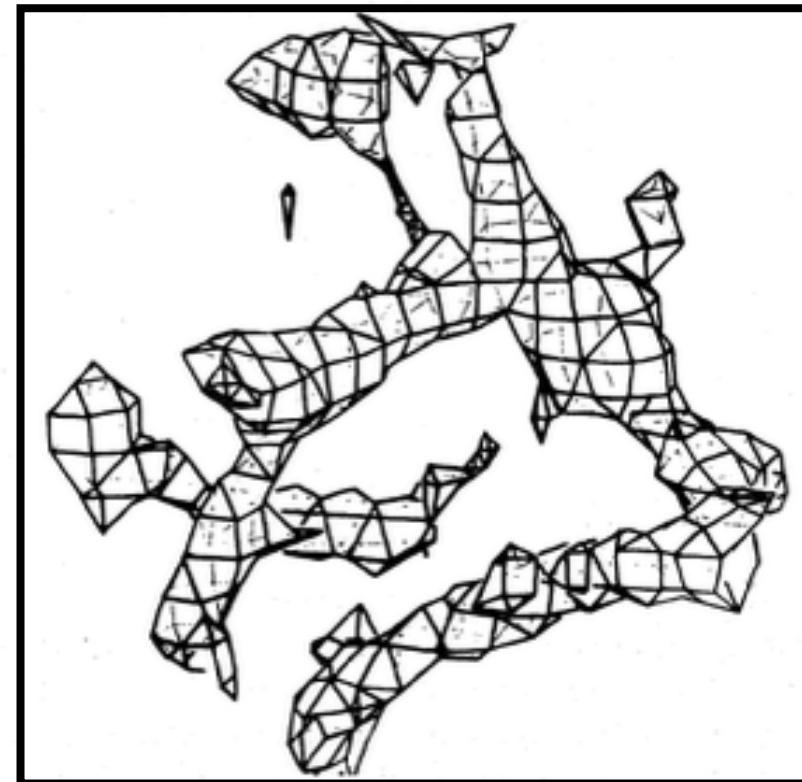


Figure 3. An example of the structures arising in 3D numerical simulations of the adiabatic scenario. The surface is a surface of constant density  $\rho \sim 2.5 \rho_0$ .

# State of art N-body simulations

**1981** Efstathiou, Eastwood, **MNRAS, 194, 503**

*Clustering of particles in an expanding Universe*

511

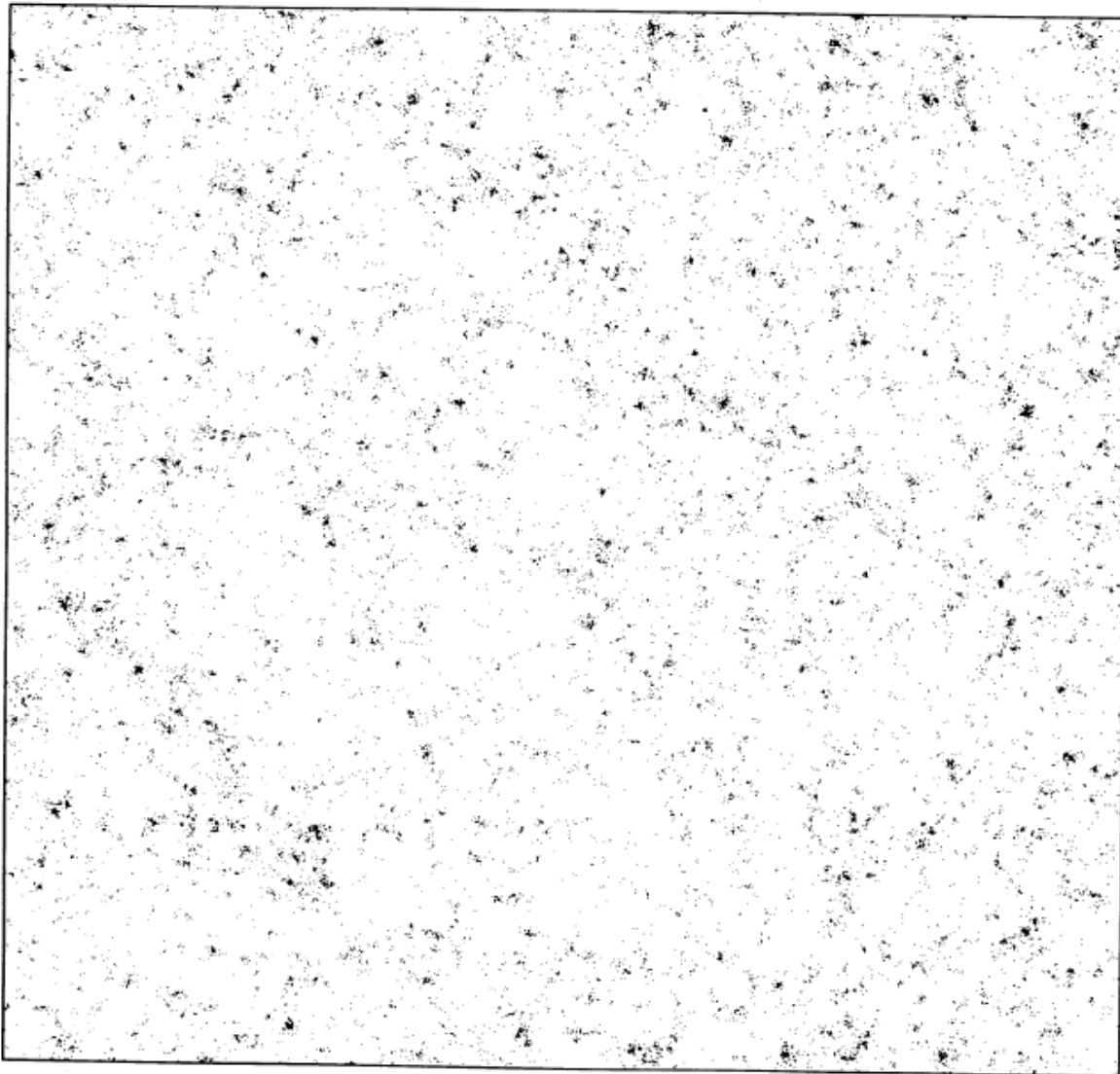


Figure 1.  $X$ - $Y$  projection of the particle positions for a 20 000-body numerical experiment after the system has expanded by a factor of 9.9. In this case the expansion follows that of an Einstein-de Sitter model,  $\Omega_0 = 1.0$ .

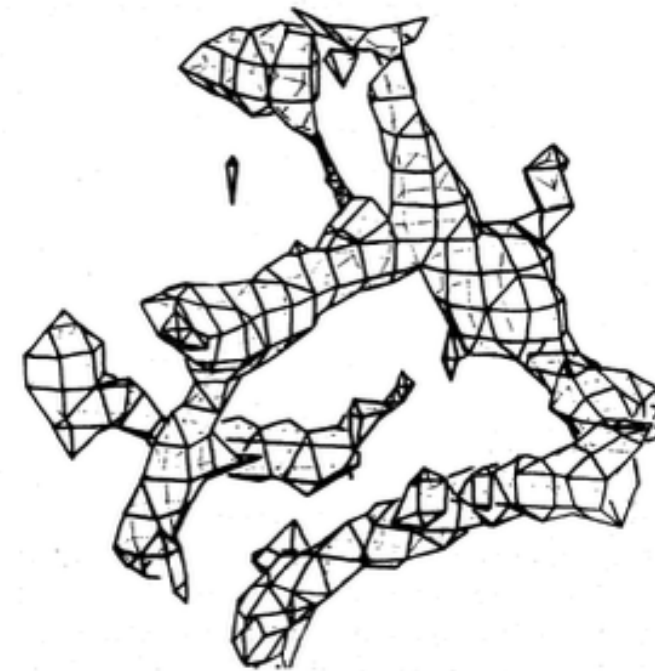


Figure 3. An example of the structures arising in 3D numerical simulations of the adiabatic scenario. The surface is a surface of constant density  $\rho \sim 2.5 \rho_0$ .

# Outline of the talk

- Brief cosmological introduction
- Beginning of the dark matter web story
  - The Zeldovich approximation
  - Geometrical and topological challenges
  - **Web of galaxies**
- Dark matter web
  - Flip-flop field as a record of halo merging
  - Multi stream field
  - A comparison project “Tracing the Cosmic Web”
  - Caustics
- Summary

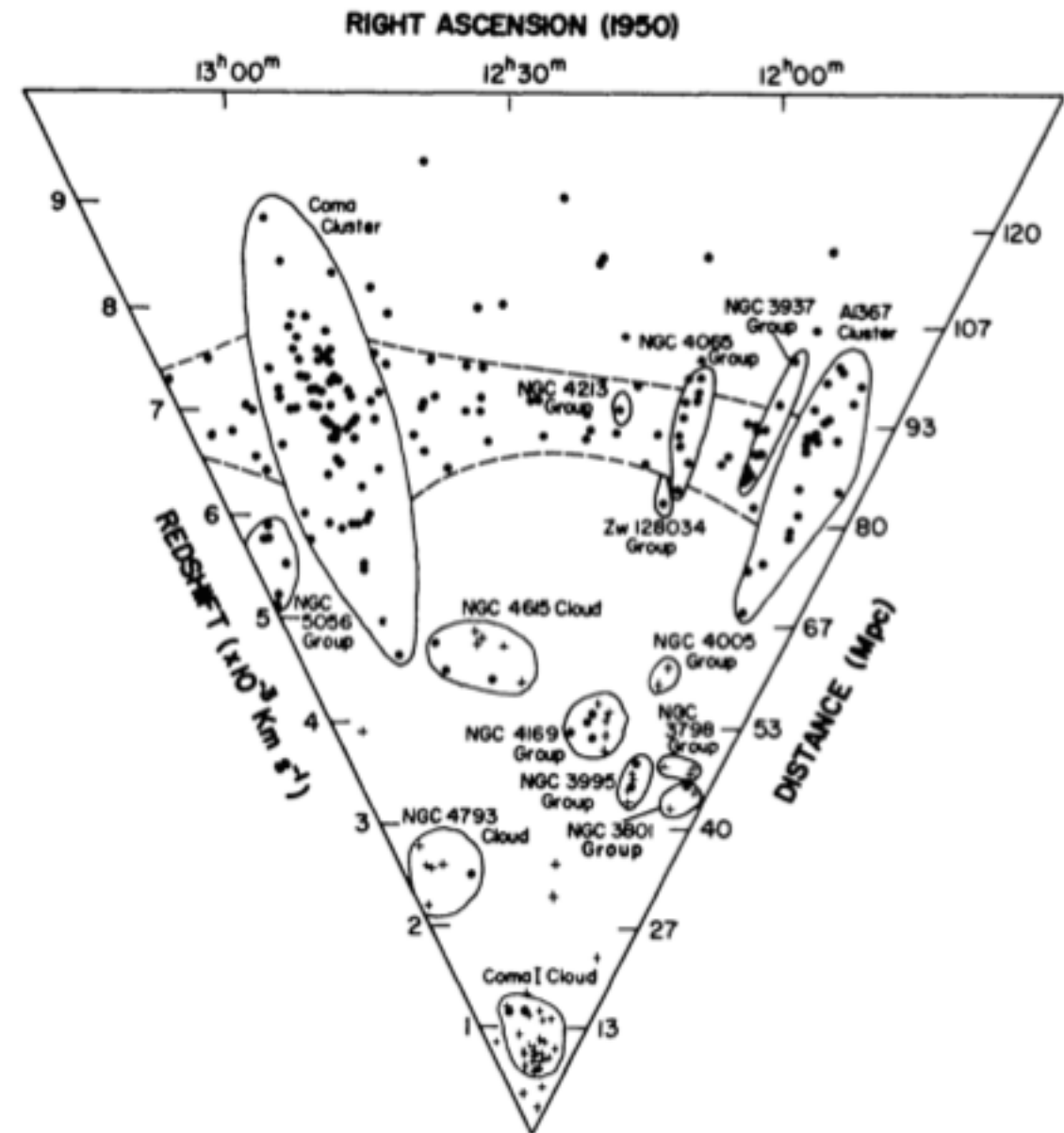
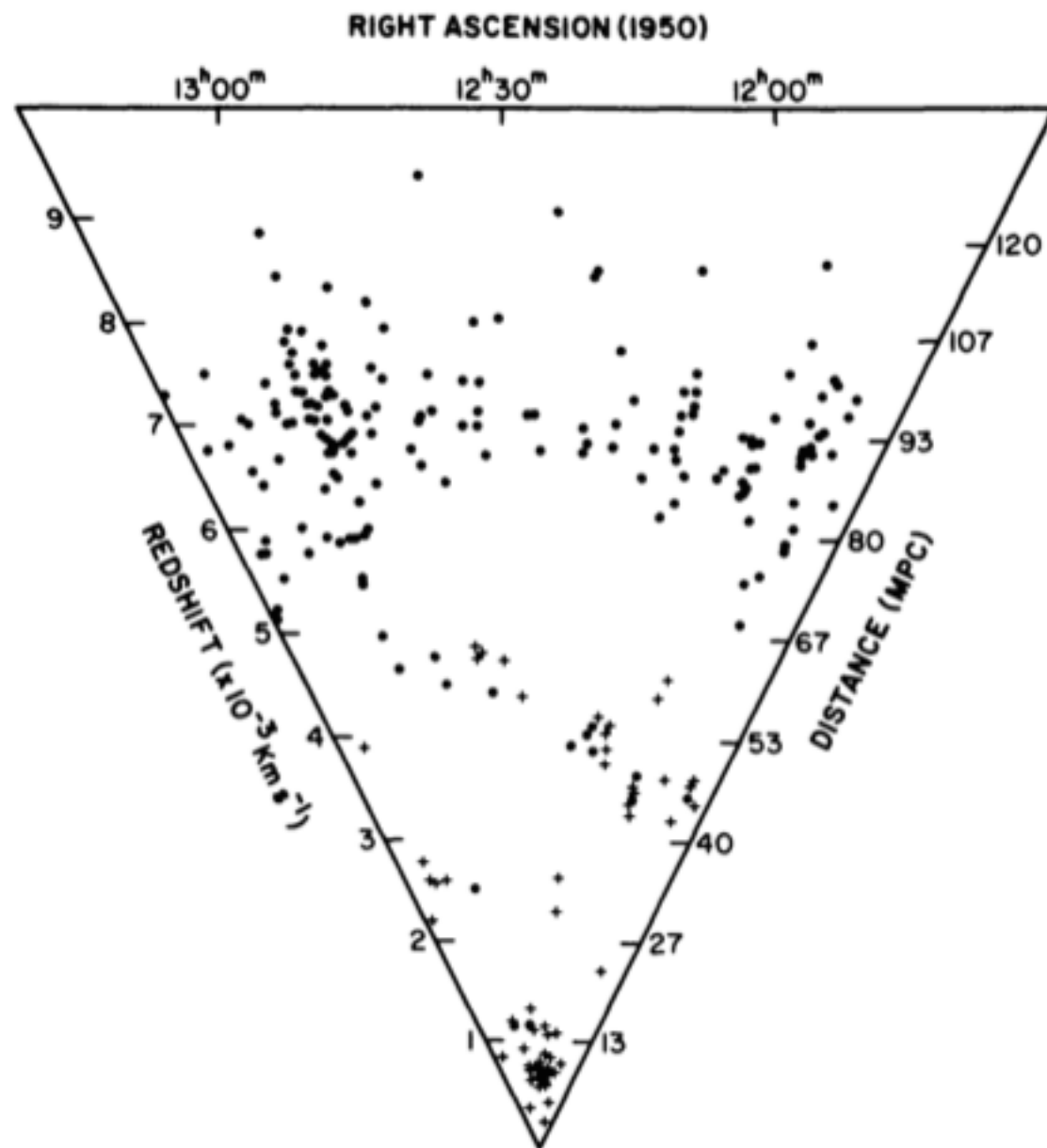
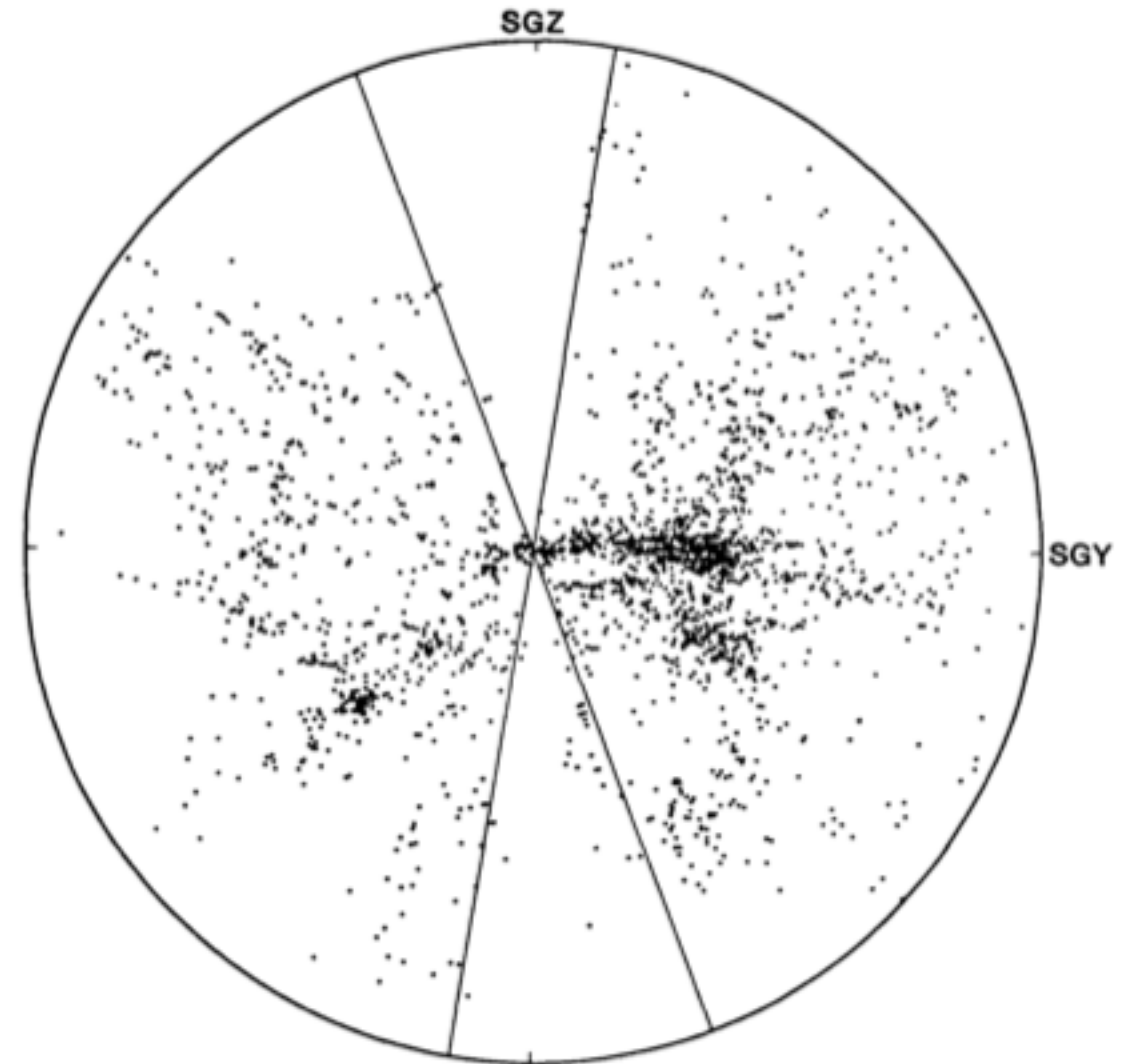


Figure 12 “Wedge diagram” of the Coma supercluster [Gregory & Thompson (40)]. As the supercluster is elongated in the east-west direction, right ascensions have been chosen as position coordinates; the galaxies lie between  $+19^\circ$  and  $+32^\circ$  declination. The angular size has been magnified about two times compared with the indicated distance scale.

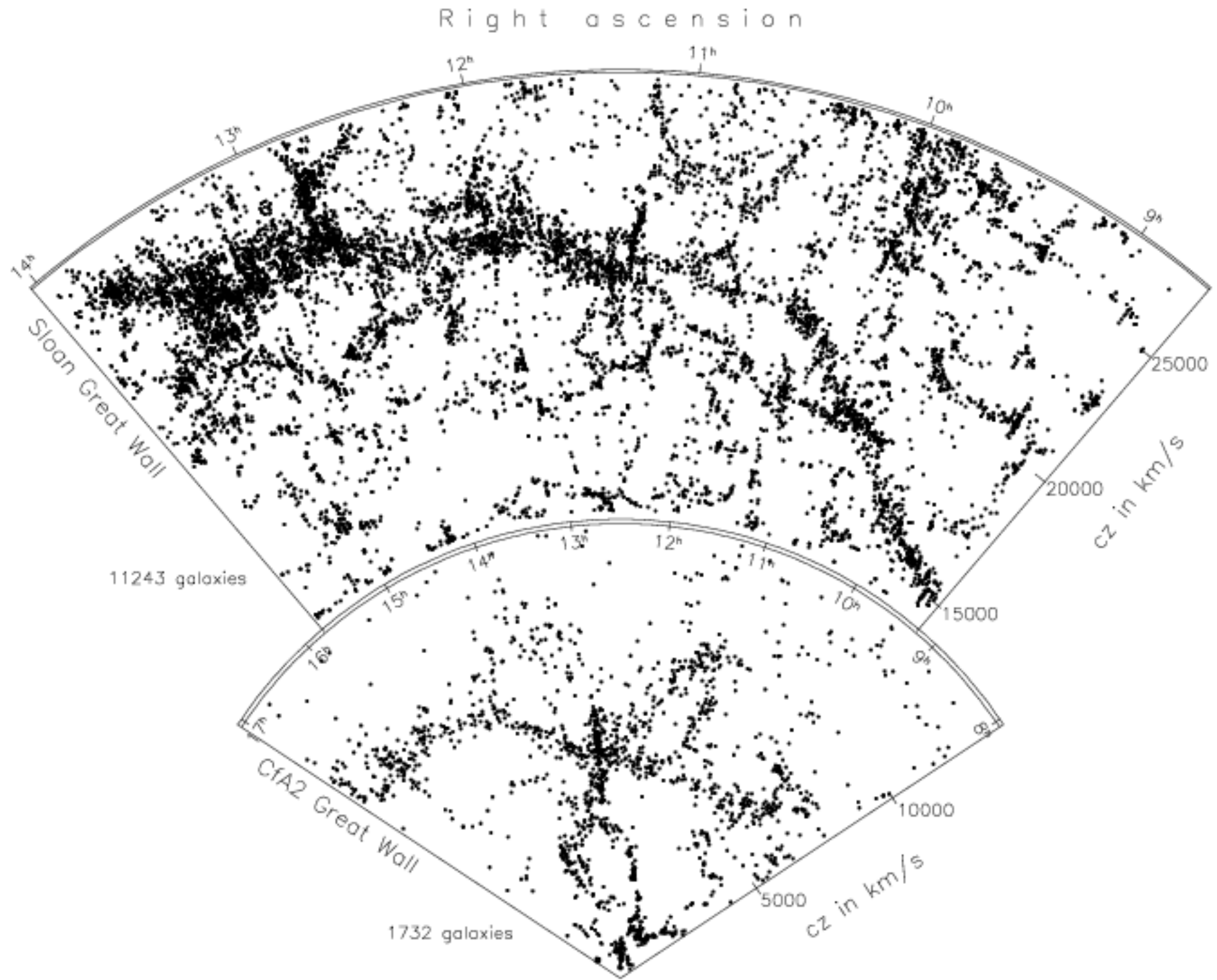
Gregory & Thompson 1978  
 see also Chincarini & Rood 1976

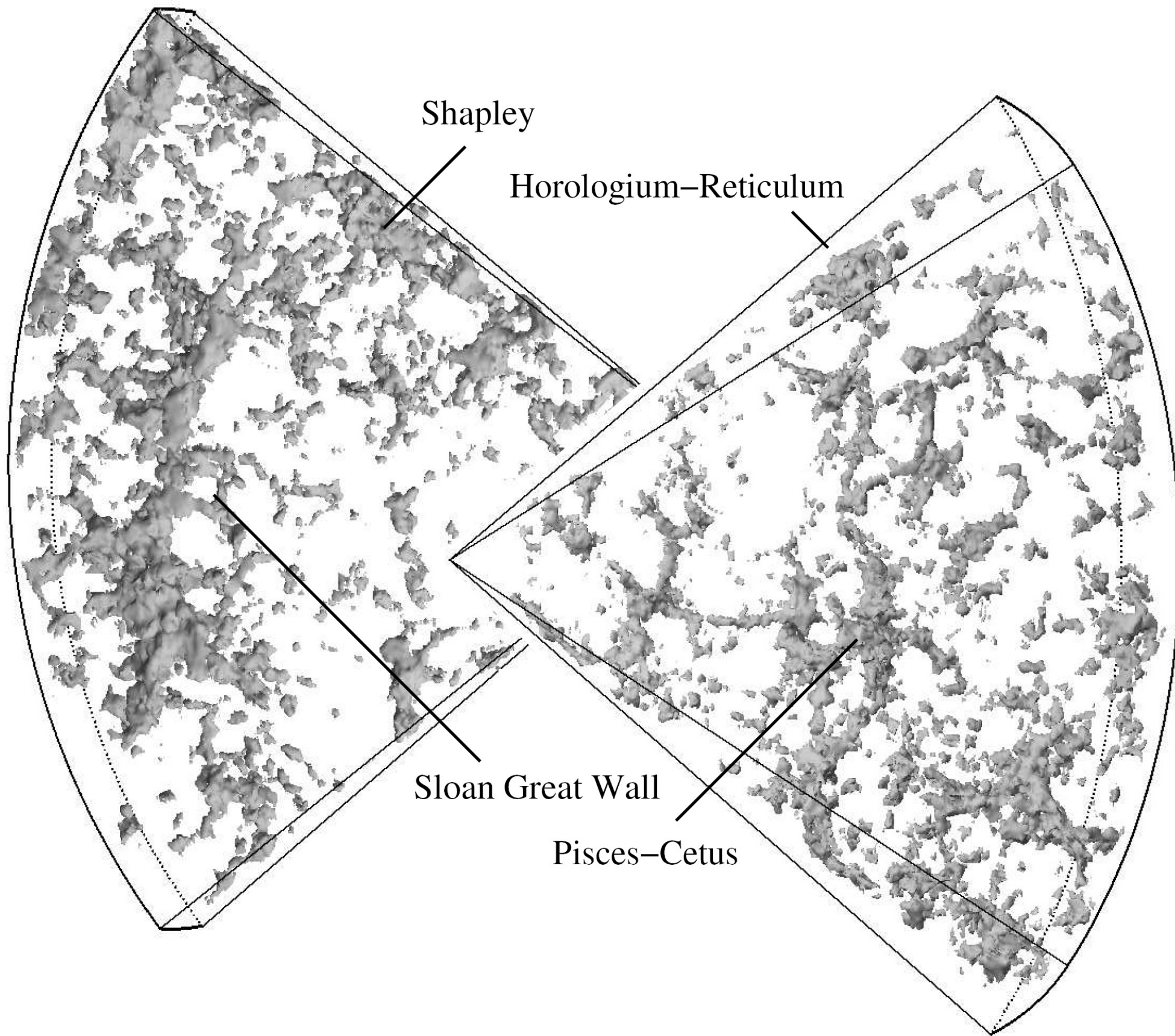


**Figure 2.** Distribution of the Shapley-Ames galaxies (1932) in (old) galactic coordinates. The zone of avoidance (dark) and of partial obscuration (grey) by the Milky Way is indicated. The supergalactic equator and parallels at  $\pm 30^\circ$  latitude are marked. Two external galaxy clouds in Hydra ( $l^I = 240^\circ$ ) and Pavo-Indus ( $l^I = 310^\circ$ ) and the elongated Dorado-Fornax-Eridanus stream or "southern supergalaxy" are outlined.



**Figure 3** All 2175 galaxies in the Nearby Galaxy Catalog (NBG) projected onto the SGY-SGZ plane. The SGY-axis is directed toward supergalactic longitude  $90^\circ$ , supergalactic latitude  $0^\circ$  ( $l^{II} = 227^\circ$ ,  $b^{II} = +83^\circ.7$ ), the SGZ-axis toward supergalactic latitude  $90^\circ$  ( $l^{II} = 47^\circ.4$ ,  $b^{II} = +6^\circ.3$ ). The radius of the outer boundary is 60 Mpc. The galactic zone of avoidance ( $b < 15^\circ$ ) is contained within the opposed wedges tilted by  $6^\circ$  with respect to the SGZ-axis. There is a zone of incompleteness ( $\delta < -45^\circ$ ), which is projected across most of the southern supergalactic hemisphere. Figures 3–6 are reproduced by courtesy of R. B. Tully (92).

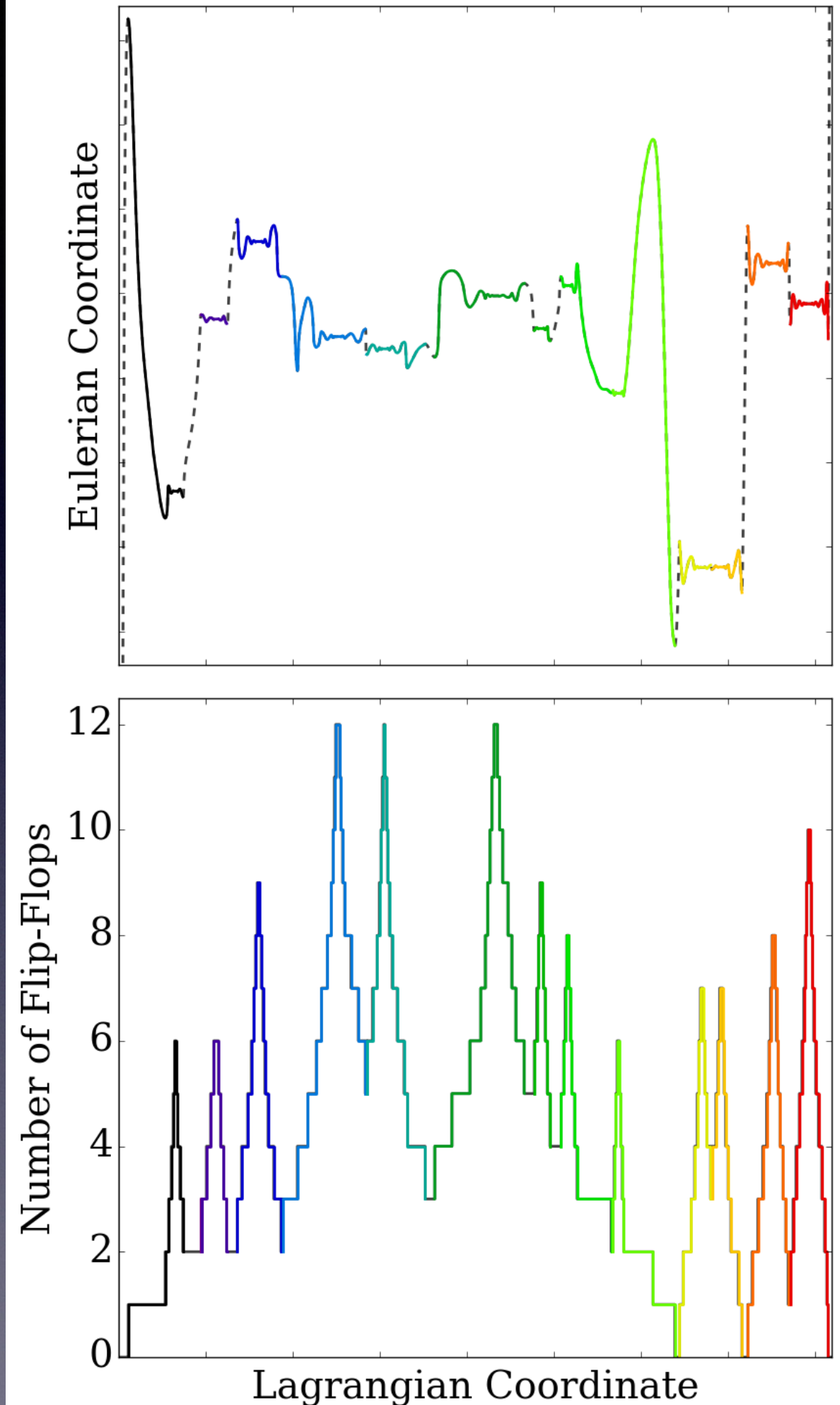
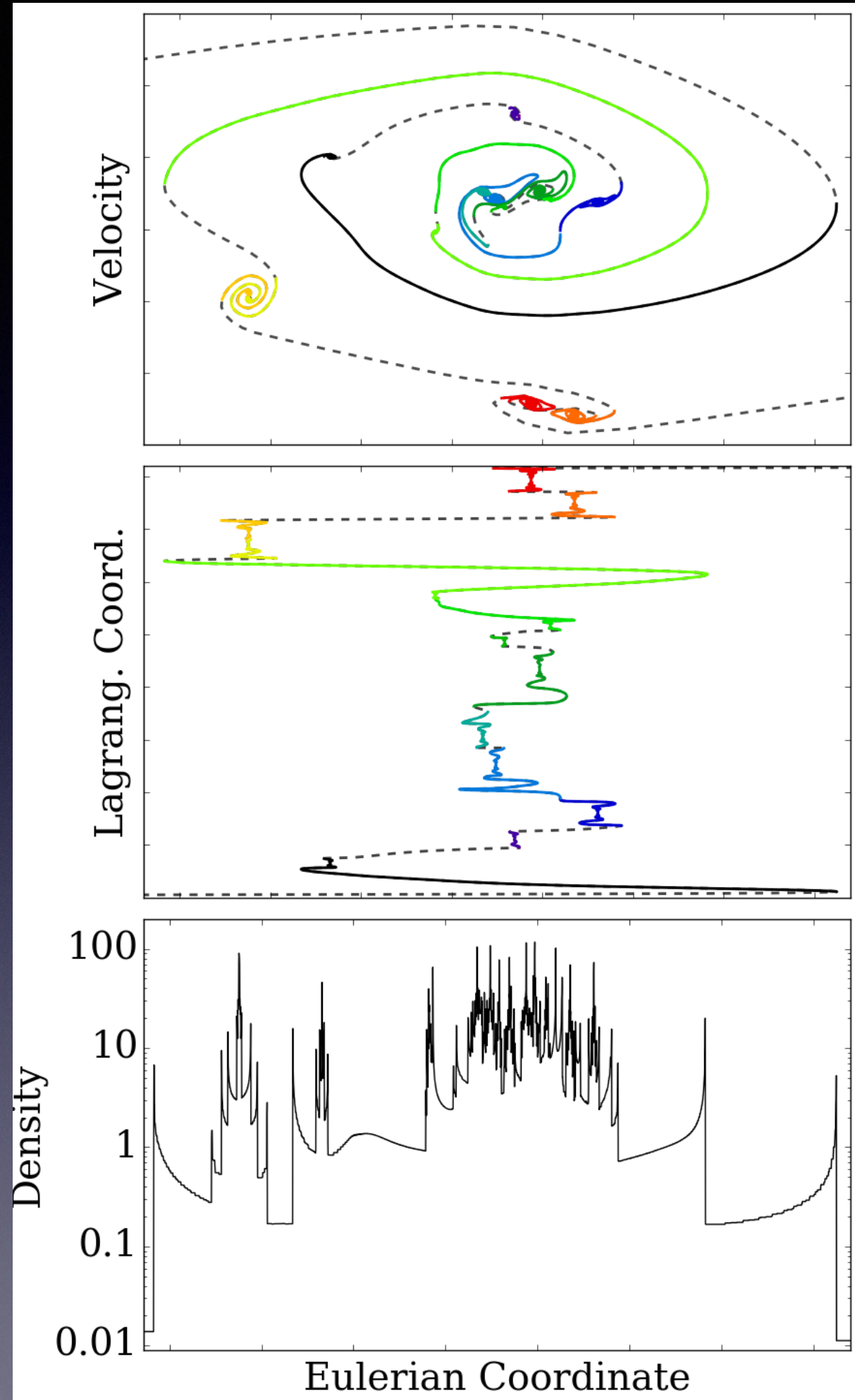




Three-dimensional **DTFE** reconstruction of the inner parts of the **2dF Galaxy Redshift Survey**

# Outline of the talk

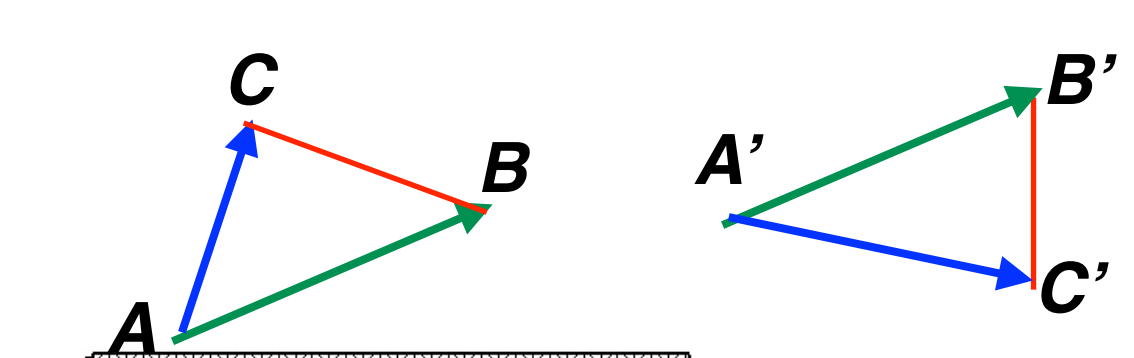
- Brief cosmological introduction
- Beginning of the dark matter web story
  - The Zeldovich approximation
  - Geometrical and topological challenges
  - Web of galaxies
- Dark matter web
  - Flip-flop field as a record of halo merging
  - Multi stream field
  - A comparison project “Tracing the Cosmic Web”
  - Caustics
- Summary



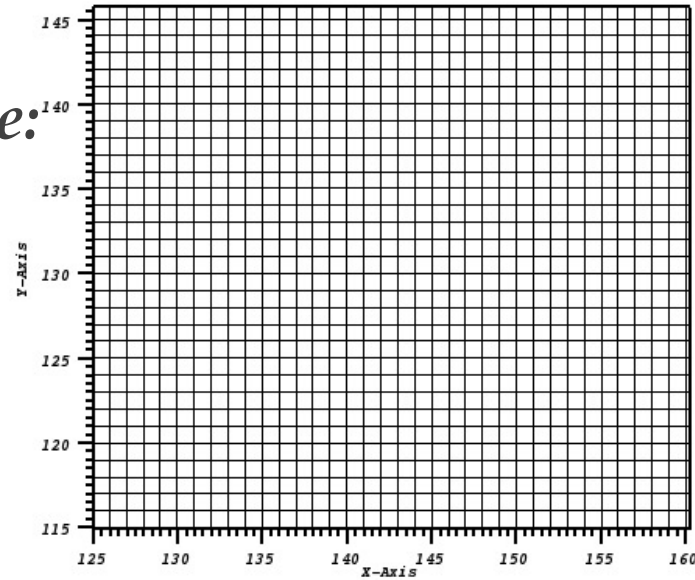
**Flip-Flop  
2D**

$$a = \frac{1}{2} \vec{AB} \times \vec{AC}$$

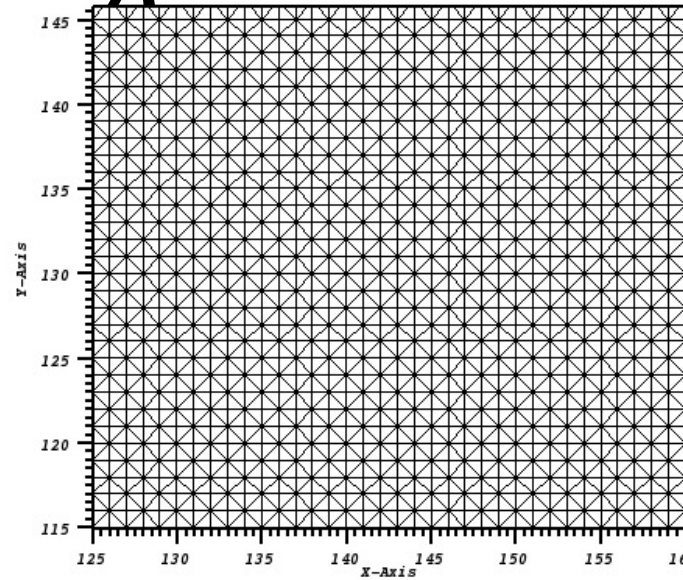
$$a' = -\frac{1}{2} \vec{A'B'} \times \vec{A'C'}$$



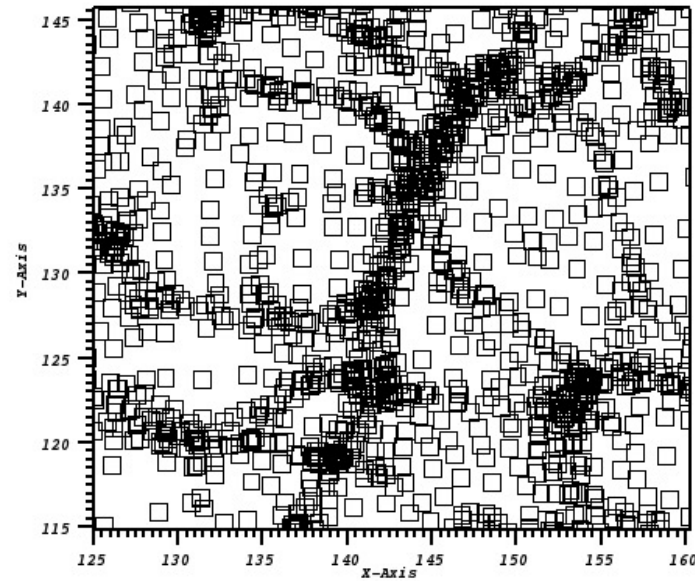
*Initial (uniform) state:  
square particles fill  
whole space*



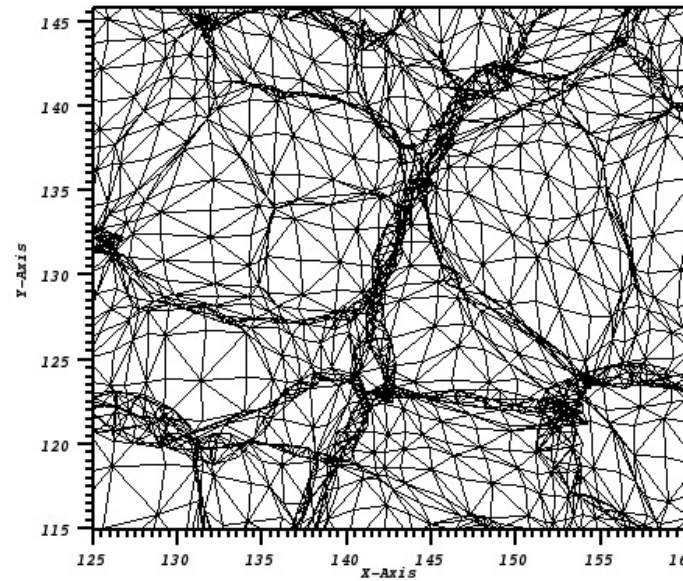
*Initial state:  
particles = vertices  
of tessellation.  
Mass is uniformly  
distributed  
within triangles*



*Particles in evolved  
state*

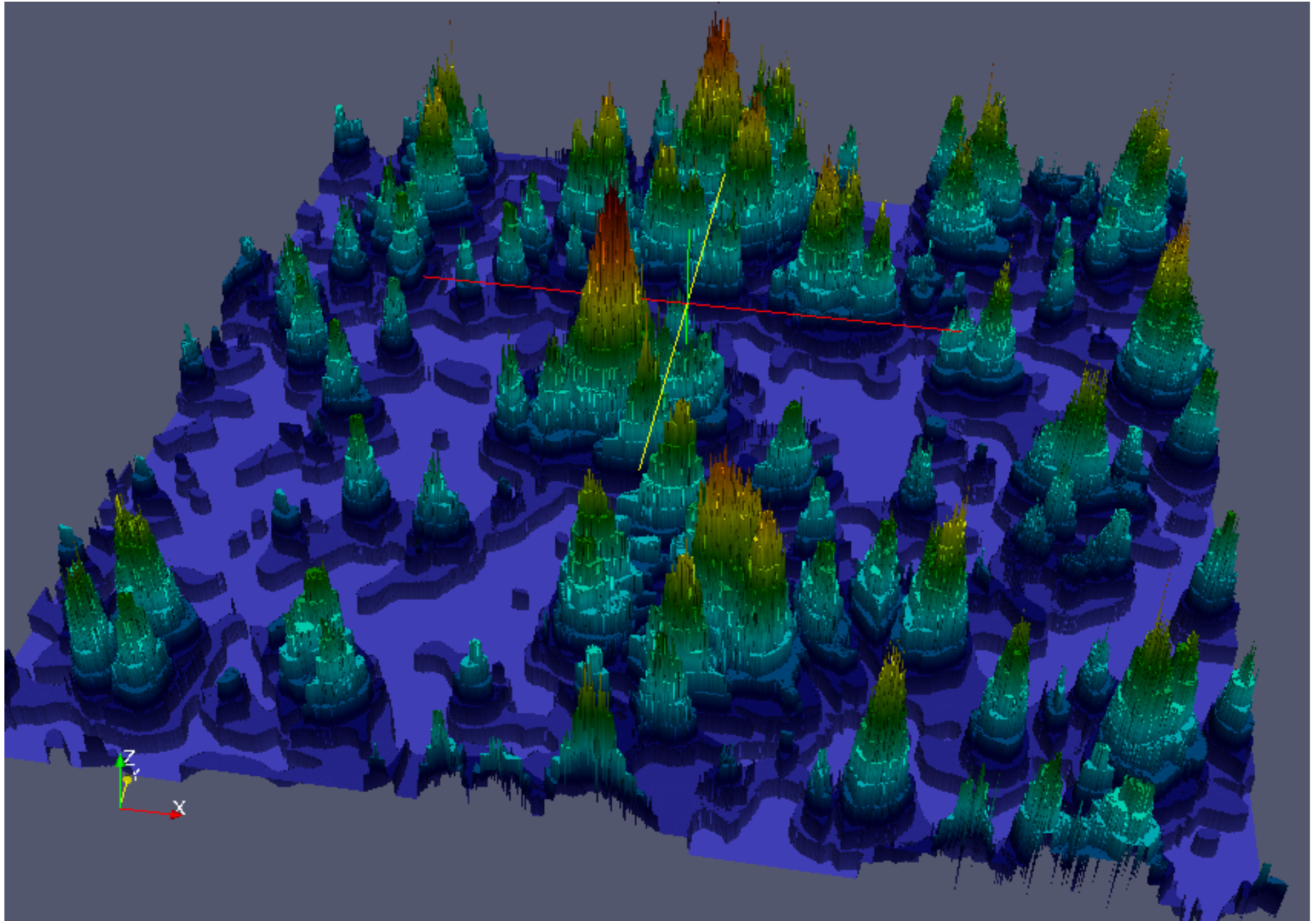


*Evolved tessellation*



**Flip-Flop on particles: change of sign of  $\det [\partial x_i / \partial q_k]$**

# Flip-Flop field in Lagrangian space in $1024^2$ simulation



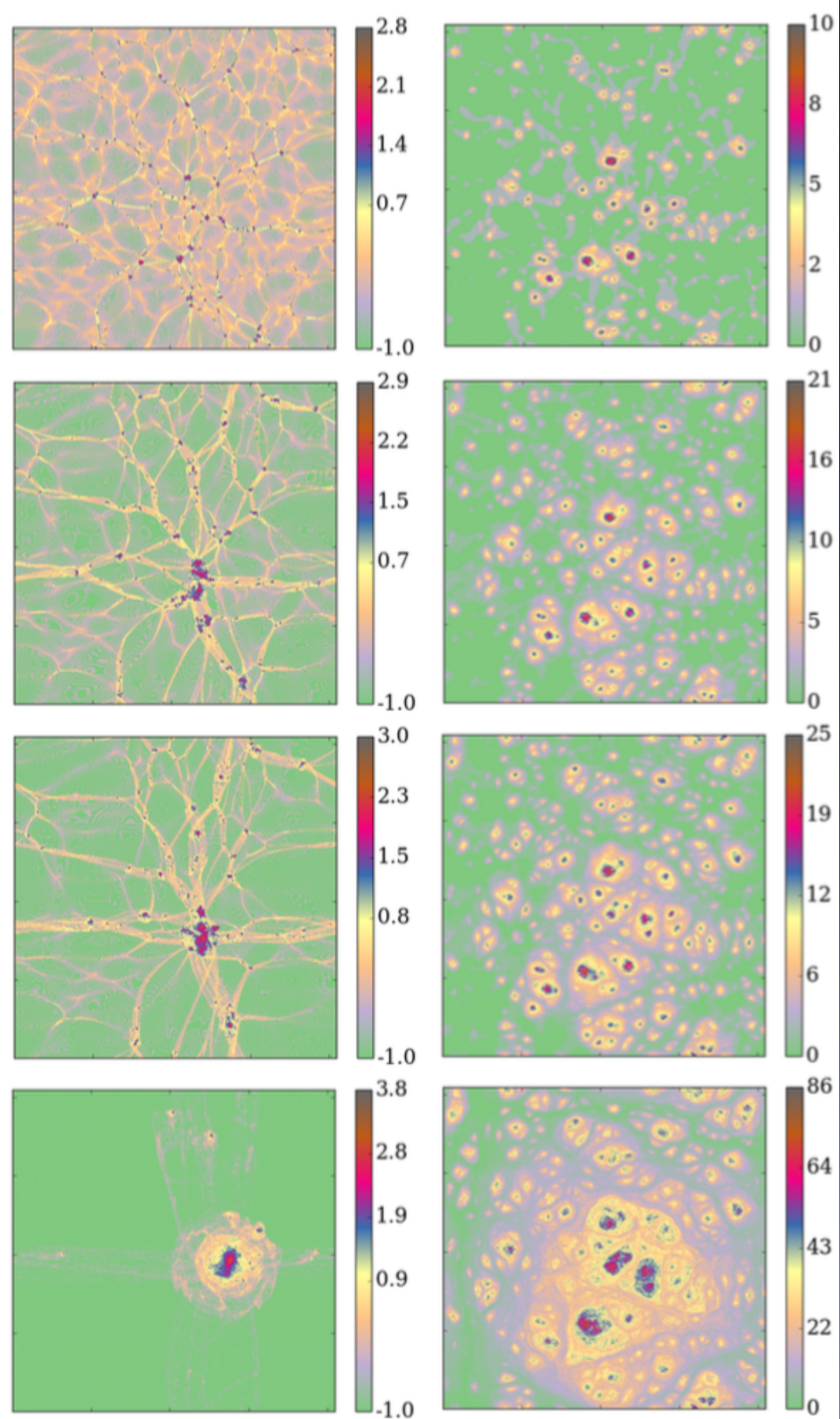
$a=1$   
'beginning' of  
non-linear stage

*density  
field*

$a=2.3$

$a=3.4$

$a=59$



*flip-flop  
field*

**Figure 2.** Evolution of structure in two-dimensional N-body simulation. Four stages are shown at  $a \approx 1.0$ , 2.3, 3.4 and 58.7 from top to bottom. The density perturbation linearly extrapolated would result in  $\delta_{\text{rms}} = 1$  at  $a = 1$ . The CIC density fields in Eulerian space are shown in the left column. The corresponding

### 3 N-BODY SIMULATIONS

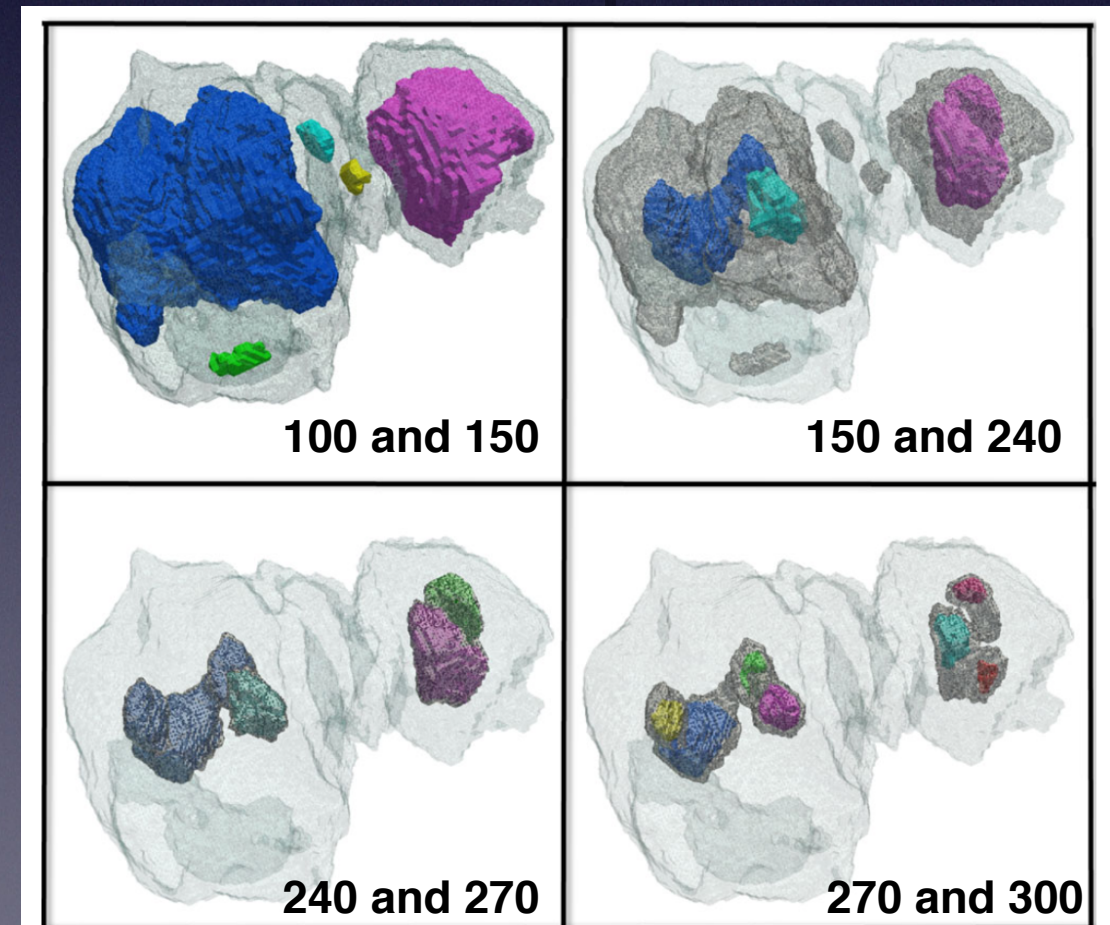
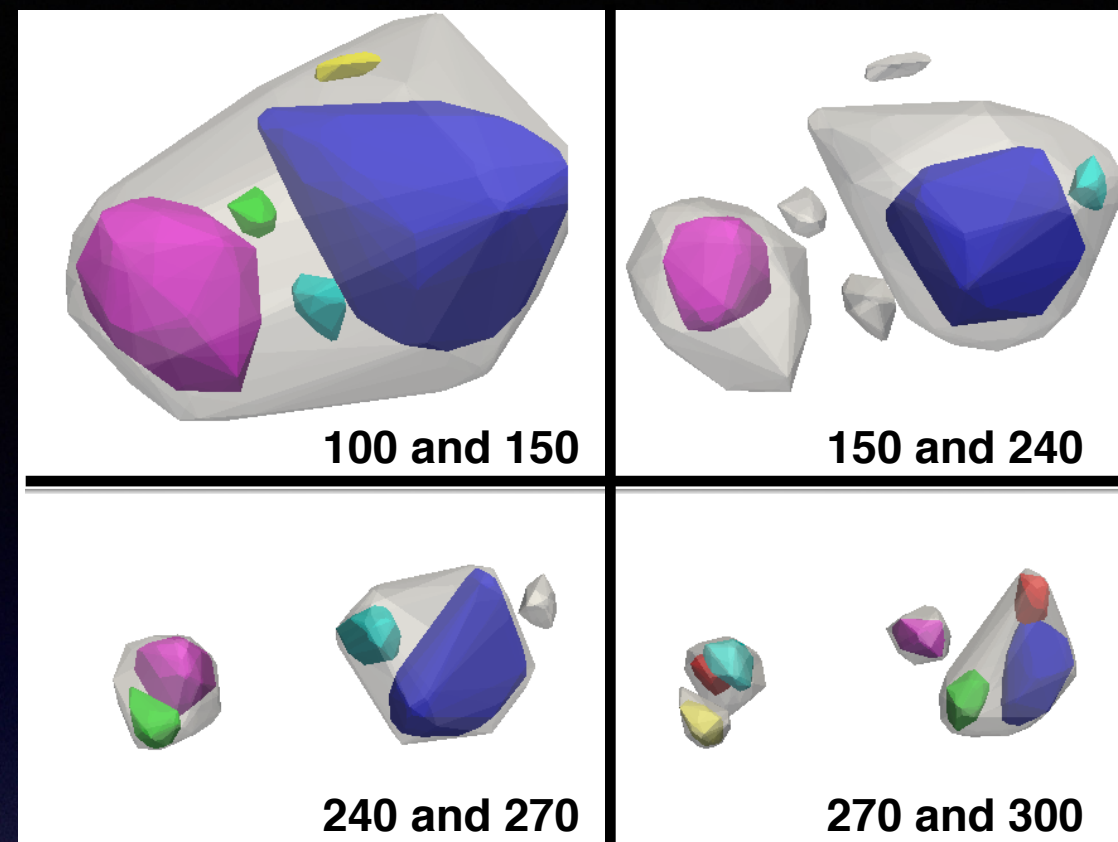
The initial conditions were generated with NGenIC code<sup>4</sup> with the standard  $\Lambda$  cold dark matter ( $\Lambda$ CDM) cosmology,  $\Omega_m = 0.3$ ,  $\Omega_\Lambda = 0.7$ ,  $\Omega_b = 0$ ,  $\sigma_8 = 0.9$ ,  $h = 0.7$  and the initial redshift  $z = 50$ . A set of simulations were carried out with a box  $1 h^{-1}$  Mpc and total mass  $M_{b,dm} \approx 1.2 \times 10^{11} M_\odot$ . For illustration purposes, we present two simulations with  $128^3$ ,  $m_{\text{part}} \approx 5.7 \times 10^4 M_\odot$  and  $256^3$ ,  $m_{\text{part}} \approx 7.1 \times 10^3 M_\odot$  DM particles with the force resolution of  $1.5 h^{-1}$  and  $0.75 h^{-1}$  kpc respectively. The chosen size of the box is obviously too small for the purpose of deriving statistically valid

Table 1. Number of particles in substructures shown in Fig. 22

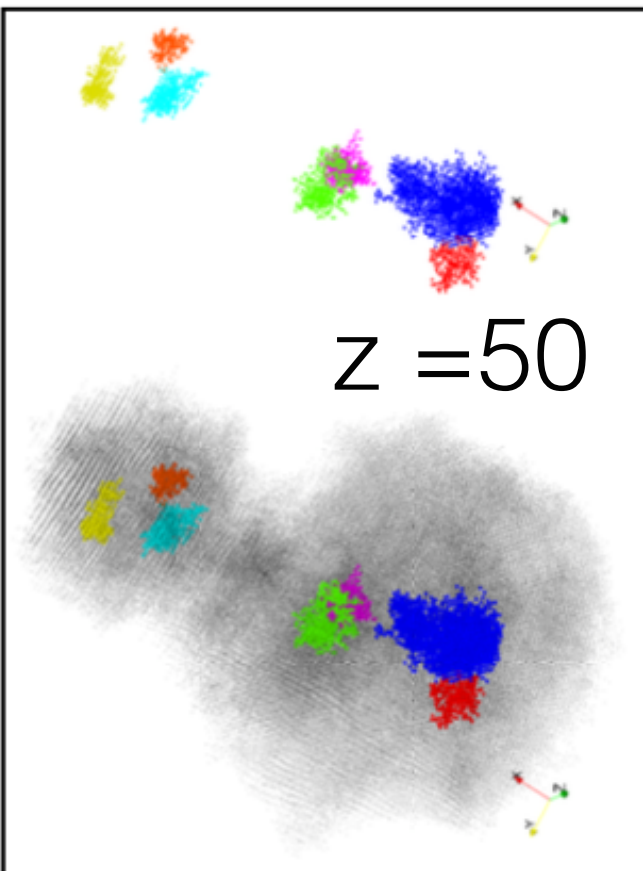
flip-flop threshold	$N_1$	$N_2$	$N_3$	$N_4$	$N_5$	$N_6$	$N_7$
100	206670						
150	61960	17035	513	308	265		
240	8698	3960	211				
270	4363	1474	753	521			
300	1976	416	405	381	286	267	178

Table 2. Approximate masses of substructures shown in Fig. 22 in units of  $10^6 M_\odot$

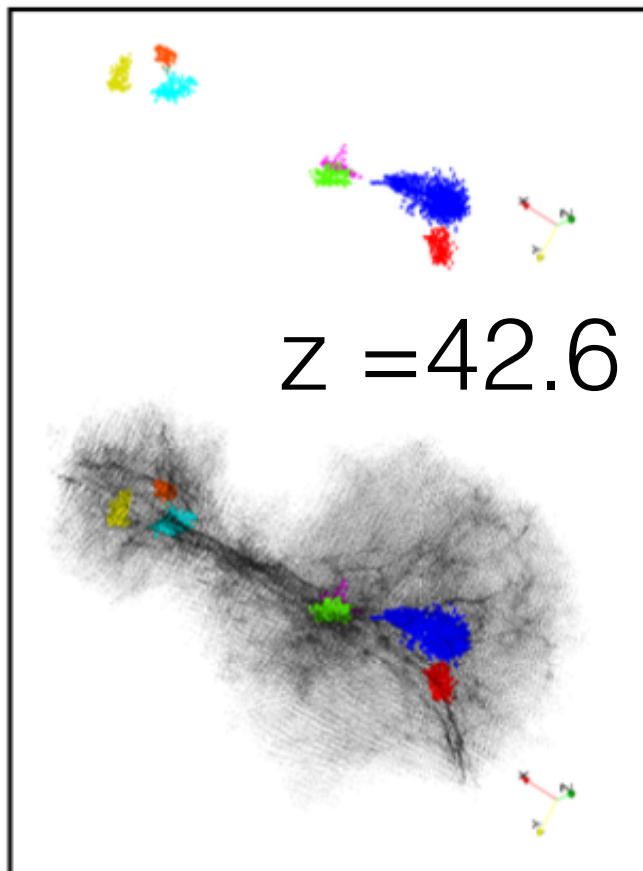
flip-flop threshold	$M_1$	$M_2$	$M_3$	$M_4$	$M_5$	$M_6$	$M_7$
100	1464.						
150	439.	121.	3.63	2.18	1.87		
240	61.6	28.1	1.50				
270	30.9	10.4	5.34	3.70			
300	14.0	2.94	2.87	2.70	2.03	1.89	1.26



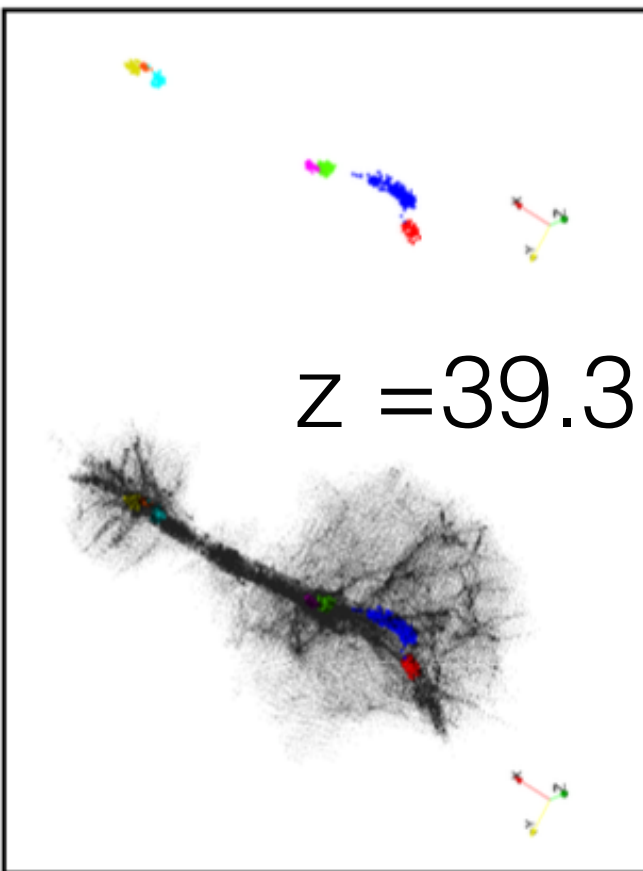
**Figure 22.** The marching cubes isosurfaces of the flip-flop field show five levels of hierarchical structure of the largest flip-flop peak in the  $256^3$  simulation in Lagrangian space. All panels show the surface of the peak



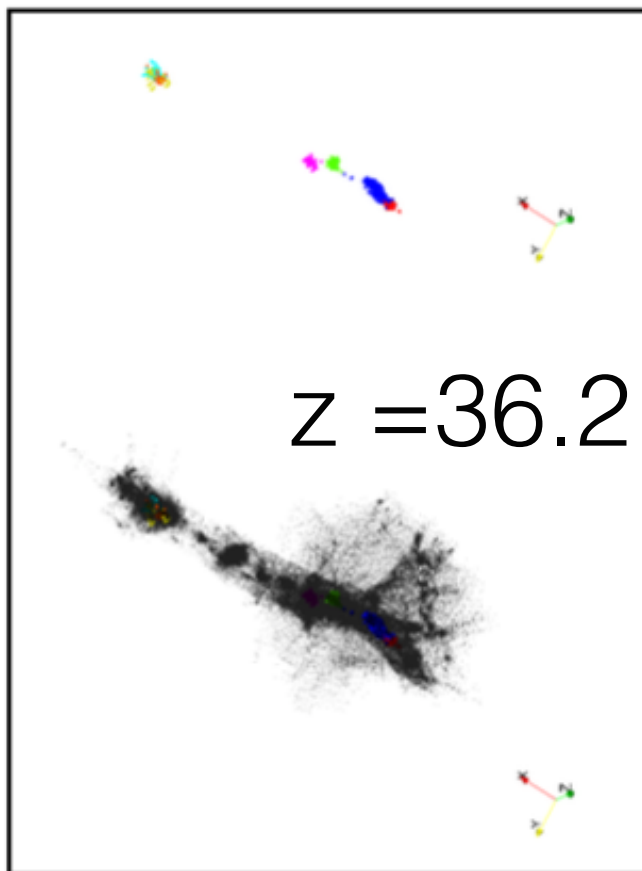
$z = 50$



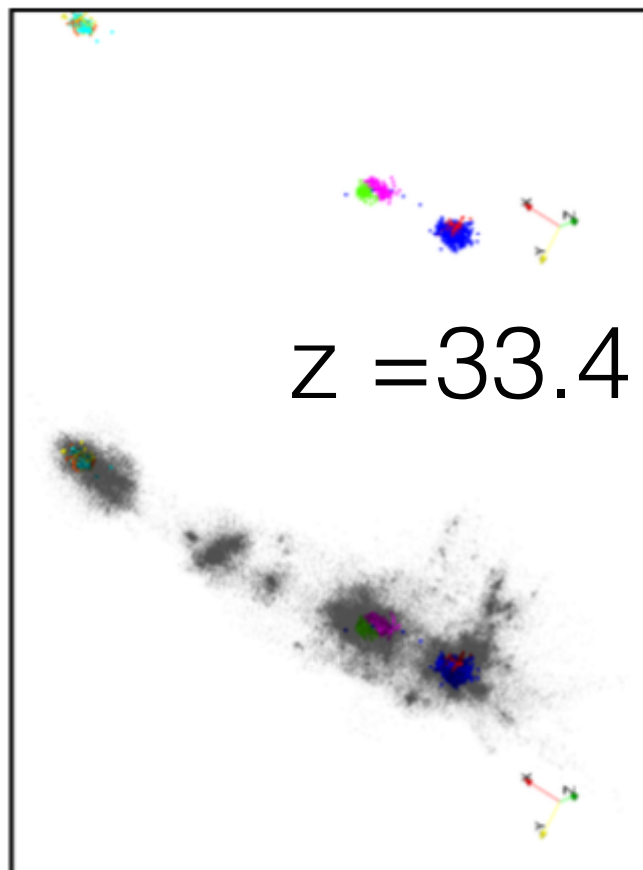
$z = 42.6$



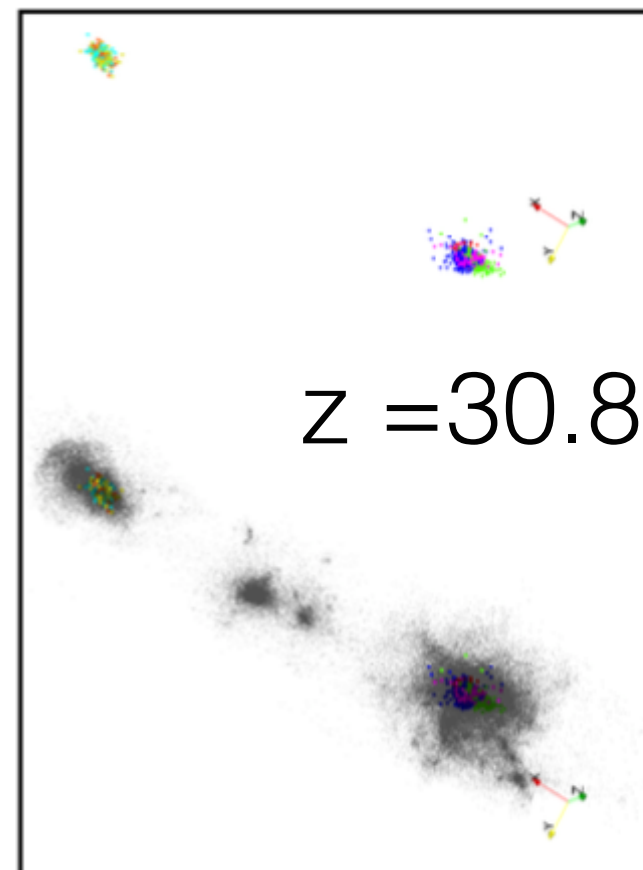
$z = 39.3$



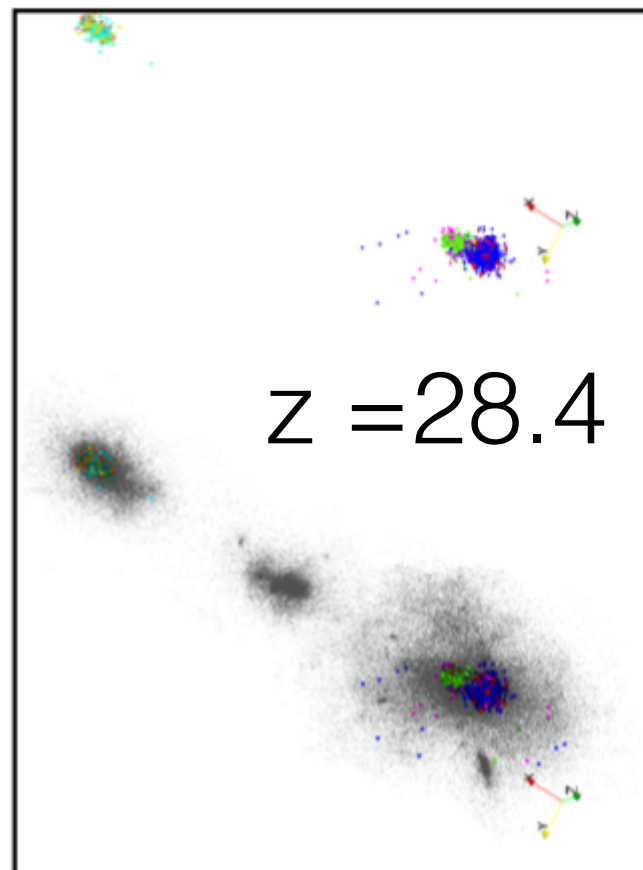
$z = 36.2$



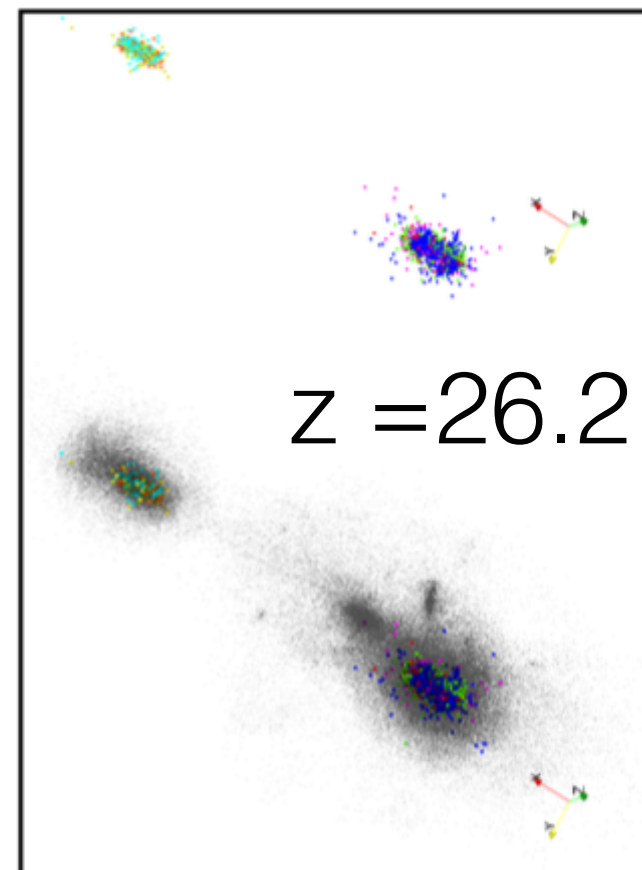
$z = 33.4$



$z = 30.8$

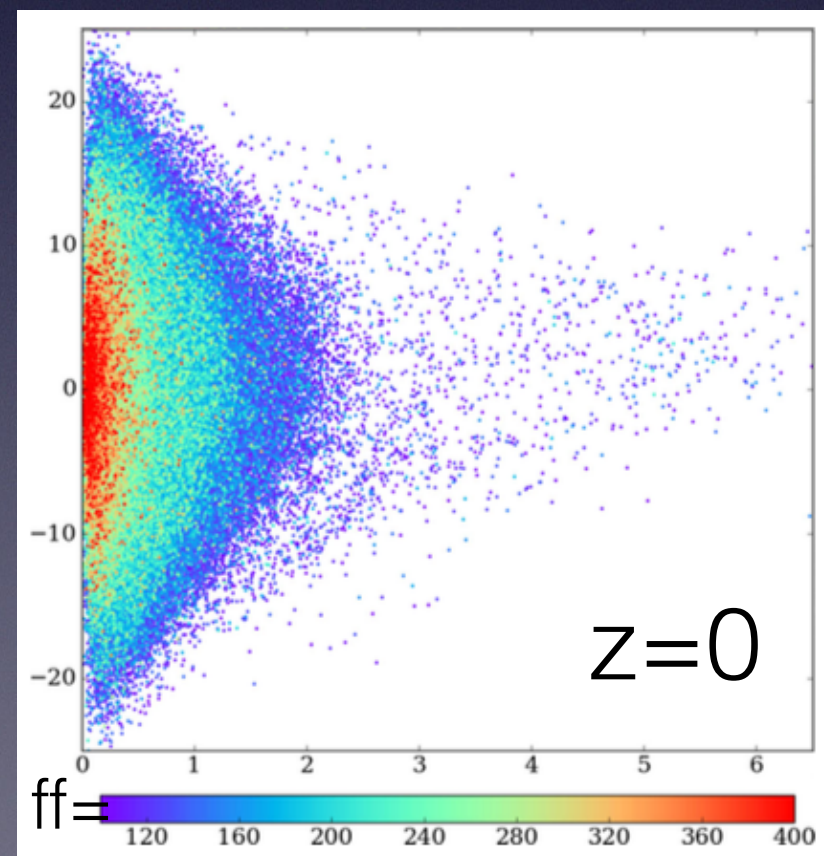
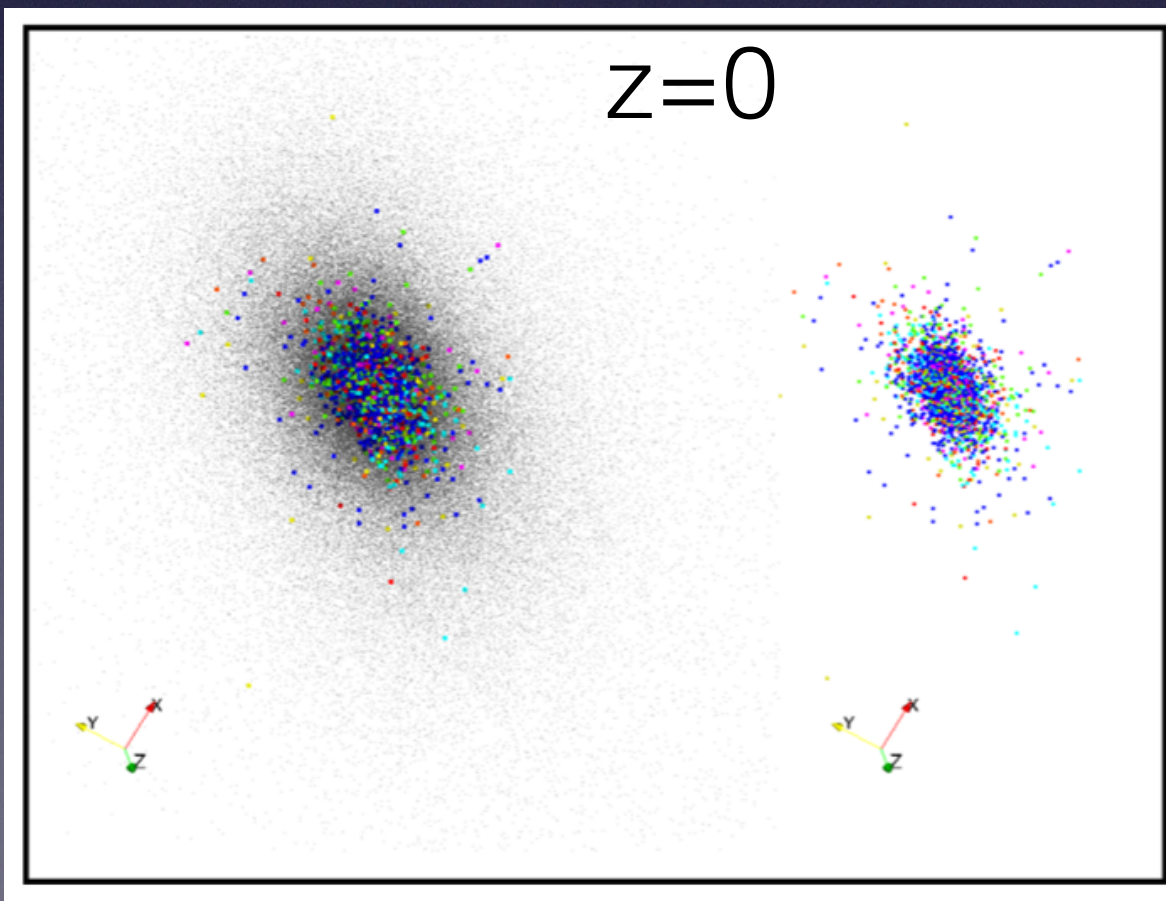
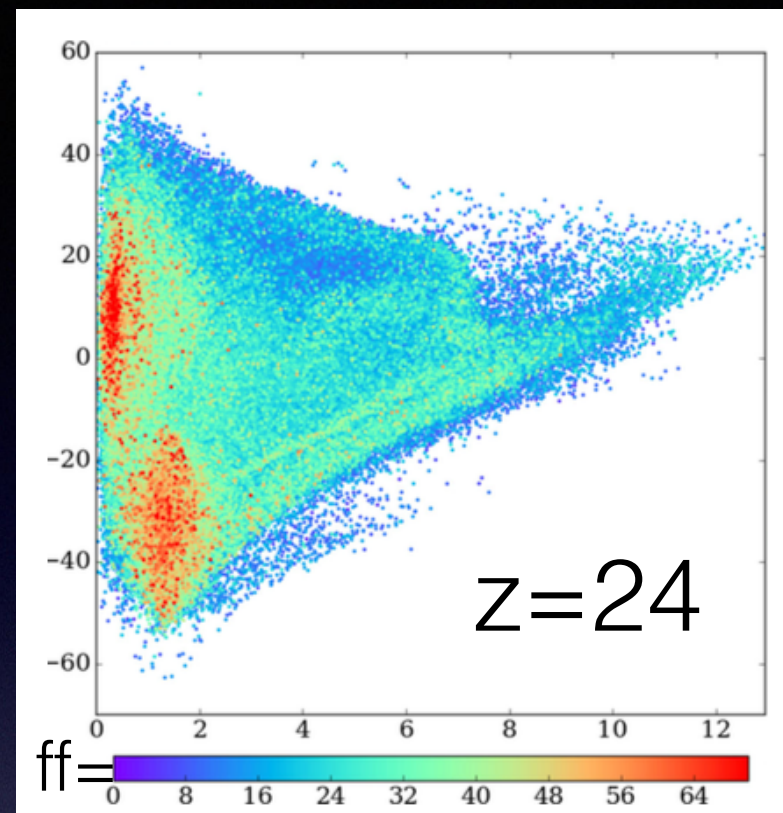
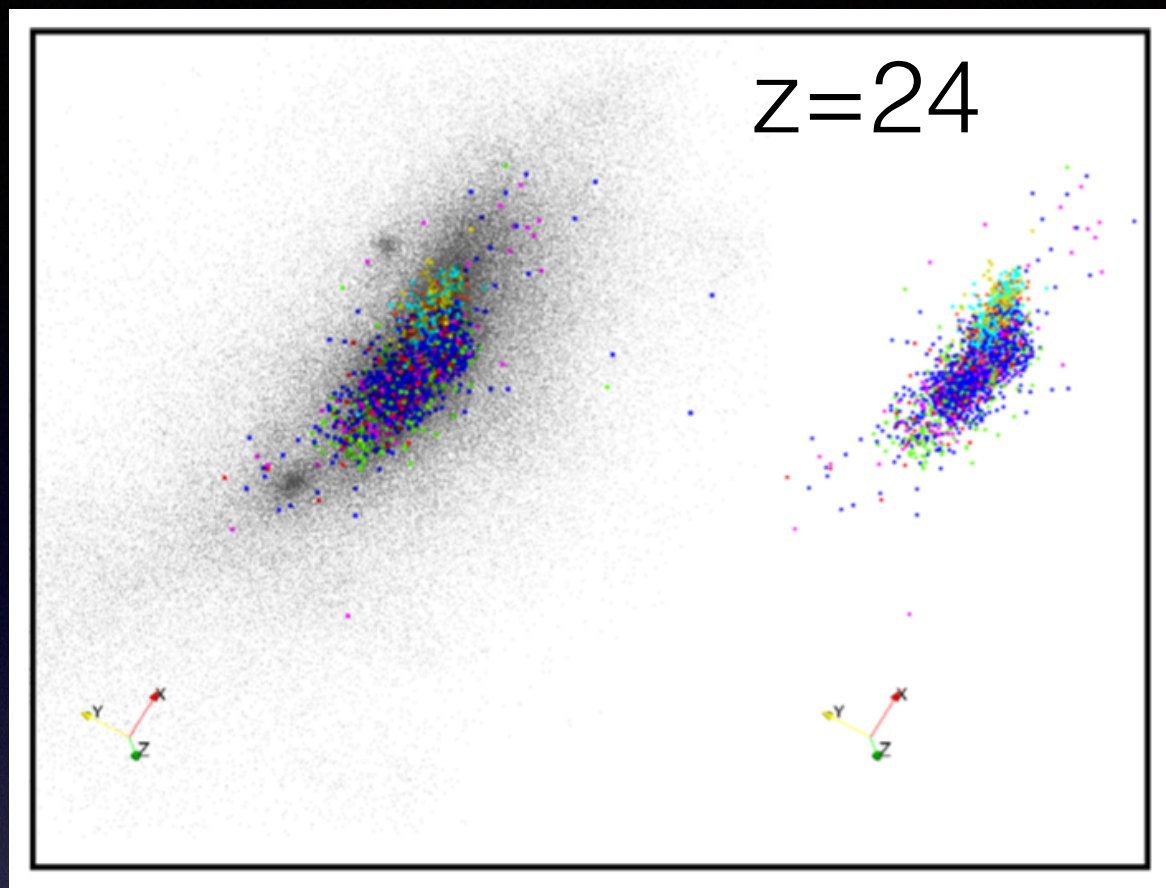


$z = 28.4$



$z = 26.2$

# “Phase space” (kpc, km/s)



# Lagrangian Space

*“Phase space” at  $z=0$*

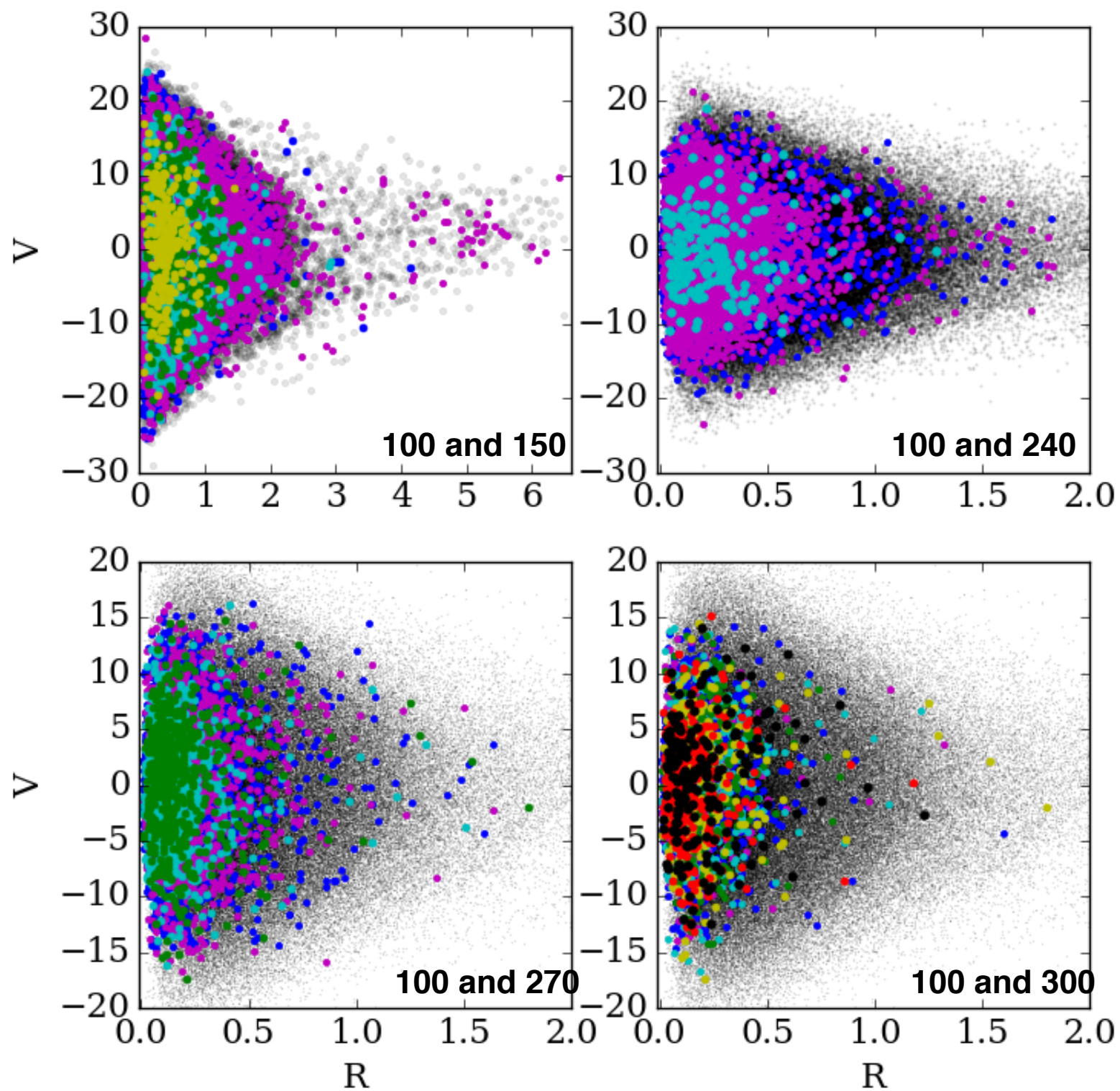
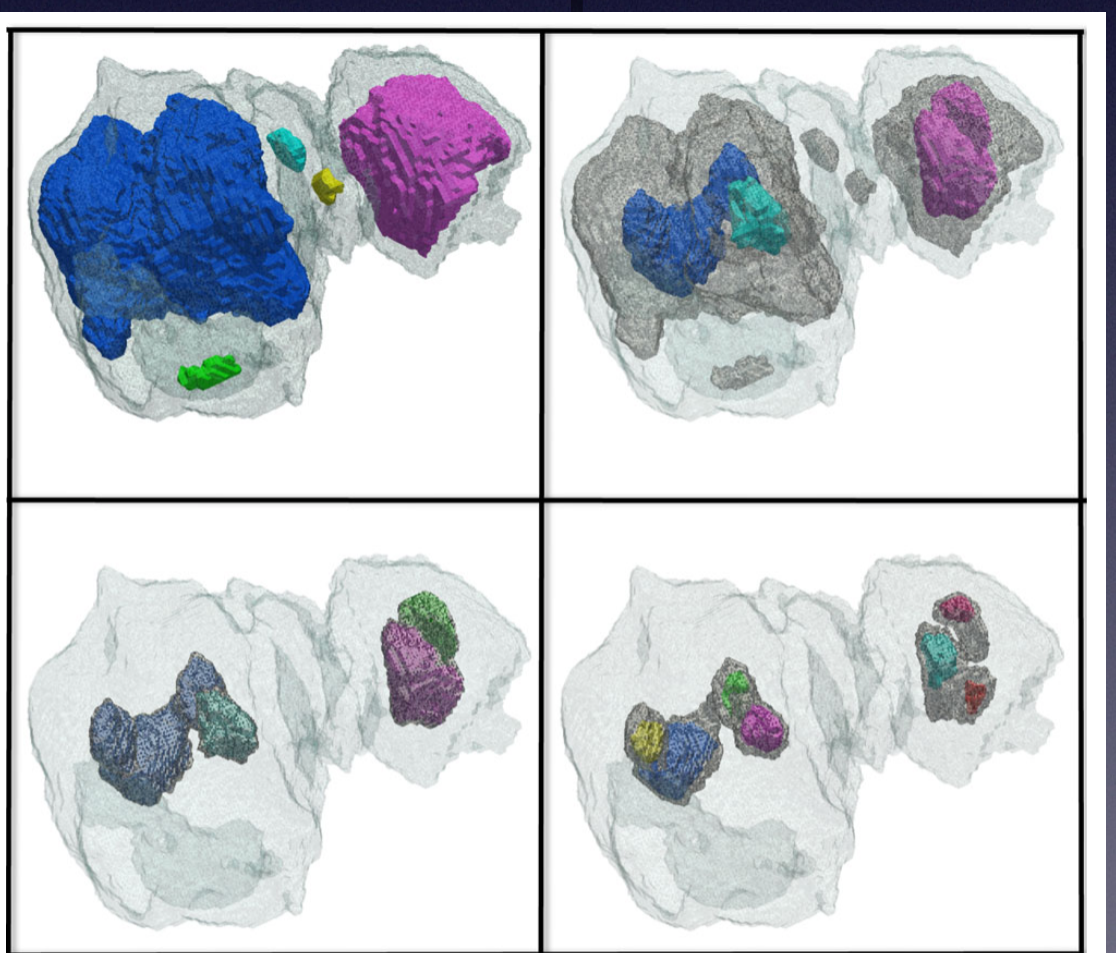
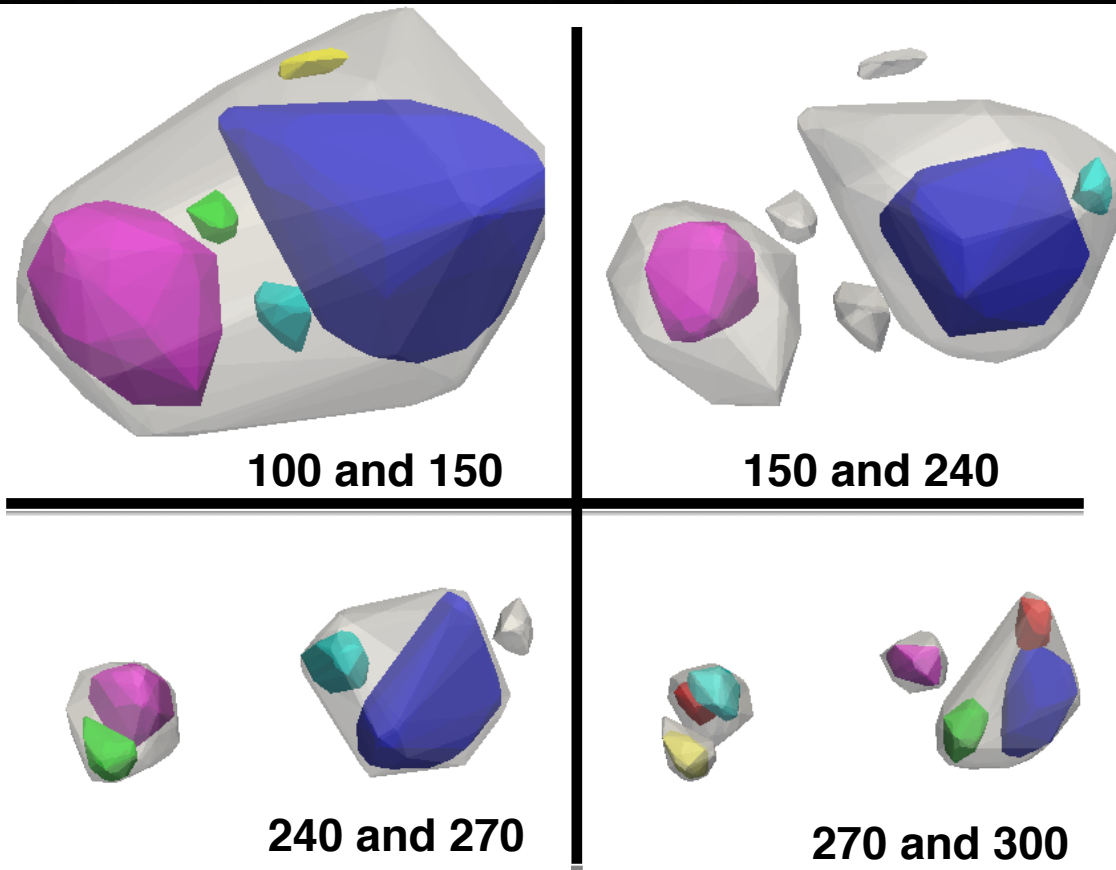


**Figure 22.** The marching cubes isosurfaces of the flip-flop field show five levels of hierarchical structure of the largest flip-flop peak in the  $256^3$  simulation in Lagrangian space. All panels show the surface of the peak

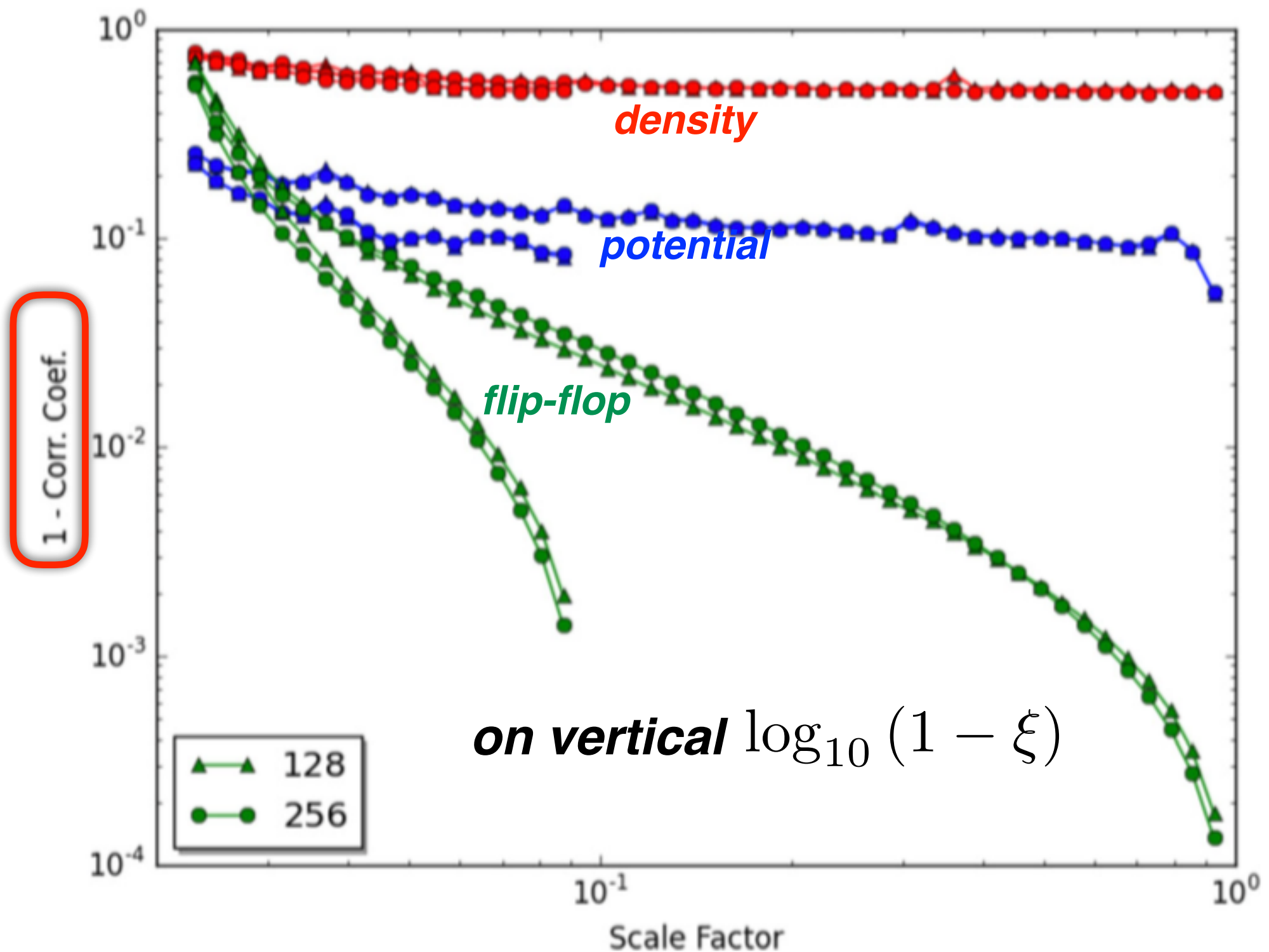
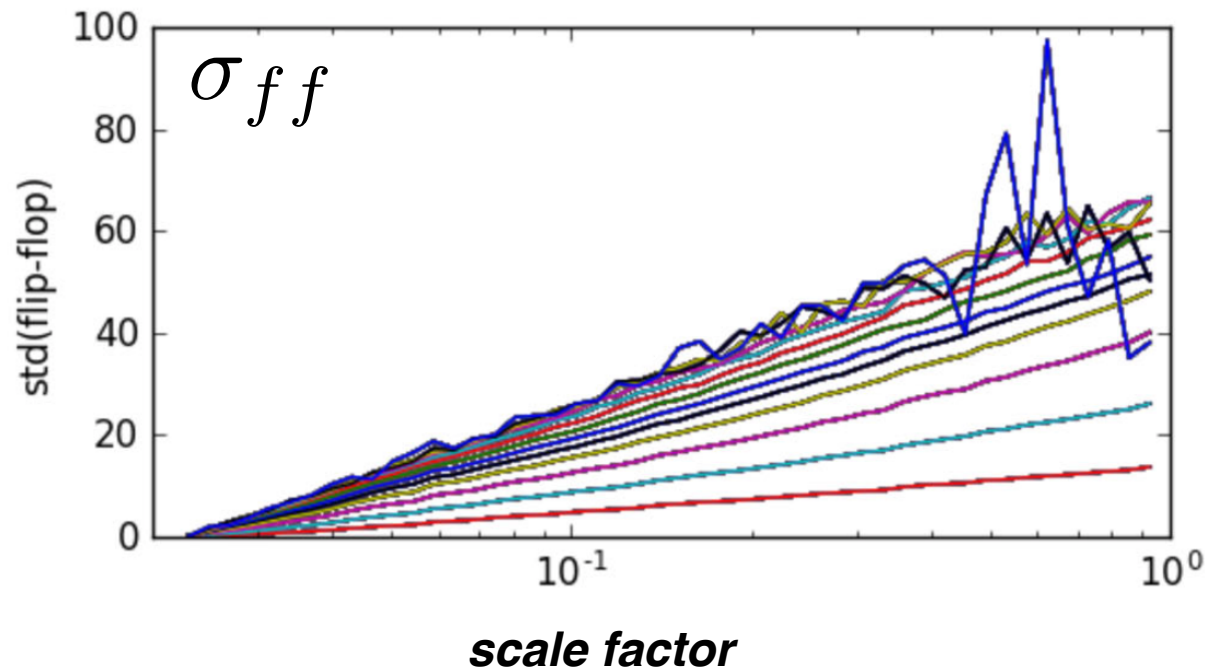
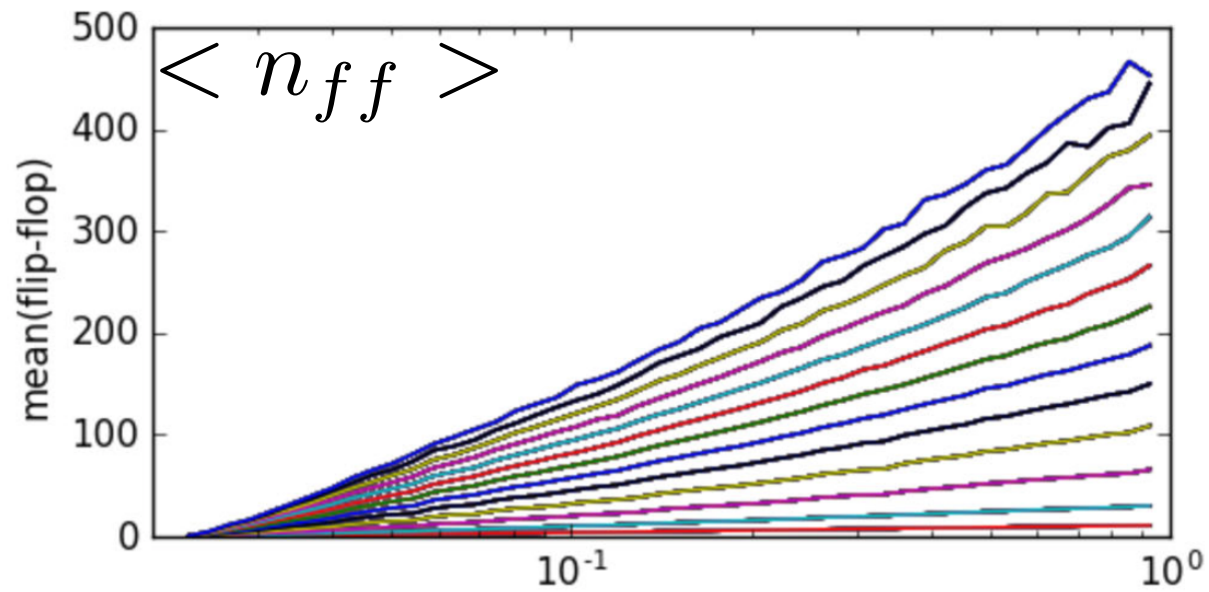


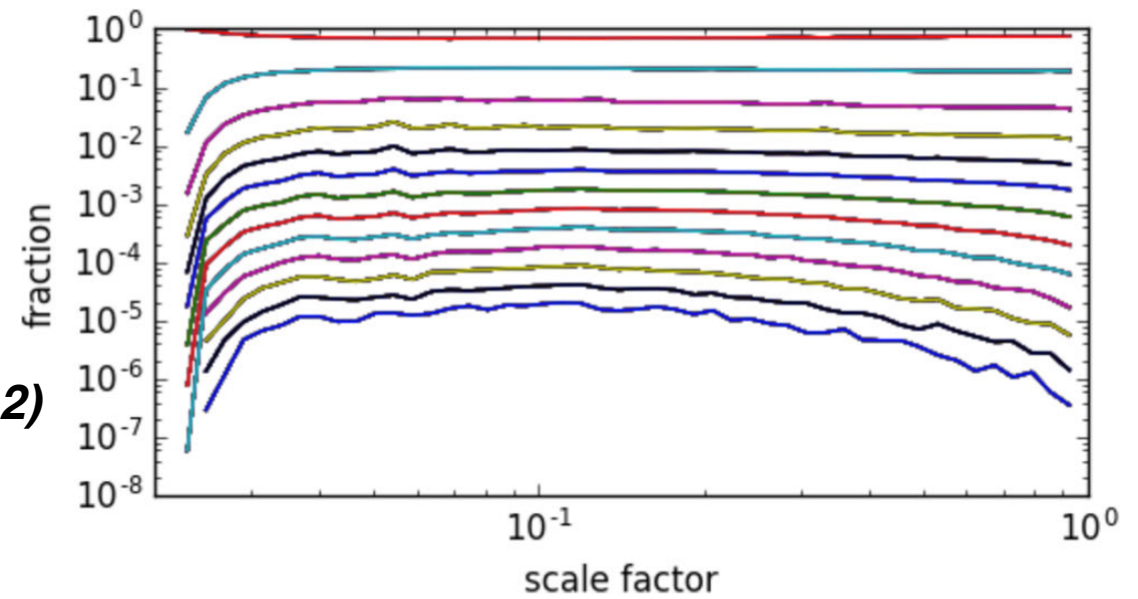
**Figure 12.** Correlation coefficient of the density  $\xi_{\rho \cdot \rho}$  (red), potential  $\xi_{\varphi \cdot \varphi}$  (blue) and flip-flop  $\xi_{\text{ff} \cdot \text{ff}}$  fields at  $a = 1$  (long curves) and  $a = 0.1$  (short curves) with corresponding fields at all previous stages. In order to see how close to unity  $\xi_{\text{ff} \cdot \text{ff}}$  is, we plot the logarithm of its difference from unity. The curves are shown for both  $N_p = 128$  (triangles) and 256 (circles) simulations.



***The rich get richer  
and  
the poor get poorer***

$$\rho(r) \propto r^{-n}$$

$$t \propto r^{n/2}$$



***Each curve corresponds to <math>\Delta(n\_{ff}(\Delta t))=(1, 2, \dots, 12)</math>***

***Vertical: mean(<math>n\_{ff}</math>) in top; std(<math>n\_{ff}</math>) in bottom in  
fraction on the right ;***

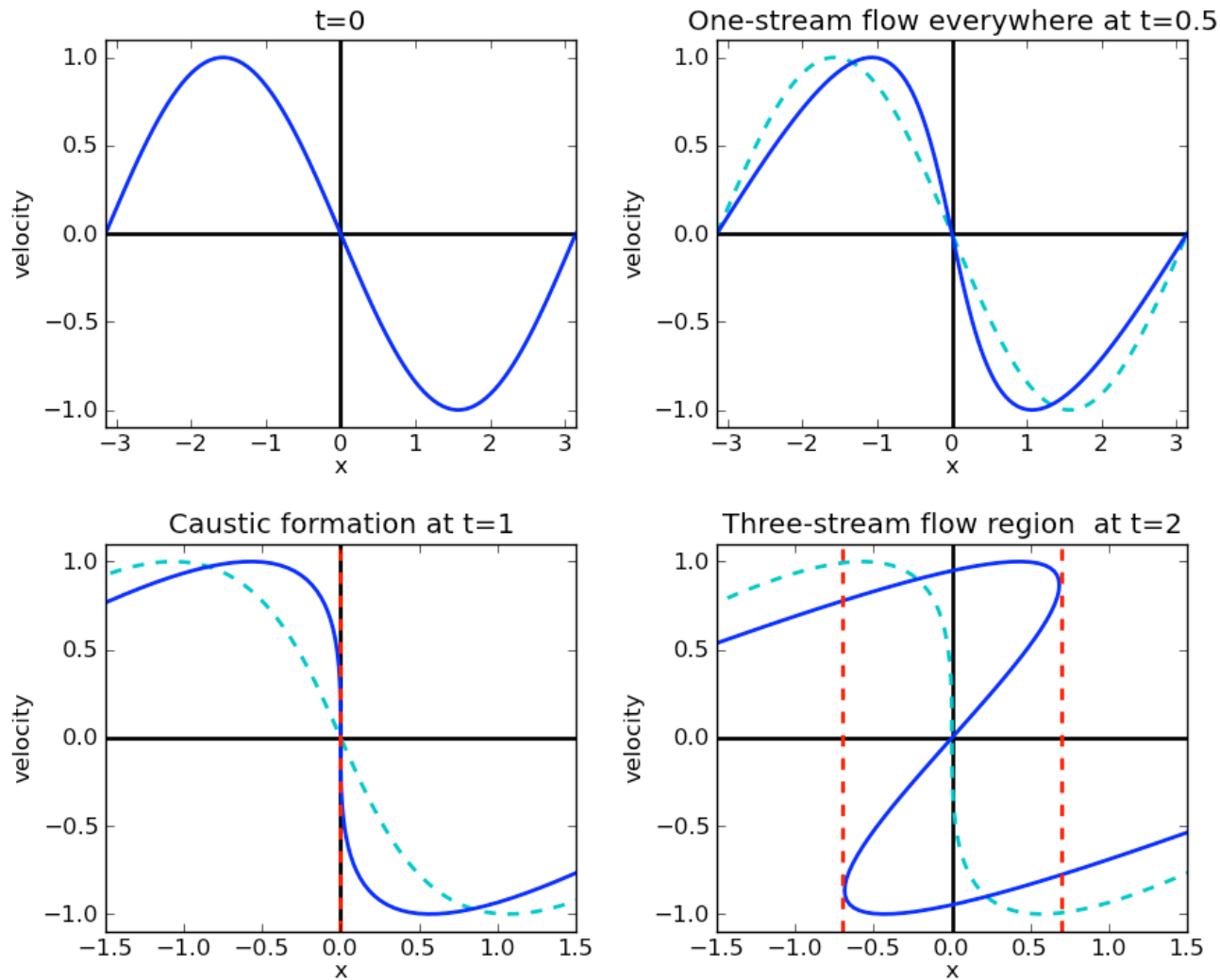
$$n_{ff}(t + \Delta t) = n_{ff}(t) + \Delta n_{ff}(\Delta t)$$

**Figure 14.** Conditional statistics of the flip-flop field as a function of the scalefactor. The particles are binned according to the change of the number of flip-flops between the outputs  $\Delta_{ff} = n_{ff}(a_{i+1}) - n_{ff}(a_i)$ . The curves are in the range  $0 \leq \Delta_{ff} \leq 12$  from the bottom to top in top two panels and in the reverse order in the bottom panel. The panels show the mean, std and fraction of the particles in each bin from top to bottom.

# Outline of the talk

- Brief cosmological introduction
- Beginning of the dark matter web story
  - The Zeldovich approximation
  - Geometrical and topological challenges
  - Web of galaxies
- Dark matter web
  - Flip-flop field as a record of halo merging
  - Multi stream field
  - A comparison project “Tracing the Cosmic Web”
  - Caustics
- Summary

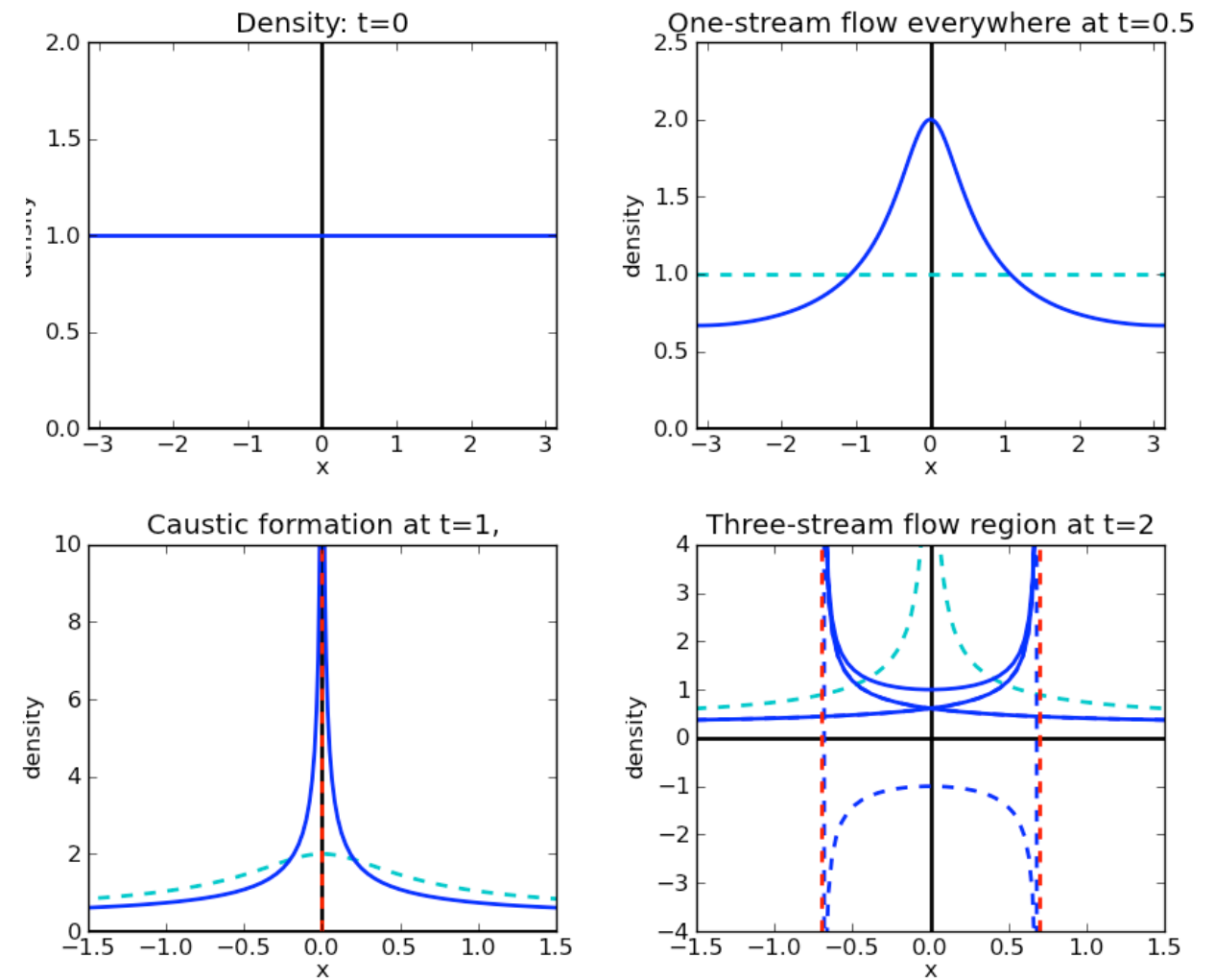
# Phase space



***Dashed lines show previous stage***

$$x = q - t \sin q$$

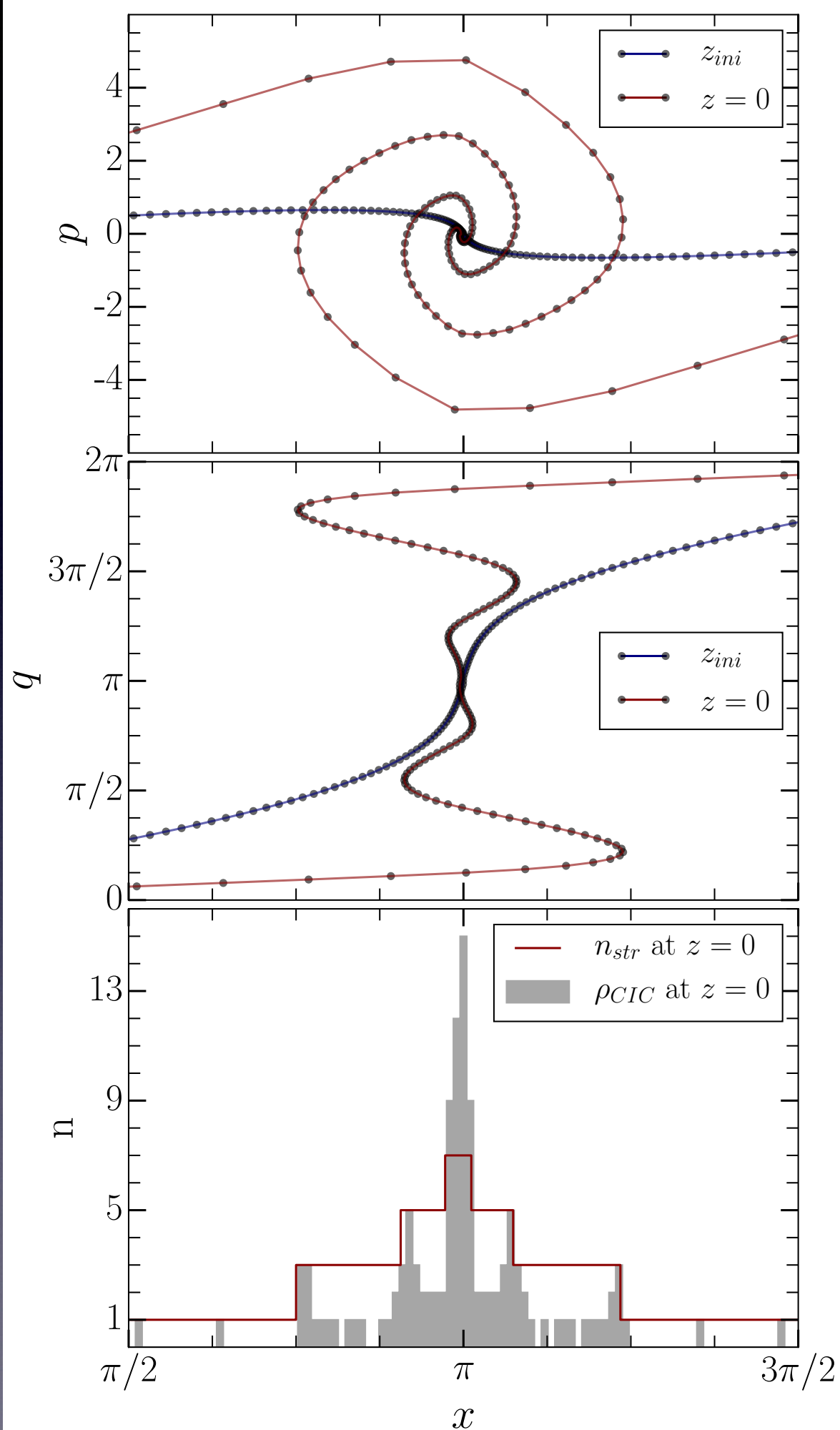
# Density



# Phase space

Lagrangian submanifold  
 $q(x)$  or  $x(q)$

$q(x)$  is multi valued (one-to-many)  
 $x(q)$  is single valued (one-to-one)



Density (gray, filled)  
V.S.

number of streams (red line)

Shandarin, Habib, Heitmann 2011 subm. 9 Nov.

Abel, Hahn, Kaehler 2011 subm. 16 Nov.

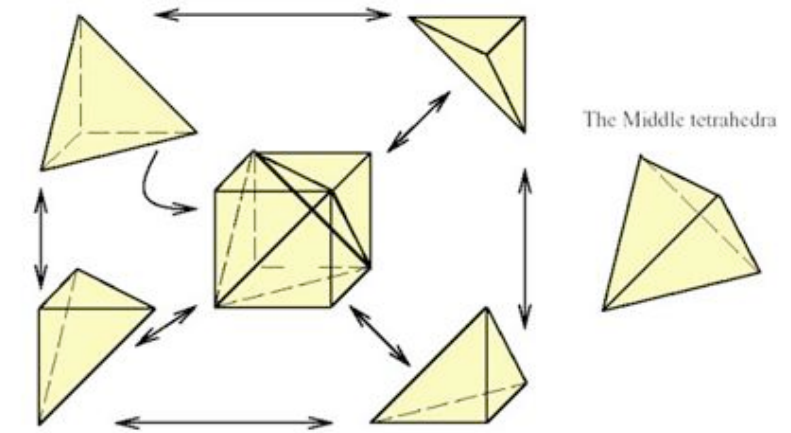
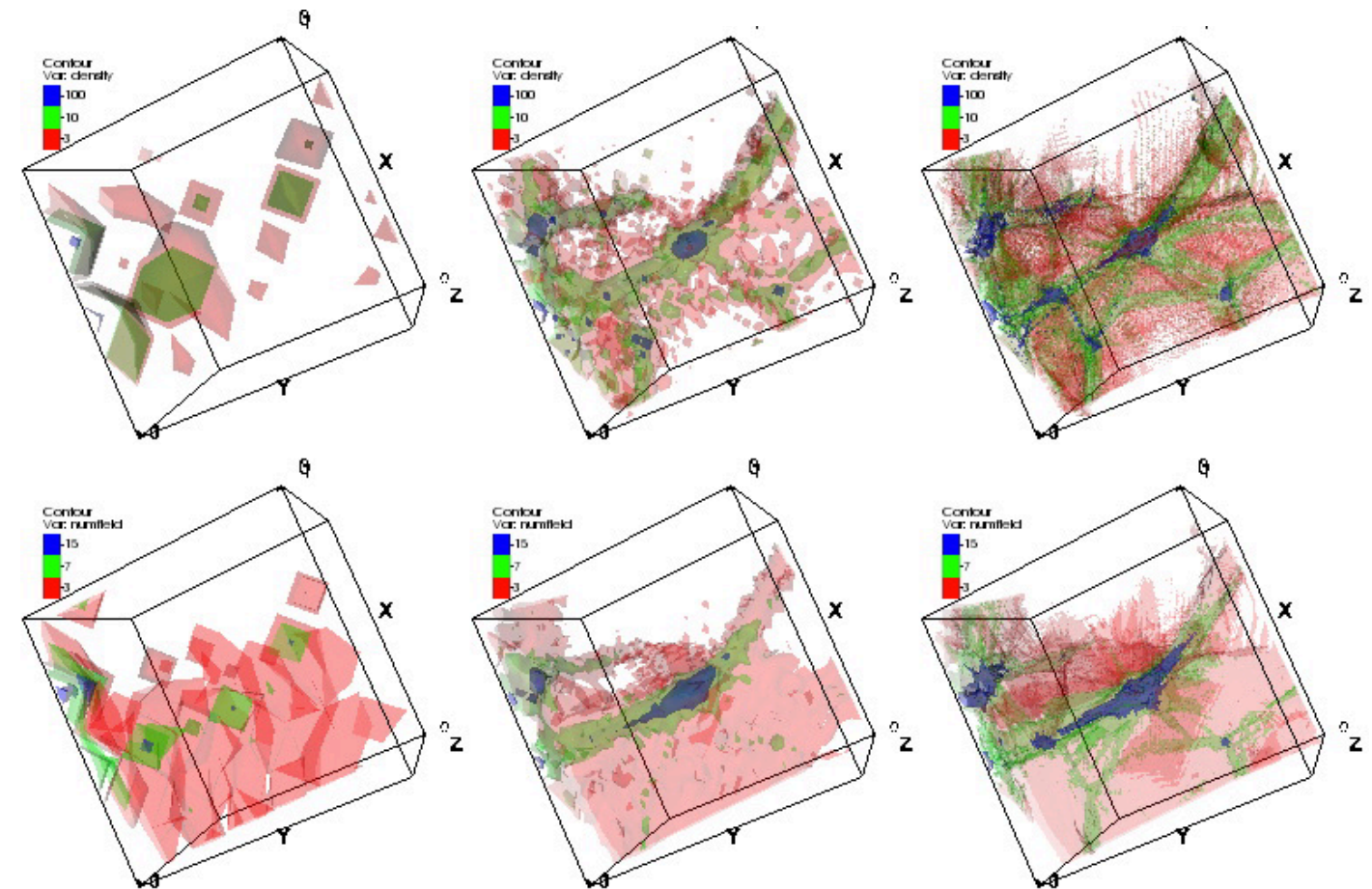
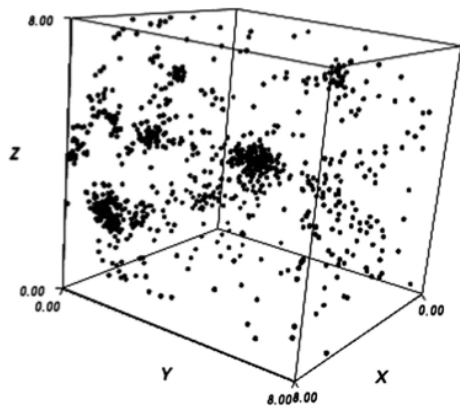


Figure 1.9: The Tetrahedra orientation within a cube

DENSITY  
FIELD



MULTI-STREAM  
FIELD

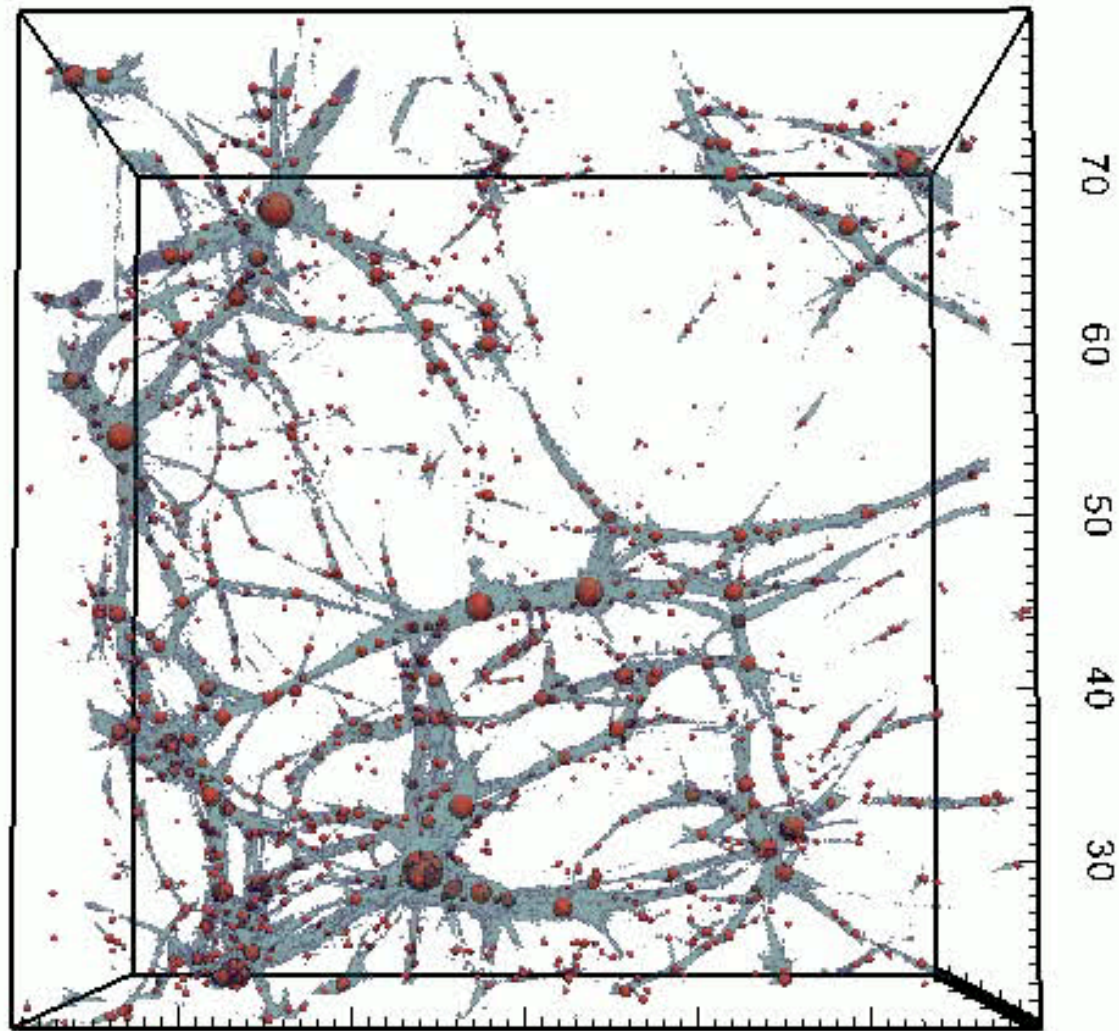


Fields are computed on a uniform 3D diagnostic grid in configuration space by projecting tetrahedra from 6D to 3D.

The refinement of 3D diagnostic grid is increasing from left to right (1, 4, 16)  
The distribution of particles remains the same in all plots.

# All halos are embedded in filaments

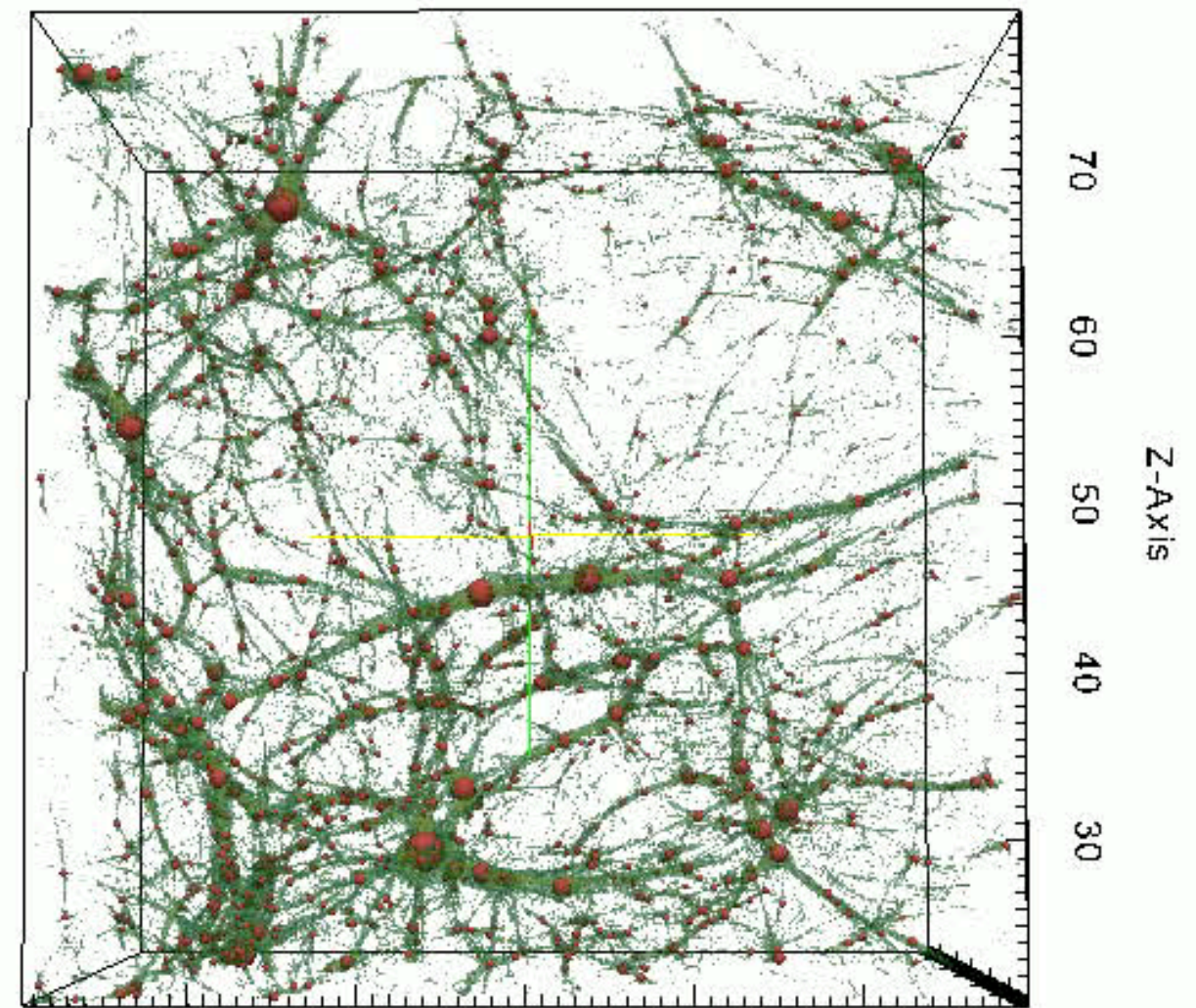
Ramachandra, Shandarin, MNRAS, 467, 1748, 2017



Y-Axis (Mpc)

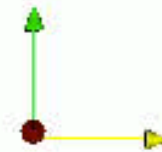
Z-Axis (Mpc)

streams

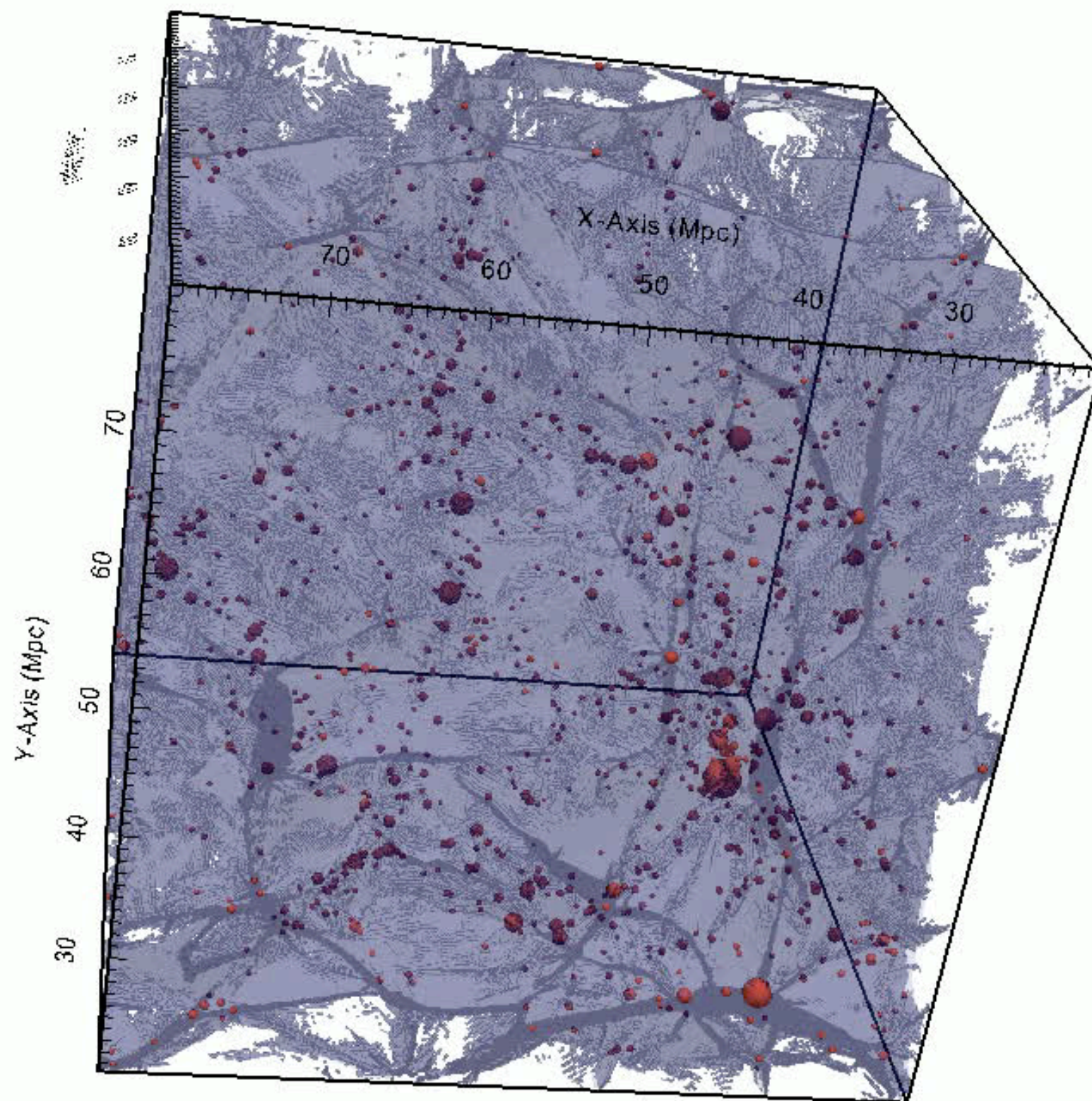


Y-Axis

Z-Axis



density



streams

# Outline of the talk

- Brief cosmological introduction
- Beginning of the dark matter web story
  - The Zeldovich approximation
  - Geometrical and topological challenges
  - Web of galaxies
- Dark matter web
  - Flip-flop field as a record of halo merging
  - Multi stream field
  - A comparison project “Tracing the Cosmic Web”
  - Caustics
- Summary

# Tracing the Cosmic Web<sup>★</sup>

Noam I Libeskind<sup>1†</sup>, Rien van de Weygaert<sup>2</sup>, Marius Cautun<sup>3</sup>, Bridget Falck<sup>4</sup>, Elmo Tempel<sup>1,5</sup>, Tom Abel<sup>6,7</sup>, Mehmet Alpaslan<sup>8</sup>, Miguel A. Aragón-Calvo<sup>9</sup>, Jaime E. Forero-Romero<sup>10</sup>, Roberto Gonzalez<sup>11,12</sup>, Stefan Gottlöber<sup>1</sup>, Oliver Hahn<sup>13</sup>, Wojciech A. Hellwing<sup>14,15</sup>, Yehuda Hoffman<sup>16</sup>, Bernard J. T. Jones<sup>2</sup>, Francisco Kitaura<sup>17,18</sup>, Alexander Knebe<sup>19,20</sup>, Serena Manti<sup>21</sup>, Mark Neyrinck<sup>3</sup>, Sebastián E. Nuza<sup>22,23,1</sup>, Nelson Padilla<sup>11,12</sup>, Erwin Platen<sup>2</sup>, Nesar Ramachandra<sup>24</sup>, Aaron Robotham<sup>25</sup>, Enn Saar<sup>5</sup>, Sergei Shandarin<sup>24</sup>, Matthias Steinmetz<sup>1</sup>, Radu S. Stoica<sup>26,27</sup>, Thierry Sousbie<sup>28</sup>, Gustavo Yepes<sup>18</sup>

*Affiliations are listed at the end of the paper*

10 May 2017

## TEST DATA: SIMULATION AND DATA SET

Each of the participants applied their web identification methods to the same Gadget-2 ([Springel 2005](#)) dark matter only  $N$ - body simulation,

with a box size of  $200 h^{-1}\text{Mpc}$  and  $512^3$  particles.

The  $\Lambda\text{CDM}$  cosmological parameters are taken from Planck ([Planck Collaboration et al. 2014](#)):

$h = 0.68$ ,  $\Omega_M = 0.31$ ,  $\Omega_\Lambda = 0.69$ ,  $n_s = 0.96$ , and  $\sigma_8 = 0.82$ .

Haloes in the simulation are identified using a standard FOF algorithm ([Davis et al. 1985](#)), with a linking length of  $b = 0.2$  and a minimum of 20 particles per halo.

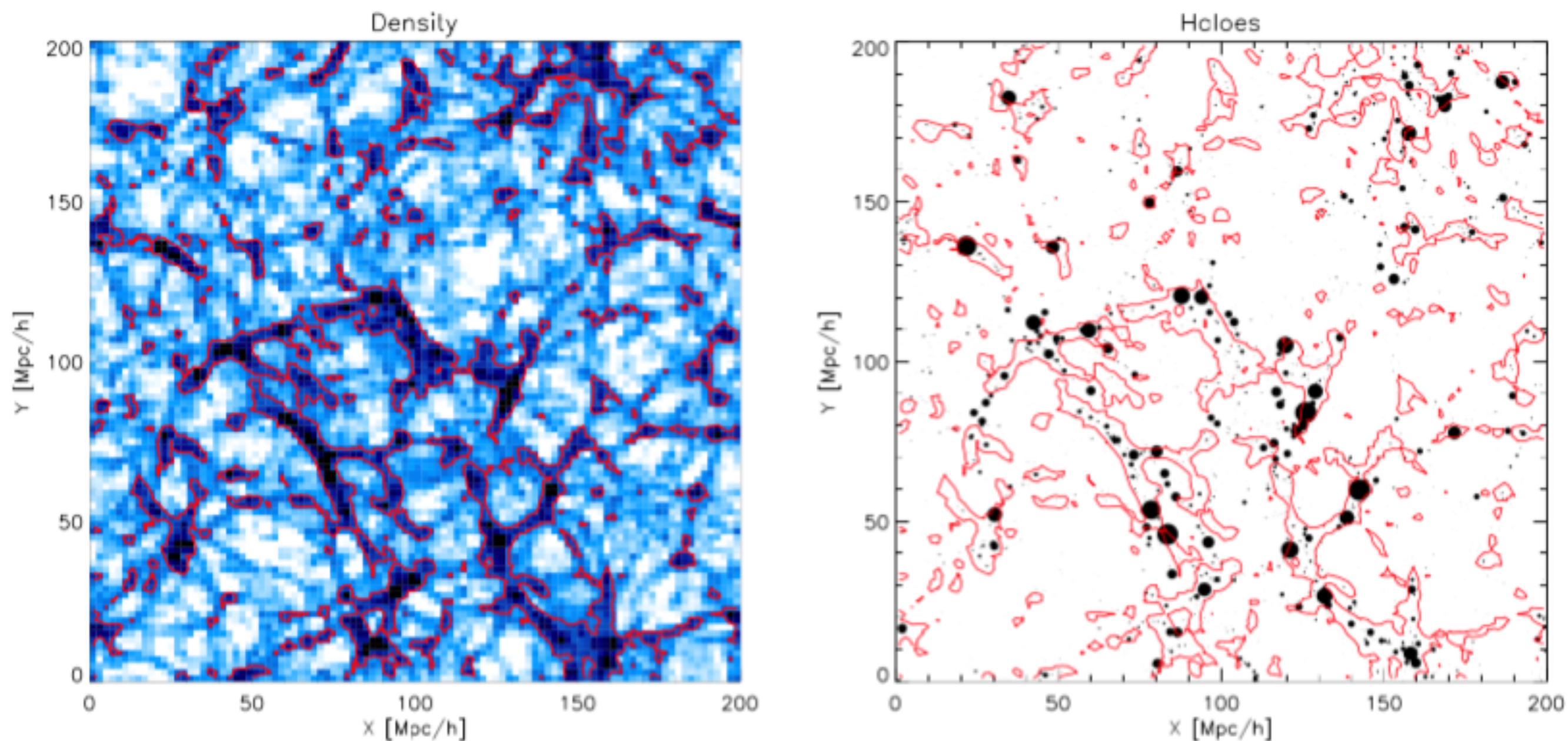
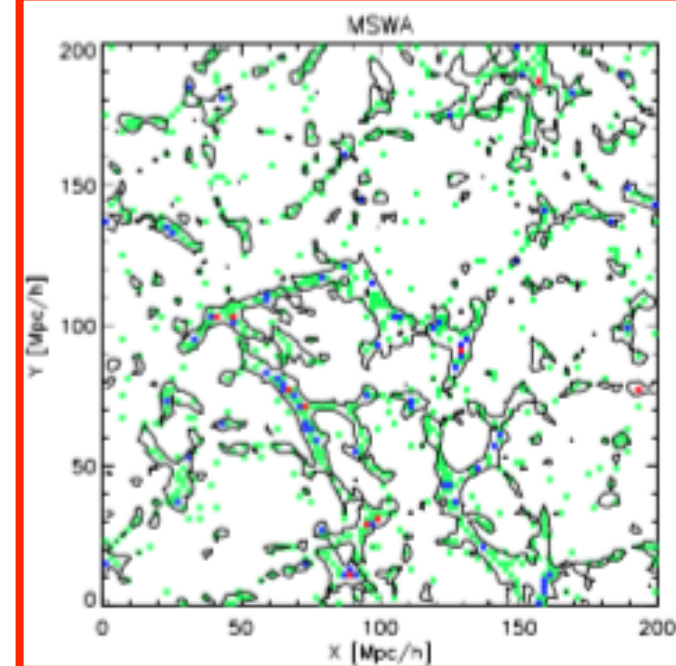
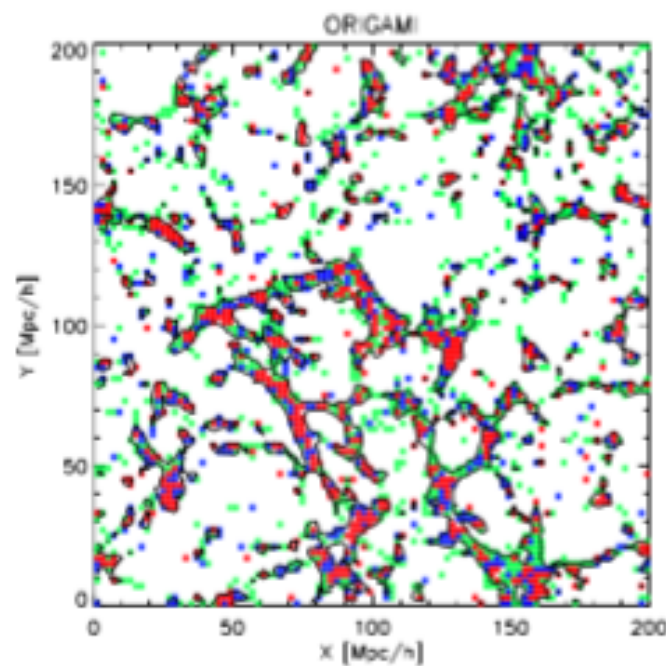
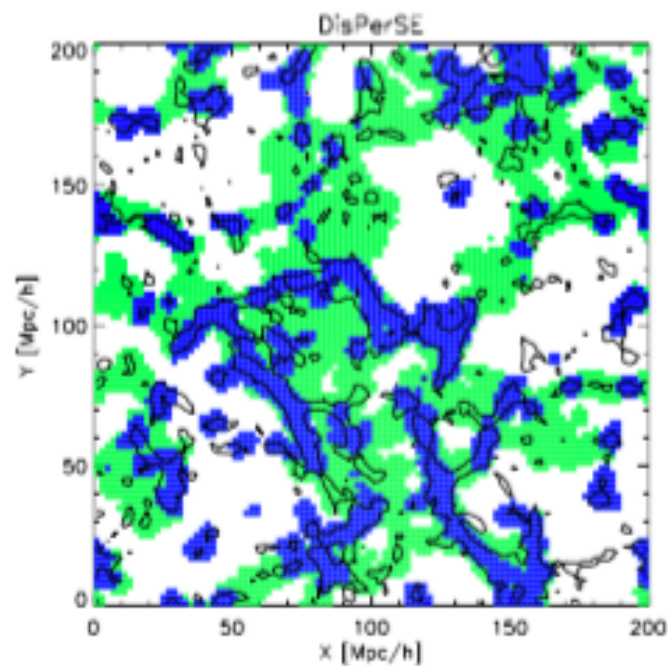
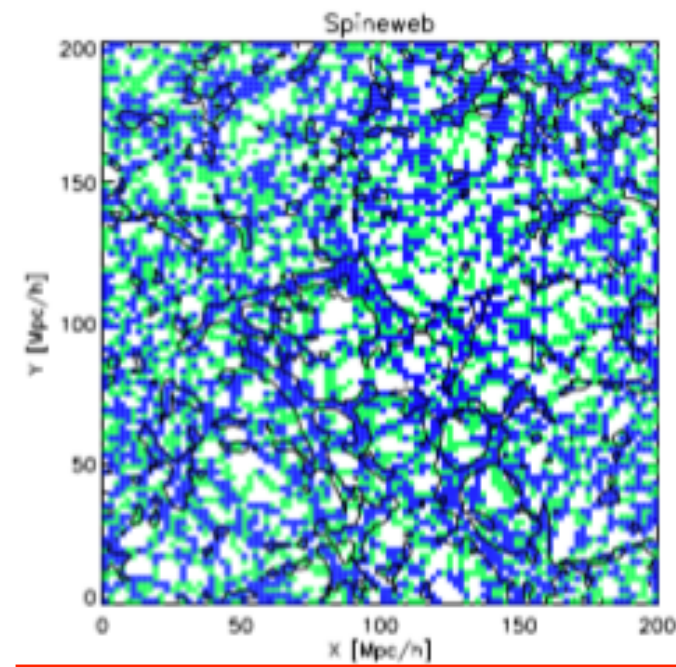
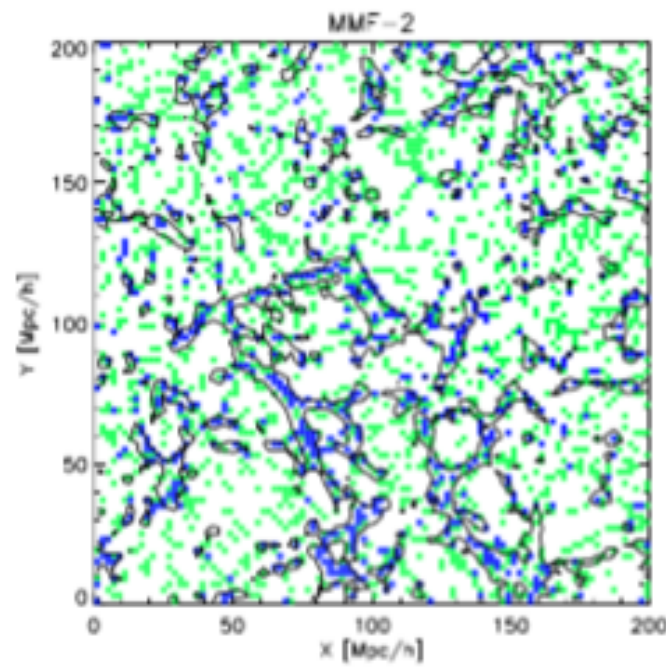
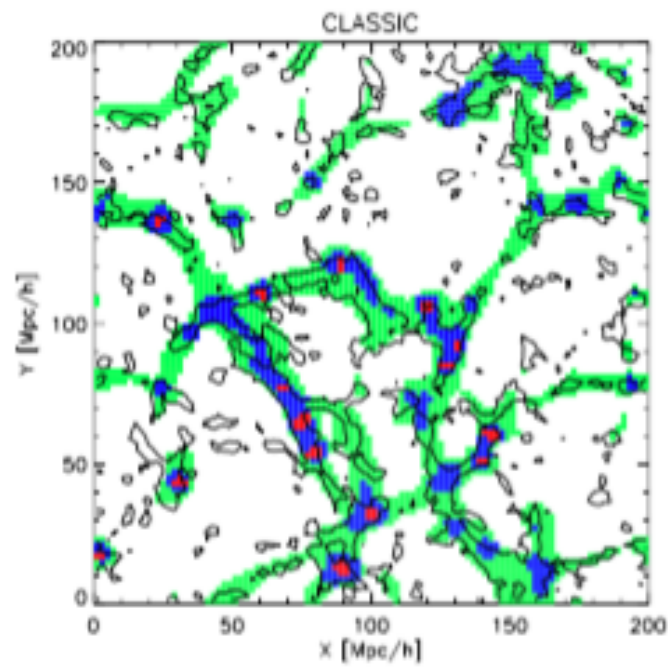
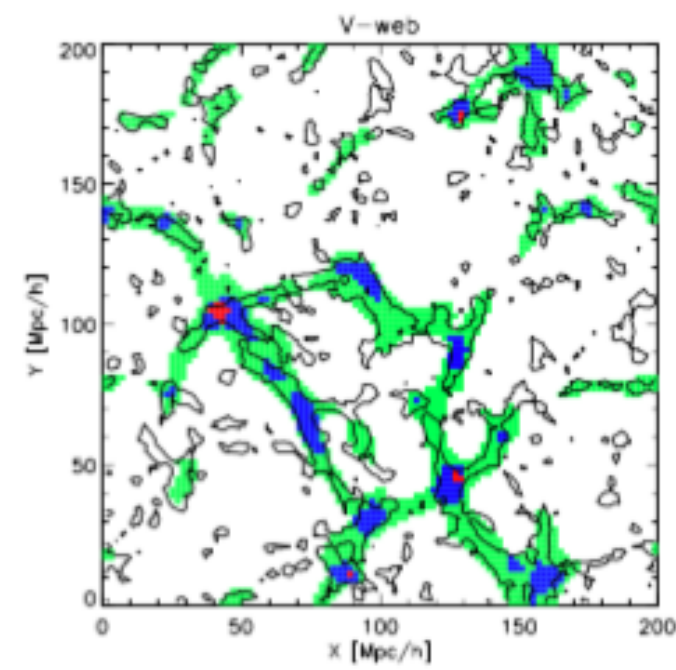
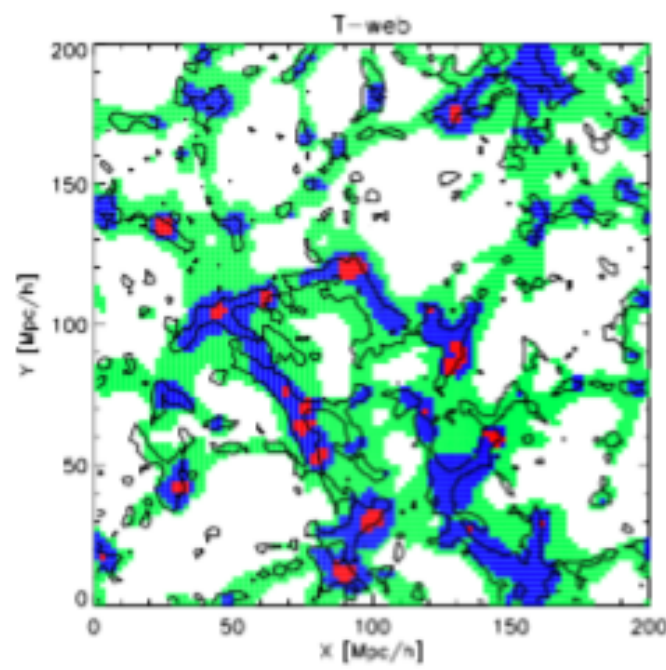
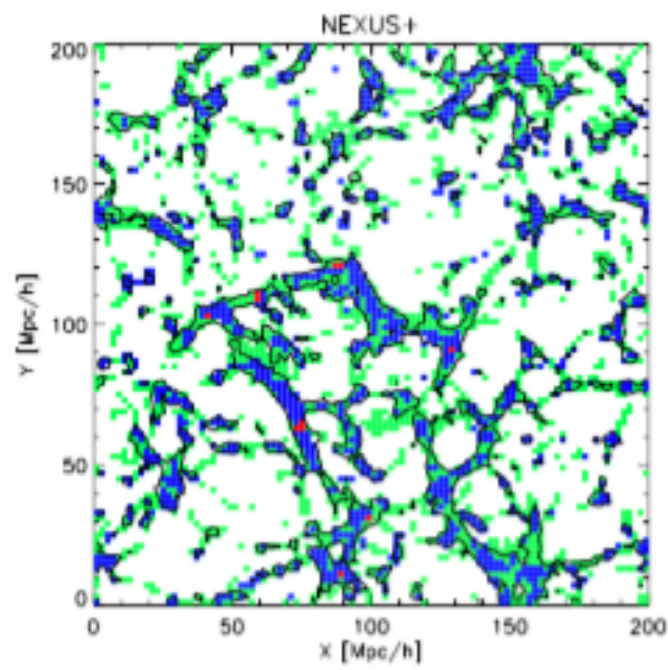
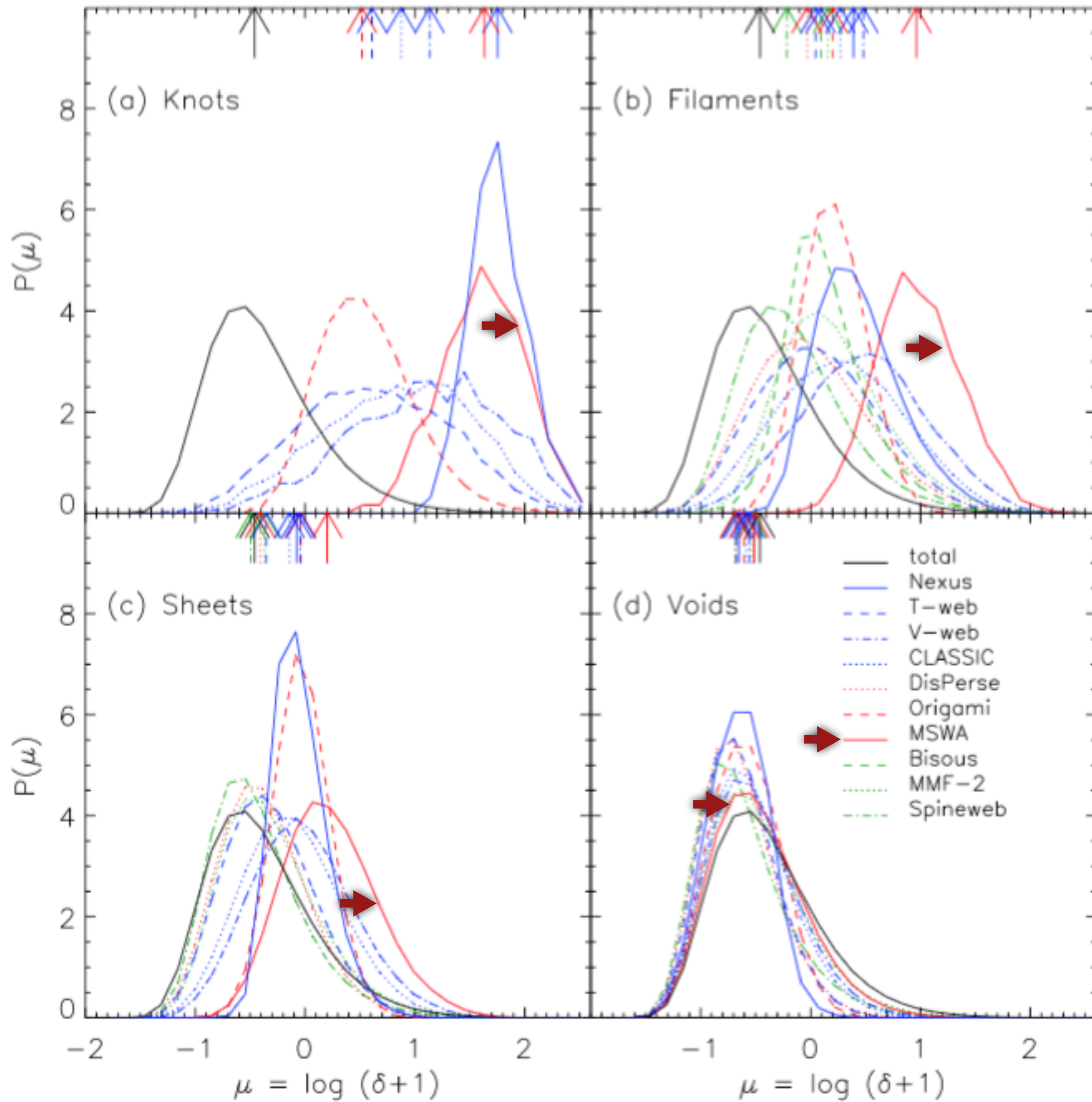


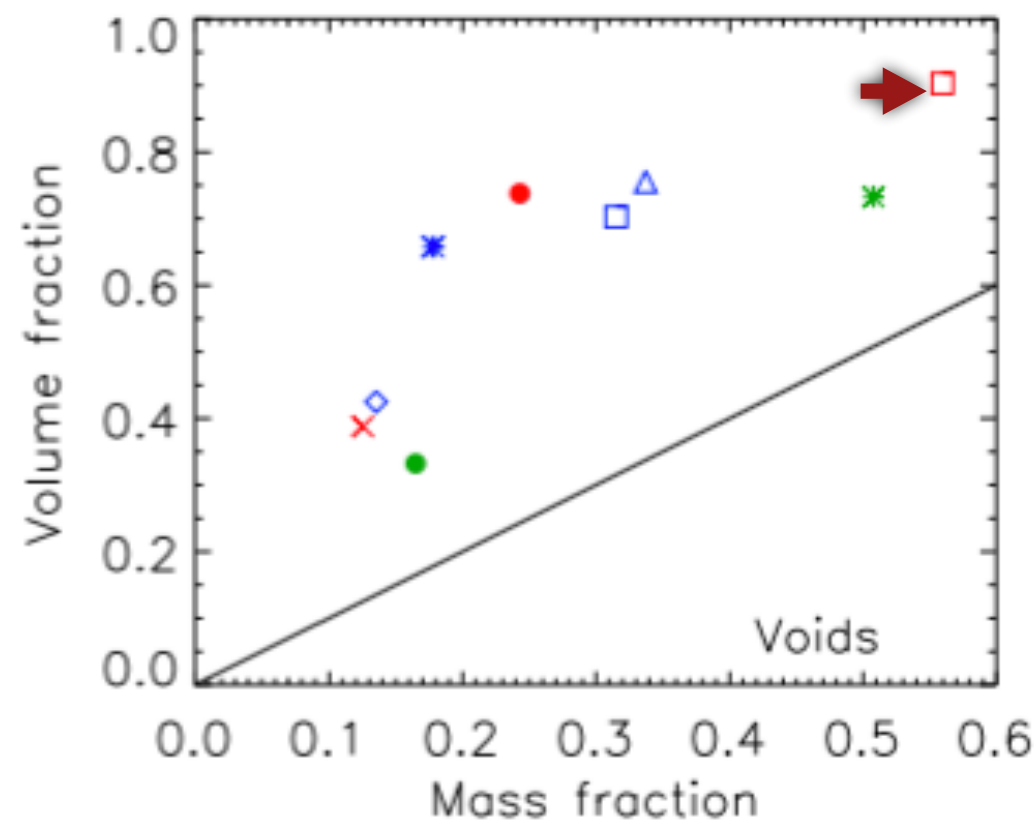
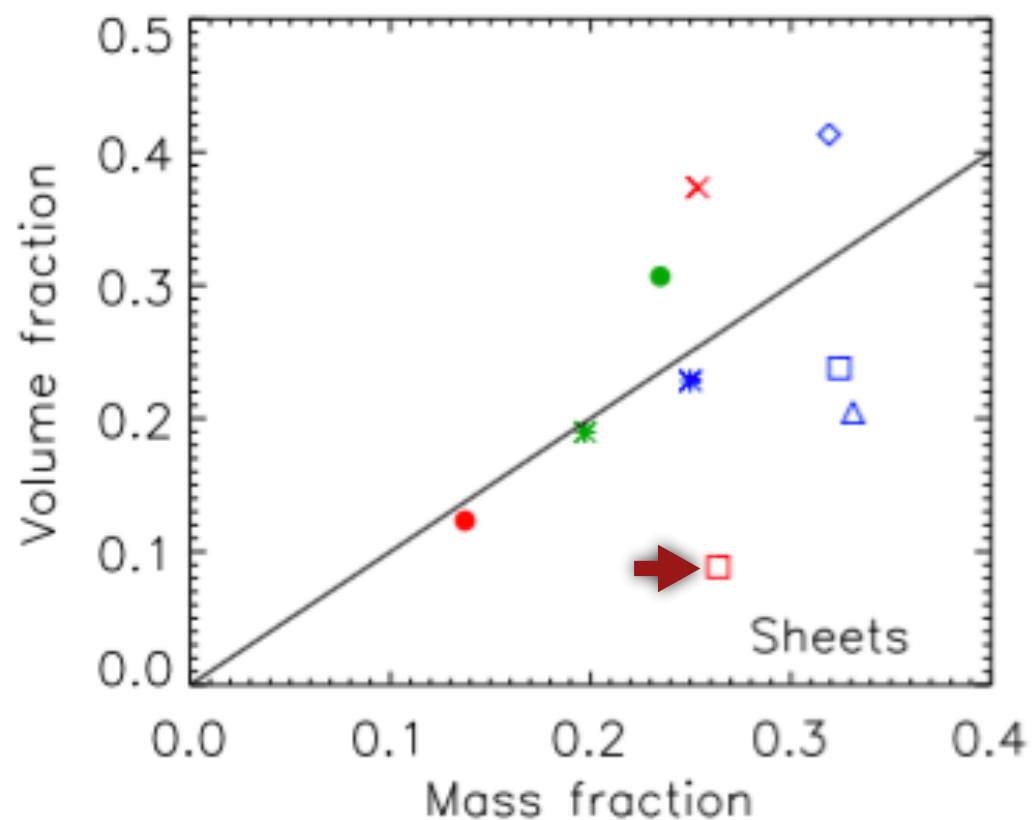
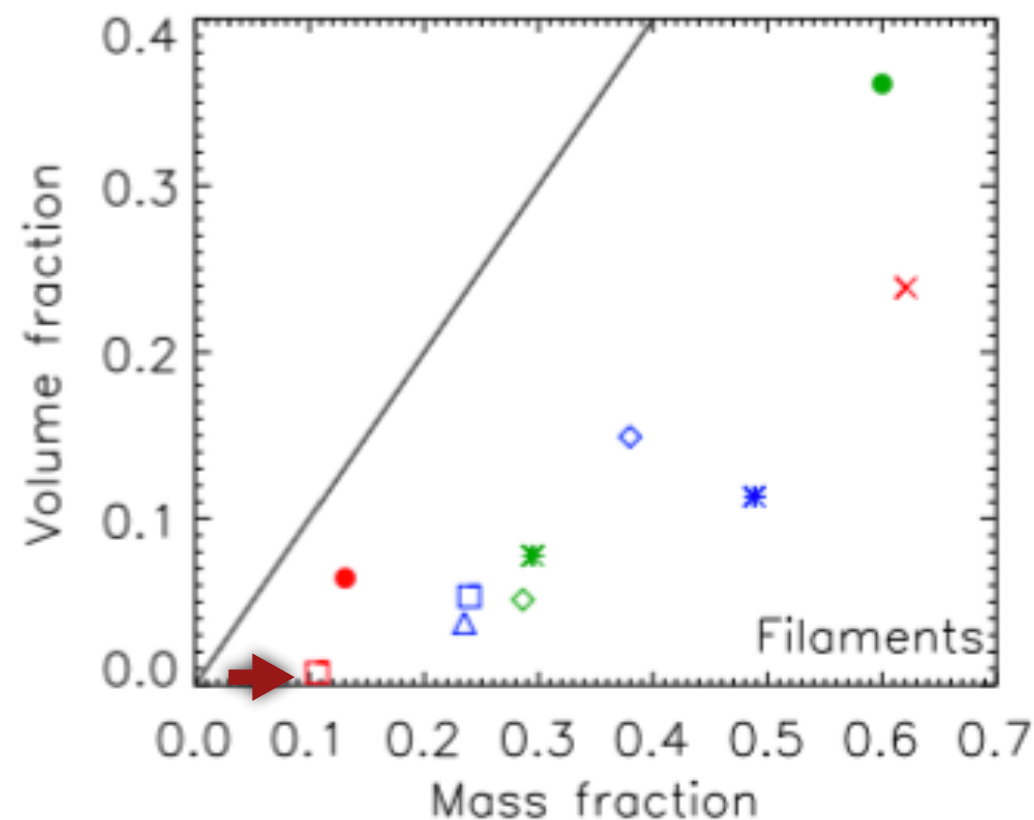
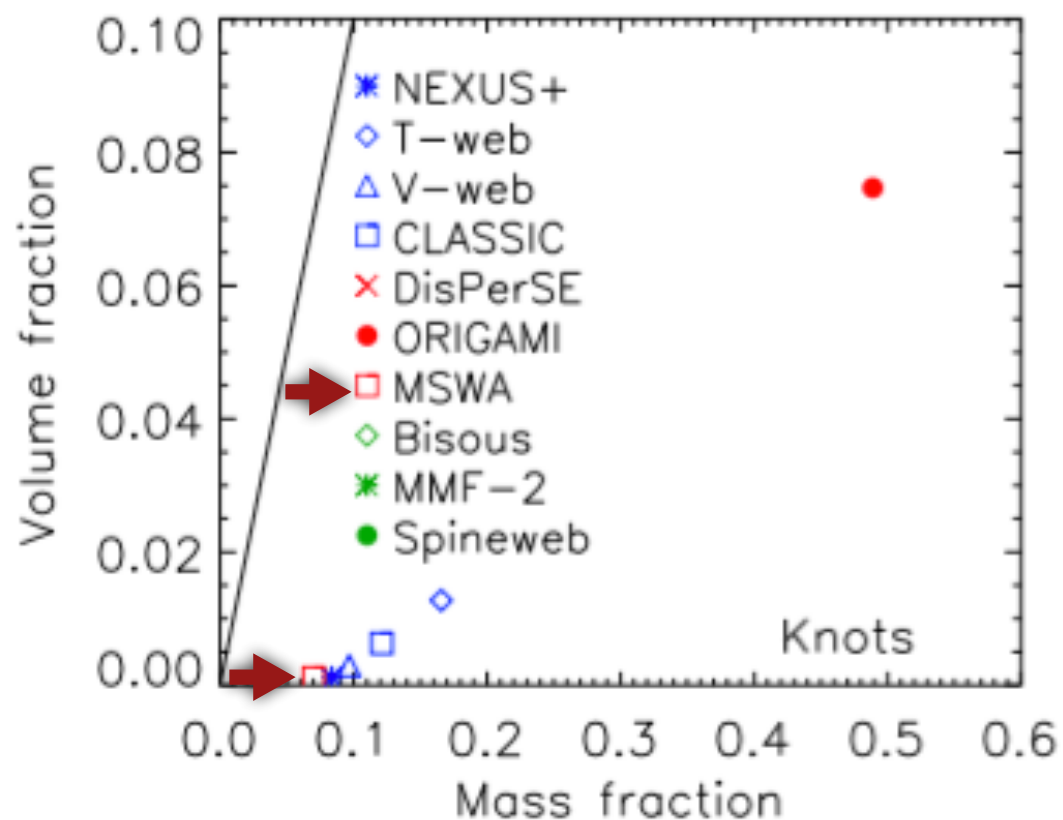
**Figure 1.** A thin slice through the cosmological simulation used for comparing the web identification methods. The left panel shows the density field in a  $2 h^{-1}\text{Mpc}$  slice with darker colours corresponding to higher density regions. The red lines show the  $\delta = 0$  contours (dividing over and under dense regions, with respect to the mean) and are reproduced in the right panel (and in Fig. 2 as black lines). The right panel shows the positions of haloes in a  $10 h^{-1}\text{Mpc}$  slice, where symbol sizes are scaled by halo mass. This same slice will be used to showcase the web identification methods in Figs. 2 and 3 as well as the level of agreement across web finders in Fig. 7.



N. R.  
S. Sh.

MSWA=  
MultiStream  
Web  
Analysis

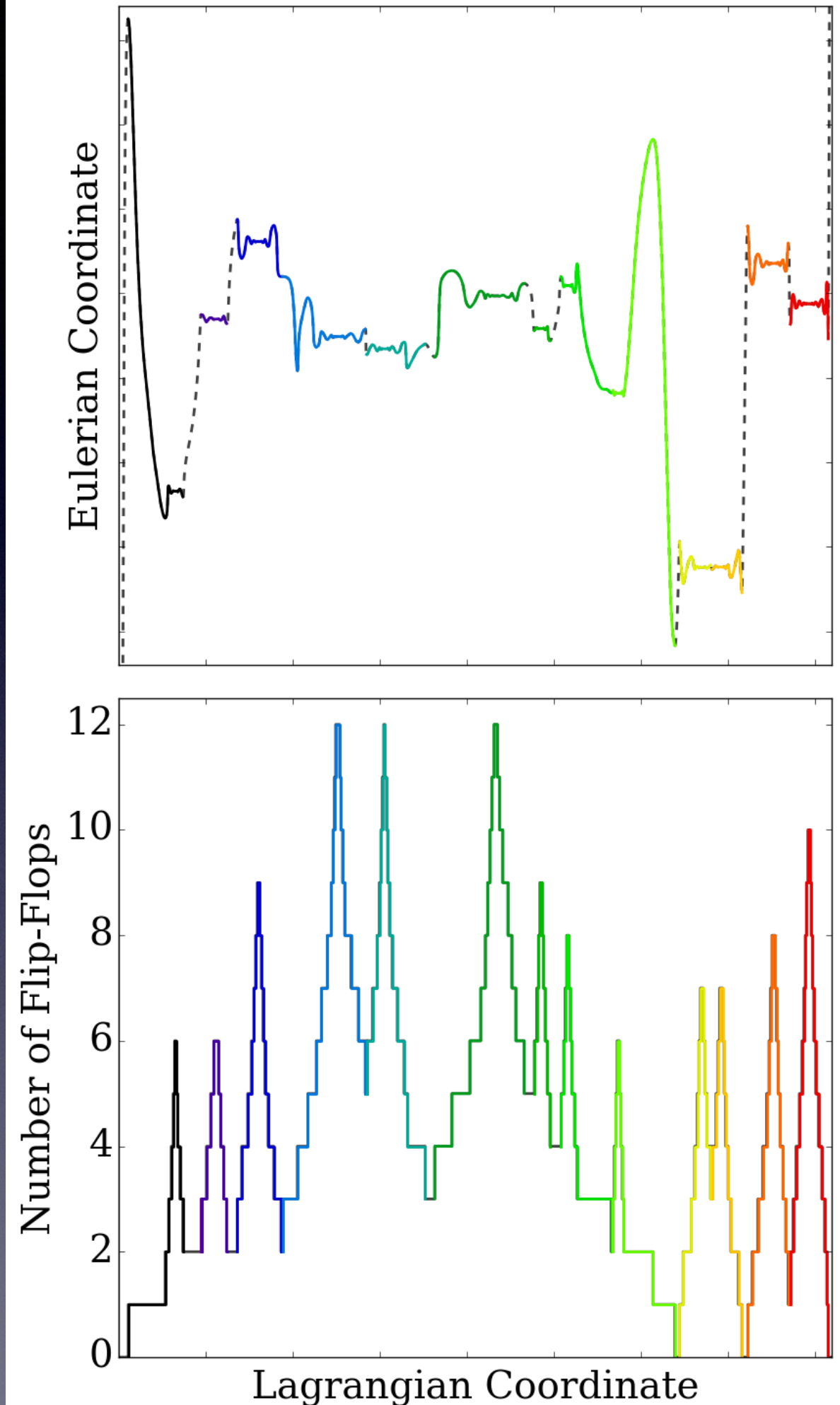
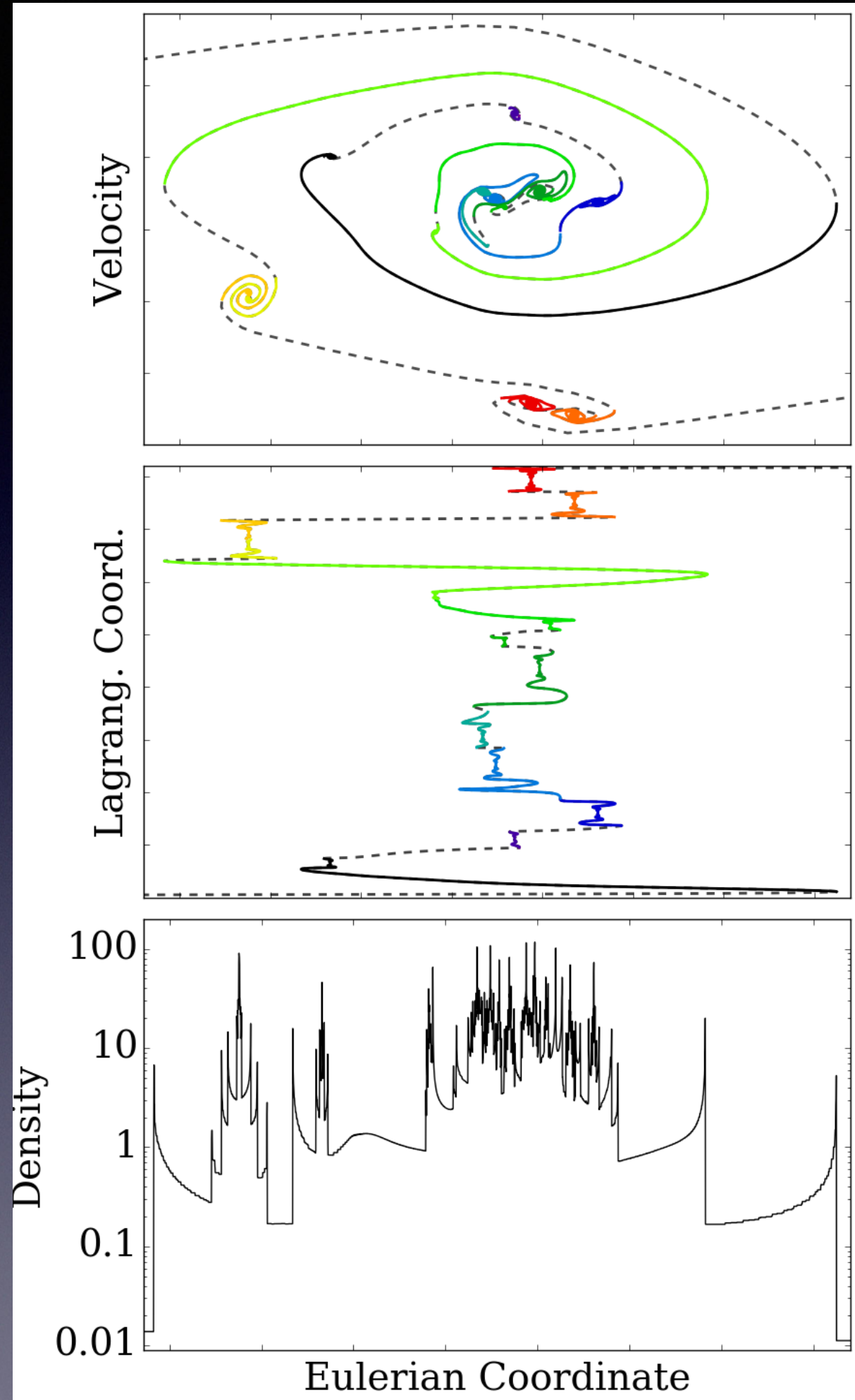




**Figure 5.** The mass and volume filling fraction of knots (top-left), filaments (top-right), sheets (bottom-left) and voids (bottom-right) as identified by the various cosmic web finders. These quantities were computed using a regular grid with a cell spacing of  $2 h^{-1} \text{Mpc}$ . The solid line shows the mean filling fraction, i.e. a slope of unity, where the volume filling fraction equals the mass filling fraction. Namely, points above this line lie in under-densities, points below it in over-densities.

# Outline of the talk

- Brief cosmological introduction
- Beginning of the dark matter web story
  - The Zeldovich approximation
  - Geometrical and topological challenges
  - Web of galaxies
- Dark matter web
  - Flip-flop field as a record of halo merging
  - Multi stream field
  - A comparison project “Tracing the Cosmic Web”
    - **Caustics**
- Summary



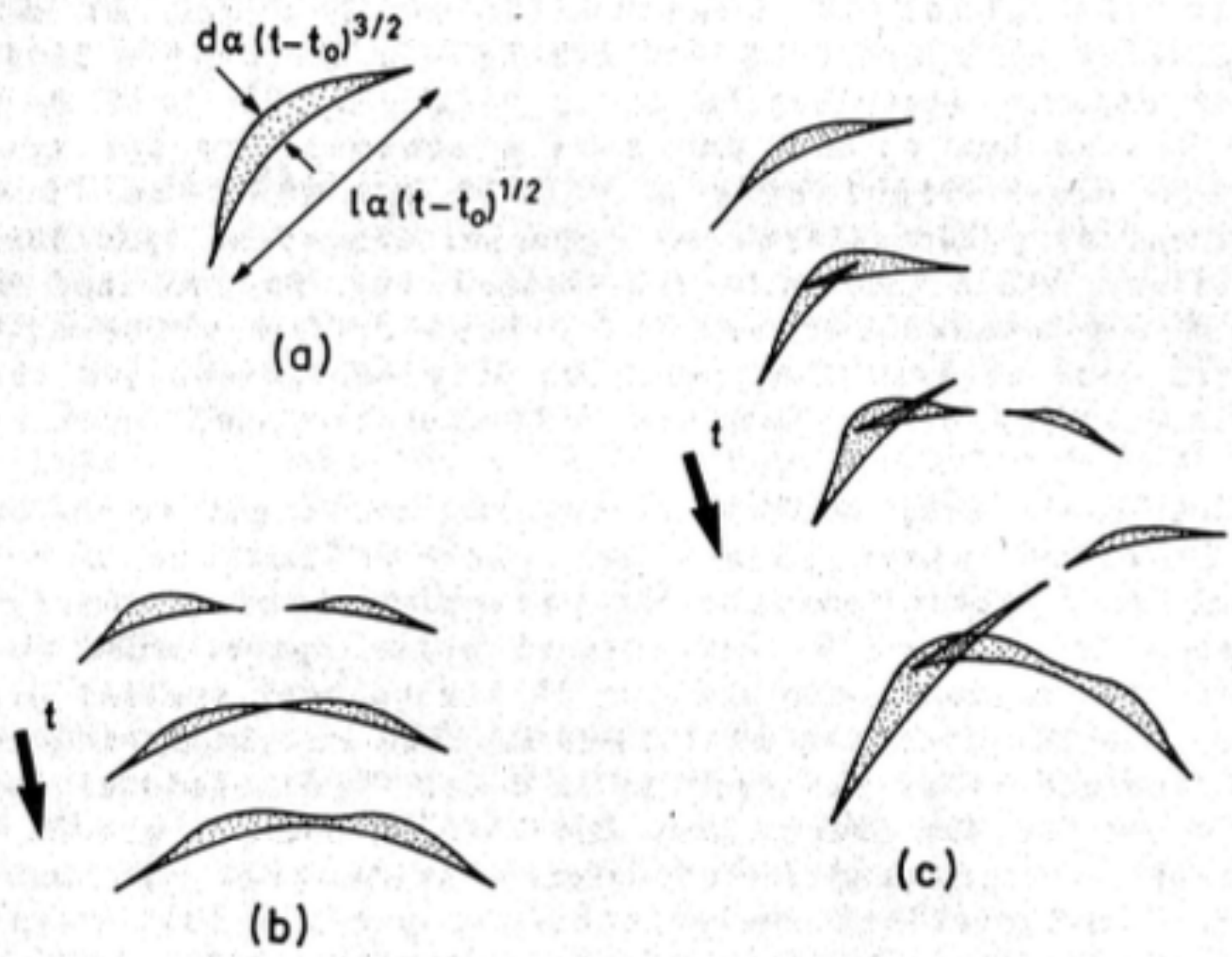
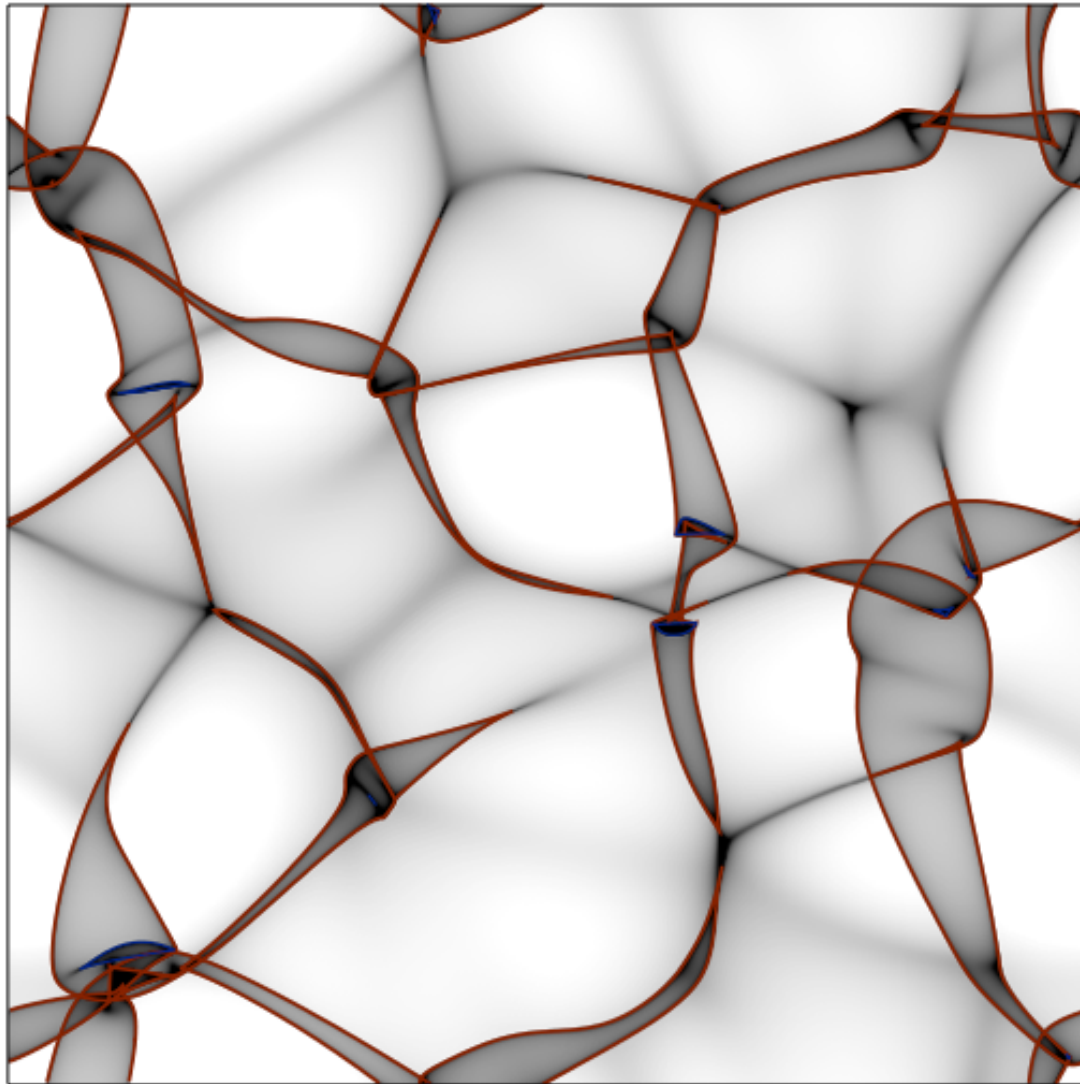


Figure 1. Examples of the general patterns arising in two-dimensional models. The dark regions are regions of three streams flows. a) 'pancake', b) and c) two types of merging of pancakes. Solid lines are caustics - lines of infinite density.

# Caustics in Zeldovich Approximation

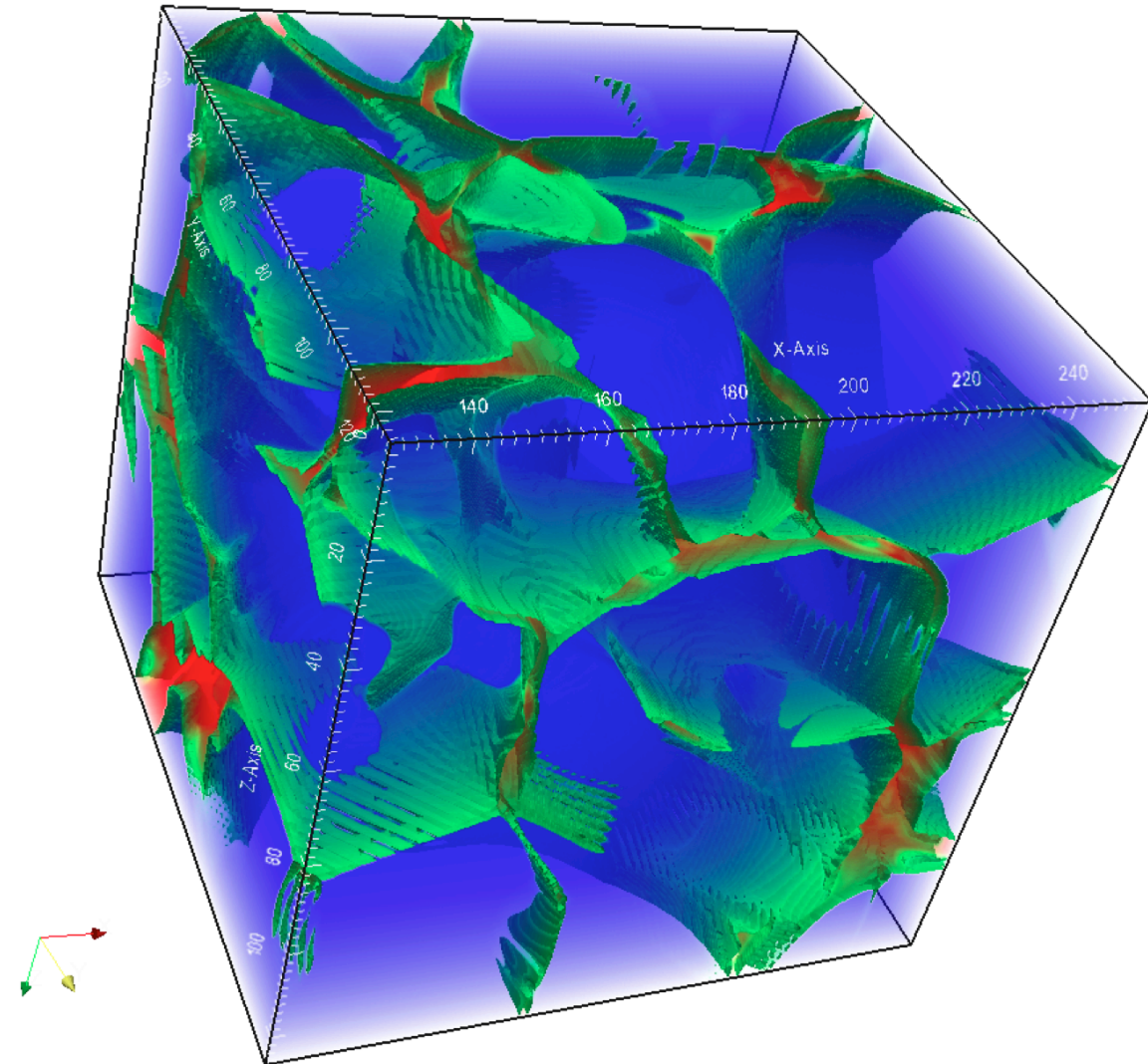
Hidding, Shandarin, van de Weygaert 2014

## Caustics in 2D



Red - Lam\_1  
Blue - Lam\_2

## Caustics in 3D



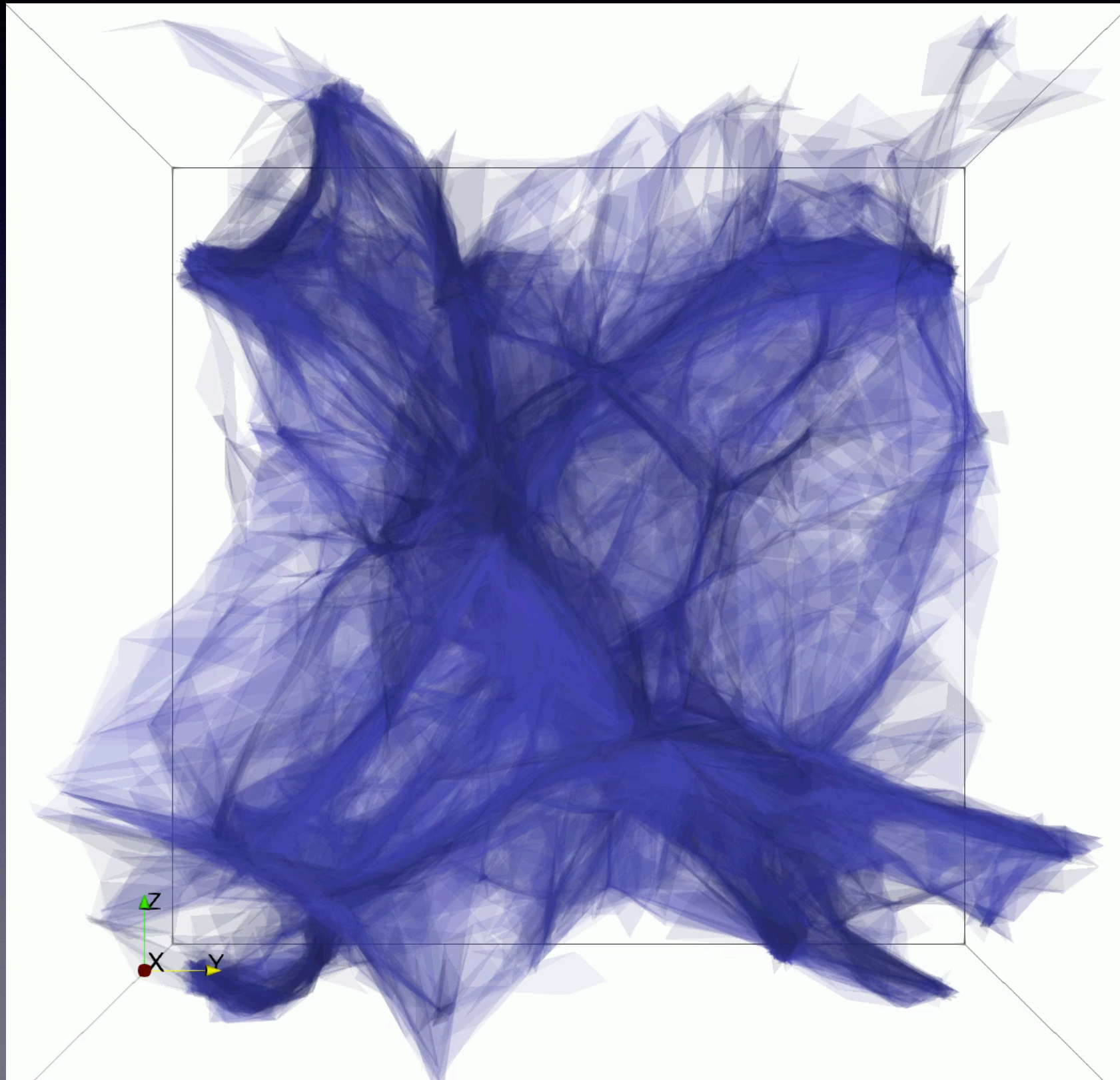
Green - Lam\_1  
Red - Lam\_2  
Lam\_3 caustics are inside  
Lam\_2 Surfaces

# Arnold 1982

$n=3$ , Euler space, series A				
type	instantaneous caustics			bicaustic
	$t < 0$	$t = 0$	$t > 0$	
$A_3$				
$A_3(+)$				
$A_3(-)$				
$A_3(+)$				
$A_3(-)$				
$A_4$				
$A_4(+)$				
$A_4(-)$				
$A_5$				

$n=3$ , Euler space, series D				
type	instantaneous caustics			bicaustic
	$t < 0$	$t = 0$	$t > 0$	
$D_4^-$				
$D_4^-(+)$				
$D_4^+(+)$				
$D_4^+(-)$				
$D_5$				

Caustics in 3D N-body simulations:  
triangle interface between neighboring tetrahedra  
 $V_1 > 0$  and  $V_2 < 0$



# Summary

## DM Web

New fields: number of streams and flip-flop fields, and caustic surfaces reveal new properties of the cosmic web. All are easy to compute from standard cosmological simulations, however require the tessellation of the initial state.

The dark matter web is defined as the part of the universe where the number of streams greater than one. It spans throughout the entire volume of the universe occupying about 10% of the volume.

The void regions occupy the rest 90% of the volume. The largest percolating void occupy about 99% of all the single-streaming regions. (A sponge topology)

The number of flip-flops as a function of Lagrangian coordinate stores information about the merging history of DM halos.

The volume and mass fractions in voids measured by MSWA=Multi Stream Web Analysis are the largest (0.90 and 0.56 respectively) of all measured by other methods in the comparison project.